

Lawrence Berkeley National Laboratory

Recent Work

Title

CHEMISTRY DIVISION QUARTERLY REPORT Dec. 1956, Jan, Feb. 1957

Permalink

<https://escholarship.org/uc/item/7r34v39q>

Author

Lawrence Berkeley National Laboratory

Publication Date

1957-03-19

UNIVERSITY OF
CALIFORNIA

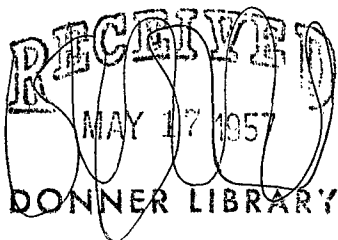
*Radiation
Laboratory*

TWO-WEEK LOAN COPY

*This is a Library Circulating Copy
which may be borrowed for two weeks.
For a personal retention copy, call
Tech. Info. Division, Ext. 5545*

CHEMISTRY DIVISION QUARTERLY REPORT

December 1956, January, February 1957



BERKELEY, CALIFORNIA

DISCLAIMER

This document was prepared as an account of work sponsored by the United States Government. While this document is believed to contain correct information, neither the United States Government nor any agency thereof, nor the Regents of the University of California, nor any of their employees, makes any warranty, express or implied, or assumes any legal responsibility for the accuracy, completeness, or usefulness of any information, apparatus, product, or process disclosed, or represents that its use would not infringe privately owned rights. Reference herein to any specific commercial product, process, or service by its trade name, trademark, manufacturer, or otherwise, does not necessarily constitute or imply its endorsement, recommendation, or favoring by the United States Government or any agency thereof, or the Regents of the University of California. The views and opinions of authors expressed herein do not necessarily state or reflect those of the United States Government or any agency thereof or the Regents of the University of California.

UCRL-3710
Chemistry - General

UNIVERSITY OF CALIFORNIA

Radiation Laboratory
Berkeley, California

Contract No. W-7405-eng-48

CHEMISTRY DIVISION QUARTERLY REPORT

December 1956, January, February 1957

March 19, 1957

Printed for the U. S. Atomic Energy Commission

CHEMISTRY DIVISION QUARTERLY REPORT

December 1956, January, February 1957

Contents

BIO-ORGANIC CHEMISTRY

On the Problem of the Primary Product of Photosynthesis	4
Alcohol and KCN Poisoning in Short-Time Photosynthesis Studies	9
Relative Radioactivities of Chlorophyll <u>a</u> and Chlorophyll <u>b</u> from Photosynthetic Studies	21
Physiology of <u>Chlorella</u> Grown in Heavy Water	22
Effect of Manganese Deficiency on CO ₂ Metabolism in <u>Nostoc</u>	25
Carotenoids in Algae in Light and Dark	28
Study of the Inhibition of Azaserine and Diaza-Oxo-Norleucine (DON) on the Algae <u>Scenedesmus</u> and <u>Chlorella</u>	29
Radiation Sensitivity in <u>Chlorella</u>	32
A Modified Method for Preparation of Carboxydismutase	33
Large-Scale Preparation of Ribulose Diphosphate (RuDP)	39
Glucose Dissimilation in a Free-Cell Neoplasm	43
Glucose Metabolism in Depancreatized Rats	52
Effect of Diisopropylfluorophosphonate (DFP) upon Brain Cholinesterase	57
Distribution of Diisopropylfluorophosphonate in Rats	59
Respiratory Metabolism of Acetate and Glycine as a Function of Age	62
The Inhibition of Ascites Tumor Growth by D ₂ O	63
Radiation Effects on Choline Chloride	68
A High-Intensity Cobalt-60 Source	72
Spectra of Copper and Chromium Complexes	76

NUCLEAR CHEMISTRY

New Isotope: Sulfur-38	79
Preparation of Gadolinium-162 and Terbium-162 by Double Neutron Capture	81
Studies of Neutron-Deficient Terbium Isotopes	81
Further Studies in Neutron-Deficient Dysprosium Isotopes	82
The Determination of Neutron-Neutron Cross Sections in Nuclear Matter	84
Triton Production in Cyclotron Bombardments	85
Half-Thickness Values for Gamma Rays in Lead	86
Fluorescence of U ⁺³	86
Deuteron-Induced Reactions of Uranium-234, Uranium-235, and Uranium-238	87
Electrostatic Calculation of Structure for Yttrium Oxyfluoride	89

*Preceding Quarterly Reports: UCRL-3629, UCRL-3595.

CHEMICAL ENGINEERING (PROCESS CHEMISTRY)

Notes on Work in Progress

Correlation of Limiting Current Density at Horizontal Electrodes under Free-Convection Conditions	91
Stability of Perforated-Plate Trays	91
Multicomponent Distillation Studies with an IBM 701-2 Frame Digital Computer	91
Electrochemical Studies in Nonaqueous Solvents	91
Liquid-Liquid Extraction and Agitation Coalescence Rates in Two-Phase Agitated Systems	92
Performance of Sphere-Packed Extraction Columns	92
Extraction Rates into Single Drops	92
Gas-Liquid Partition Chromatography (GLPC)	92

GENERAL CHEMISTRY

Metals and High-Temperature Thermodynamics

Absolute-Lifetime Apparatus	93
Ground State of S ₂	93
Stability of SiO and GeO Solids	93

Basic Chemistry

Ruthenium Chemistry	94
The Heat of Formation of the Ferrate Ion	94
The Second Ionization Constant of H ₂ Se	94
Kinetics of Rapid Reactions	94
Determination of the Molecular Structure of Aluminum Hydride	95
Heat Capacities of Metals between 0.1° and 4.2°K	95
Hydrogen Bonding in Formic Acid System	96

CHEMISTRY DIVISION QUARTERLY REPORT

December 1956, January, February 1957

Radiation Laboratory and Department of Chemistry
University of California, Berkeley, California

March 19, 1957

BIO-ORGANIC CHEMISTRYM. Calvin, Director
Edited by B. M. Tolbert

ON THE PROBLEM OF THE PRIMARY PRODUCT OF PHOTOSYNTHESIS

Helmut Metzner and Barbara Metzner

In studying the primary products of photosynthesis and CO_2 dark fixation, one normally kills the algae with boiling ethanol and extracts the cells with the same solvent. The following experiments were conducted to see whether or not this procedure can give reliable figures for the distribution of C^{14} -labeled compounds within the living cell. One has to remember that hot ethanol cannot inactivate enzyme systems immediately; on the contrary, the enzymatic processes are enhanced for a certain time by the rising temperature. It therefore seems to be more advisable to stop the metabolism by effective enzyme poisons or to kill the algae by deeply cooled organic solvents. The last procedure, however, has the disadvantage that the sugar phosphates may be partly phosphatased afterwards, because not all solvents destroy the phosphatases.

The first series of experiments was started with cold acetone (between 0° and -70°C), which in neutral solution precipitates most plant proteins strictly reversibly. Between ethanol and acetone experiments there are clear and reproducible differences (Table I). First of all, the total fixation of C^{14}O_2 is magnified in all experiments with cold acetone, whereas the difference remains within the limits of probable error if one kills the algae with acetone at 0°C . The shorter the photosynthesis period the more pronounced we find the ethanol:acetone discrepancy in total fixation, even with acetone at 0°C . Besides this there is a difference in the balance of activity distribution: All experiments with ethanol killing give a satisfactory balance, i. e., if one adds up the activities of the alcohol-soluble fraction and the insoluble material, one finds the activity of the original suspension. The deviation lies within the range of probable error, normally $< 10\%$. Acetone experiments do not give a good balance. If one fractionates the acetone suspension into the acetone-soluble material and the acetone-insoluble lot, and then washes this precipitate with water followed by 95% ethanol, one finds that the sum of the activities of all these fractions lies below 100% (Table II). This loss is greater as the time the algae have been assimilating CO_2 is shorter. It is easily demonstrated that this is not merely a temperature effect. Attempts were made to kill the algae with cold ethanol (-20°C) and

Table I

Total C¹⁴O₂ fixation of Scenedesmus

Exp. No.	PS	Temp of acetone	Counts ^a	Counts after ethanol killing
6	2 min	0°	24,376,000	25,207,000
12a	2 min	-25°	22,908,000	15,452,000
8	2 min	-70°	18,056,000	15,894,000
6	30 sec	0°	4,334,000	4,309,000
10	30 sec	-20°	9,032,000	8,490,000 ^b
6	5 sec	0°	679,000	531,000

^aFigures are corrected to "Counts/min x 1 ml wet packed cells.

^bTemperature of the ethanol -20°C.

Table II

Balance of the activity distribution after killing with acetone

Exp. No.	PS	Temp. of acetone	Suspension	Acetone fraction	Water extract	Ethanol extract	Insoluble	Loss	Loss %
6	2 min	0°	24,376,000	9,571,000	9,058,000	1,871,000	1,116,000	2,760,000	11
6	30 sec	0°	4,334,000	1,137,000	1,992,000	198,000	105,000	902,000	21
6	5 sec	0°	679,000	102,000	330,000	---	5,000	242,000	36
10	30 sec	-20°	9,032,000	254,000	5,740,000	111,000	79,000	2,848,000	32
12a	2 min	-25°	22,088,000	2,957,000	11,424,000	831,000	1,240,000 ^a	5,636,000	26

^aIncludes the activity adsorbed on the filter paper.

to extract the insoluble material with water and acetone; in this control experiment the loss of activity was less than 3%. Very pronounced losses were found when acetone-dry ice mixtures were used instead of pure acetone. Because these suspensions are bubbling rapidly after the addition of the algae, it is not easy to get exact figures for the total fixation, but we may be sure that the loss of activity is more than twice that we find with pure acetone solutions of the same temperature.

These observations lead us to the conclusion that a certain portion of the $C^{14}O_2$ is fixed as a part of a labile compound, which is split during the killing with ethanol. The difference in the total fixation (loss in activity, compared with the acetone experiments) shows that a part of this compound gives off the $C^{14}O_2$; the good balance after the ethanol killing demonstrates that the rest is converted to a stable product. If we compare the chromatograms of the ethanol and acetone series we find that in all acetone experiments there is much less PGA (< 25%). Therefore we must conclude that the labile product is converted to PGA. That all differences between the two different killing methods are much more pronounced in short-time experiments demonstrates that the labile substance originates very early and should be one of the first photosynthesis products--if not the first intermediate itself.

Pouring algal suspensions into acetone-dry ice mixtures, one sees a tremendous evolution of CO_2 ; this gas was formerly dissolved when cold acetone alone was used. There is much less $C^{14}O_2$ fixation to be observed afterwards than after killing with pure acetone. We have to assume that the difference represents loss during the bubbling, and that this is not caused by a splitting of the labile compound, but more probably by an exchange of the primarily fixed $C^{14}O_2$ with $C^{12}O_2$, which is in great surplus. To prove this exchange an absorption vessel with $Ba(OH)_2$ was attached to the suction flask with the filter, on which the acetone-dry powder was separated from the solvent and washed with water and ethanol. The precipitated $BaCO_3$ was re-suspended in ethanol and an aliquot brought to a plate (Table III). Counting these plates, we found a high proportion of C^{14} . In these experiments, too, the biggest evolution of $C^{14}O_2$ was to be observed after short-time photosynthesis experiments.

Table III

Loss of activity during the acetone killing of <i>Scenedesmus</i> and activity of the $C^{14}O_2$ evolved					
Exp. No.	PS	Temp of acetone	Total fixation	Loss of activity	Activity of $BaC^{14}O_3$
6	2 min	0°	24,376,000	2,764,000	157,000
6	30 sec	0°	4,334,000	903,000	825,000
6	5 sec	0°	679,000	242,000	714,000 ^a
11	30 sec	-25°	1,560,000	no balance calculated	87,000
12b	2 min	-25°	19,538,000	4,620,000	902,000
12b	2 min ^b	-25°	23,436,000	4,626,000	712,000
12b	10 sec ^b	-25°	3,915,000	578,000	2,681,000 ^a

^aFor explanation the bad balance of the 5-sec and 10-sec experiments see the text.

^bBefore killing with acetone addition of 10^{-2} mol NH_2OH .

In another series the acetone-dry powder was resuspended in distilled water in a modified Thunberg vessel. To avoid a $C^{14}O_2-C^{12}O_2$ exchange this suspension was flushed with a stream of nitrogen. In all these experiments only a small amount of $C^{14}O_2$ ($< 0.1\%$) could be detected. This may demonstrate that we are dealing with a real exchange phenomenon, which is enhanced by spreading the dry powder on the filter paper. There remains to be answered the question whether the first step of CO_2 fixation within the living cell is an enzymatic process or not. It could be observed that nitrogen flushes double the amount of $C^{14}O_2$ out of the Thunberg vessel, if the powder is not suspended in water but in an acidified solution of NaF. This effect has to be compared with the *in vivo* evolution of CO_2 by *Chlorella*, recently discovered by Warburg. Warburg also describes the extreme lability of the responsible enzyme system, and thus we may understand why we find such small carbon dioxide amounts set free from dry powder, which we prepared from acetone suspensions without special care to exclude interfering substances. We have to improve the method of preparation of the dry powder or have to isolate the responsible enzyme to demonstrate *in vitro* the effect discovered by Warburg.

If the labile fixation product loses $C^{14}O_2$ we have to study the question whether the usual counting procedure can give conclusive values. Adding up the activities of all soluble fractions and the remaining dry powder as well as the $C^{14}O_2$ developed during the filtration process, we find that in short-time photosynthesis experiments (5 sec and 10 sec) the sum exceeds the activity of the original suspension (Table IV). The only interpretation seems to be the assumption that the activity of the original suspension is not correctly determined. Actually we find that plates with the acetone suspension lose about 5% of their activity within 4 days. Therefore we must conclude that the counting of aluminum plates gives unreliable values. This error will be very great in experiments with only a few seconds' photosynthesis. Presumably the same must be true also for the counts of single fractions.

Table IV

Balance of the relative activity distribution after killing with acetone including the activity of the CO_2 evolved during the preparation of the dry powder

Exp. No.	PS	Temp of acetone	Total fixation	Acetone fraction	Water fraction	Ethanol fraction	Insoluble	$BaC^{14}O_3$	Σ
6	2 min	0°	100	39.3	37.2	7.7	4.6	0.6	89.4
6	30 sec	0°	100	26.2	46.0	4.6	2.4	19.0	98.2
6	5 sec	0°	100	15.0	48.5	0.0	0.7	105.2	169.4
12b	2 min	-25°	100	23.1	36.6	3.6	13.1 ^a	4.6	81.0
12b	2 min ^b	-25°	100	53.5	8.7	3.0	15.0 ^a	3.0	83.2
12b	10 sec ^b	-25°	100	58.0	10.6	0.7	15.8 ^a	68.5	153.6

^aIncludes the activity adsorbed on the filter paper.

^bBefore killing with acetone addition of 0.01 mol NH_2OH .

What do we know about this labile product? The ethanol seems to split the compound into PGA with the C^{14} in the carboxylic group. It is likely that the original compound is a phosphate ester of a branched-chain β keto acid. A comparison of the chromatograms of the acetone and the ethanol experiments has not yet shown any new spot. We therefore have to expect that the labile product does not survive the vacuum concentration of the solution and the following chromatographic separation. To isolate the first product we have two chances: First of all to inhibit the decarboxylating enzyme, which may be identical with the carboxydismutase, or to trap the compound to get a more stable derivative. To achieve this we tried to stop the metabolism of the algae by the addition of NH_2OH (~ 0.01 mol) immediately before the killing with acetone. In these experiments we found, after 30 seconds' photosynthesis, a much higher $C^{14}O_2$ fixation than with pure acetone killing. (Table V) This hydroxylamine effect was much less pronounced in a following 2-minute experiment. In addition to this, the activity of the acetone filtrate is considerably higher. Therefore it appears that we have got a very acetone-soluble and fairly stable derivative of the compound we are searching for.

Table V

Influence of NH_2OH upon the total $C^{14}O_2$ fixation and the relative amount of acetone-soluble material					
Exp. No.	PS	Temp. of acetone	Killing procedure	Total fixation	Acetone-soluble material
11b	30 sec	-25°	Pure acetone	1,579,000	16.5%
11b	30 sec	-25°	Acetone after NH_2OH	4,240,000	94.4%
12b	2 min	-25°	Pure acetone	19,538,000	23.1%
12b	2 min	-25°	Acetone after NH_2OH	23,436,000	53.5%
12b	10 sec	-25°	Acetone after NH_2OH	3,915,000	58.0%

The chromatograms of the acetone filtrates of these hydroxylamine experiments have a new spot in the region of the sugar phosphates. Phosphatase actually changes the R_F values, so that we may say that the yet unidentified spot must be a phosphate ester. Identification reactions of the phosphatased product are being carried out.

ALCOHOL AND KCN POISONING IN SHORT-TIME PHOTOSYNTHESIS STUDIES

Otto Kandler

In the study of the distribution of assimilated C^{14} in the different intermediary products it is of fundamental importance to inactivate all enzymes as simultaneously as possible without destroying the intermediary products. This can be achieved only approximately, however, and this paper compares the effect of poisoning with alcohol or KCN on the distribution of activity.

Materials and Methods

In all experiments *Chlorella* cultivated in shakers for 3 days was used. The algae were washed twice on the centrifuge and eluted in M/300 KH_2PO_4 to a 1% suspension. This suspension was stored in the dark at room temperature awaiting the removal of each successive sample. The over-all storage time from the first to the last sample varied between 2 and 3 hours. From a given suspension a series of experiments was carried out; 5 ml was used for each sample. A modified "lollipop" with a second opening in the wider top part instead of an outlet in the bottom part was used. The flat part of the lollipop was surrounded by a water jacket, so as to maintain the temperature at 17°C. Bicarbonate and alcohol were injected into the suspension through the upper openings by a syringe, in order to kill the cells in the light.

After injection of 100% alcohol to the suspension (end concentration 80%), 100 λ was taken out in order to estimate the total fixation. The rest was centrifuged and washed three times with 20% alcohol. The residue was suspended in 5 ml of water; 100 λ of this suspension was used to determine the activity already fixed in insoluble material. The extract was concentrated in vacuum and chromatographed as usual. To analyze the phosphate areas the spots were cut out, eluted, dephosphorylated with purified polydase, and chromatographed again. In the following tables the activity is always expressed in percent of the total activity fixed. It is assumed that the loss in activity (10 to 25%) by evaporating down is not selective.

Results

In order to see how gradual killing by alcohol would change the distribution of activity, an alcohol concentration that would not stop photosynthesis immediately was injected together with $C^{14}O_2$. After 10 sec the reactions were stopped by adding a large amount of alcohol, to 80% concentration. As shown in the appropriate columns of Tables VI, VIII, and X, there is more PGA and less sugar phosphates under these conditions than in the control. Therefore if killing by alcohol changes the distribution of activity, PGA is favored.

KCN enters the cells very quickly, and in high concentrations inhibits most enzyme reactions. When KCN (end concentration M/10 to M/100) is added together with $C^{14}O_2$ in the light, and the algae are extracted after 10 sec illumination, the fixation is equivalent to 0.1 to 0.2 sec of normal photosynthesis. Therefore, KCN is particularly convenient for stopping CO_2 fixation. In

earlier experiments¹ it has been shown that light phosphorylation, even under these high KCN concentrations, continues unchanged at least for a few minutes. Thus, it seemed likely that the assimilation products can change even after KCN poisoning. It was hoped that some of the unstable products, split by the normal methods, would be transformed to more stable products during that period.

The following tables (Tables VI - XIII, one table per series of experiments) represent the results of several experiments in which normal short-time photosynthesis was stopped by different concentrations of KCN. In each experiment the conditions after the injection of KCN were different; either the light was turned off simultaneously with the addition of KCN or illumination was continued until the start of alcohol extraction after 10 to 30 seconds of contact with KCN.

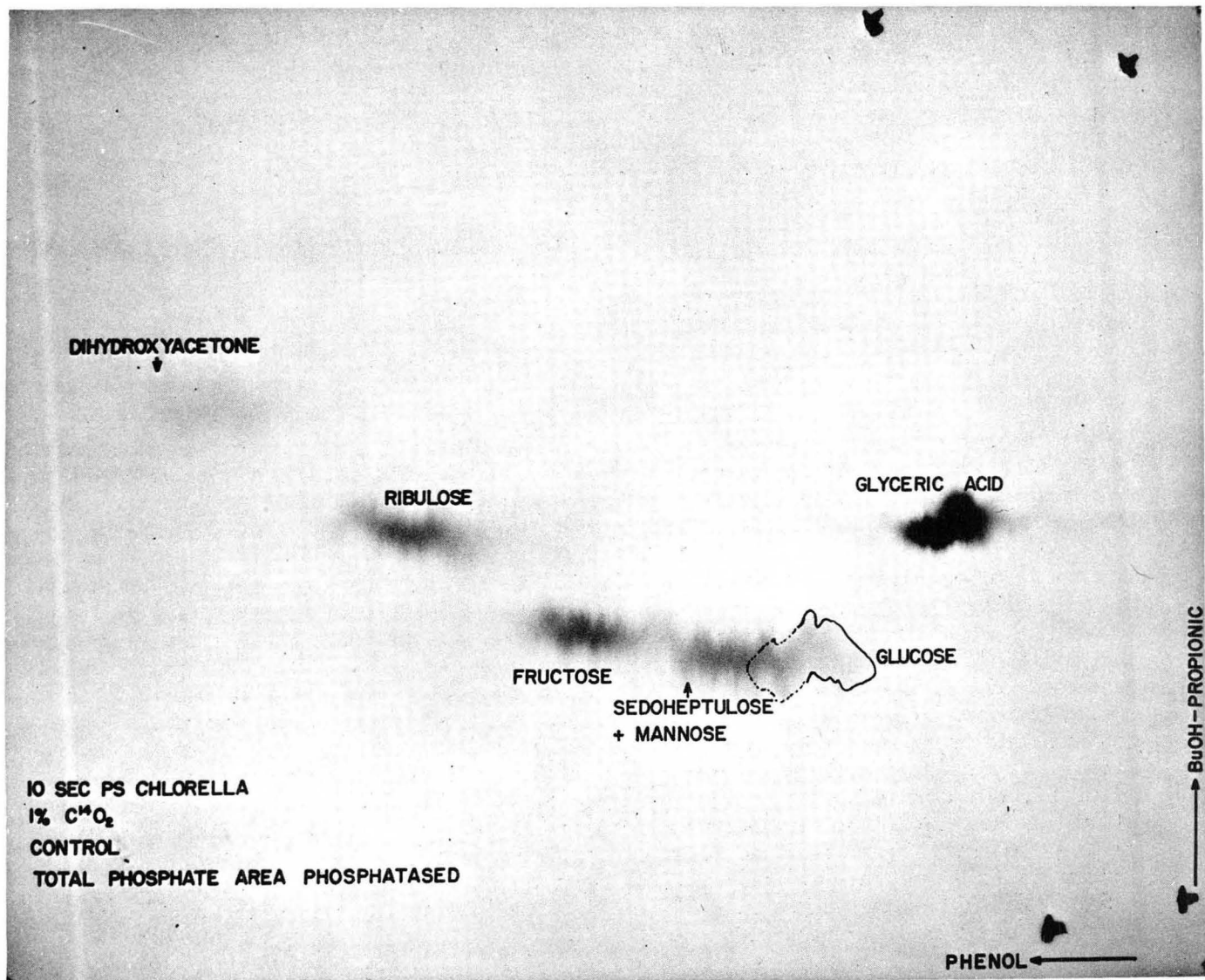
It can be seen in the tables that the PGA portion decreases strongly after KCN poisoning with illumination continued, whereas there is a large rise in the diphosphates. With the light turned off at the injection of KCN the distribution of activity is similar to that without KCN; the principal change has occurred in the acid fraction, which was more active.

The analysis of the diphosphate yielded two new spots besides the usual components (ribulose, fructose, sedoheptulose, and glucose), as shown in Figs. 1a and 1b. Also, on the chromatograms from samples without KCN, two corresponding spots could be detected, but here they never contain more than a fraction of 1% of the total activity.

When slightly acid buffer (pH 5.6) was used in paper electrophoresis, Spot I split into a mobile component (migrating like a monobasic acid) and a neutral component, whereas Spot II was entirely neutral. In alkaline buffer (pH 9.5 to 10.5) both spots moved like monobasic acids. After heating in weak acetic acid, Spot I moved to the position of Spot II on the chromatogram. It is likely that we are dealing with an acid lactone. When material from a 10-sec experiment is heated with newly prepared silver oxide, about 45% of the activity disappears after the first 10 min, and in the following hours there is only a gradual, but continuous, decrease of activity. The substance was found to be stable to heating in weak alkali or acid at 120°C for 1.5 hr, and its behavior on the chromatogram was not changed. There was no loss of activity, either. Attempts to show carbonyl groups by heating in a saturated HCl solution for 1.5 hr (120°C) were negative. There was no change in the chromatographic properties of the substances.

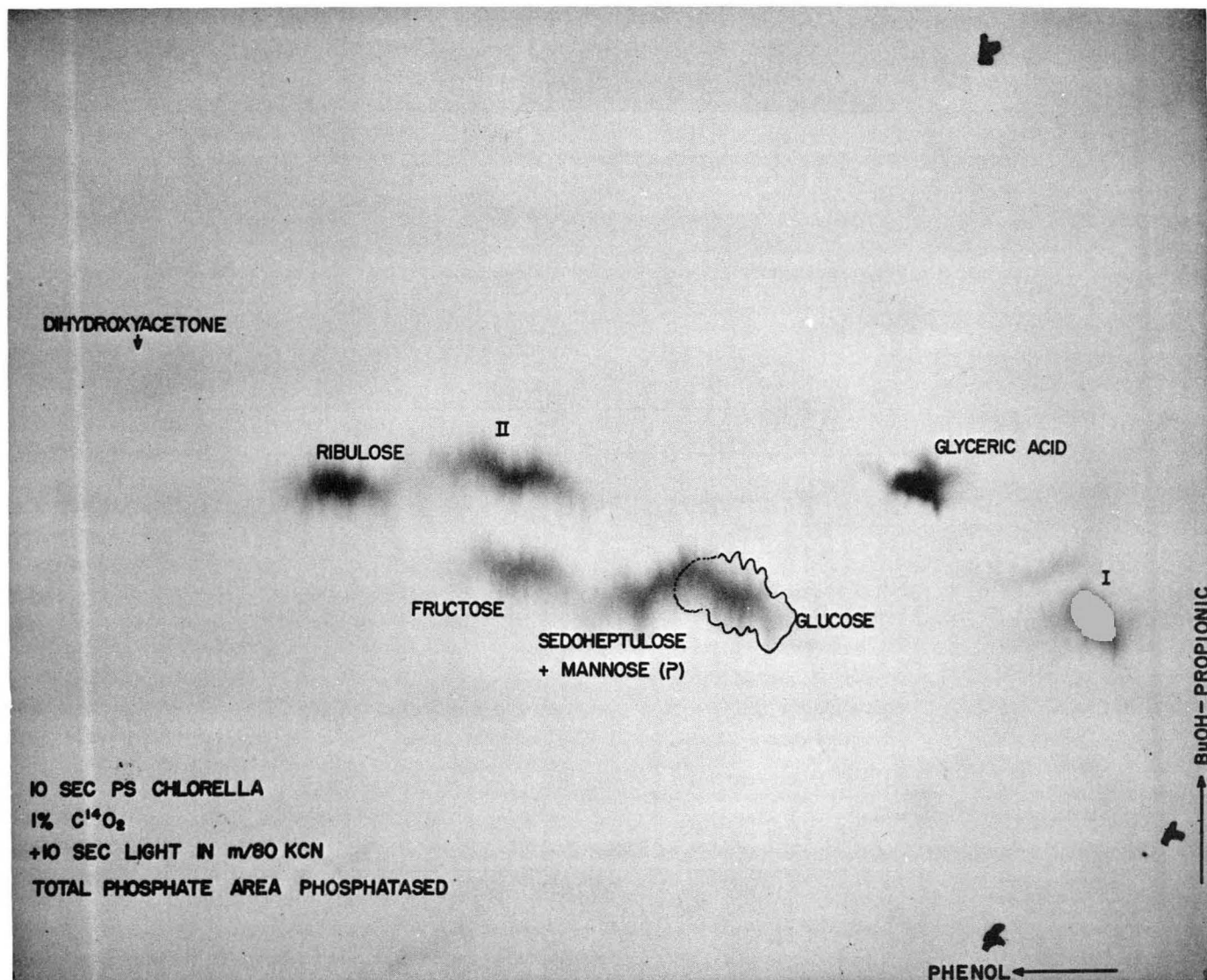
It seems likely that the unknown compound(s) is rather closely related to the early products of CO₂ fixation in algae.

¹O. Kandler, *Naturwissenschaften* 42, 390 (1955).



ZN-1689

Fig. 1a. Two-dimensional chromatogram of the phosphatased total-phosphate area from Experiment 1, Table XI. The outlined glucose area was defined by added carrier glucose on the paper.



ZN-1688

Fig. 1b. Two-dimensional chromatogram of the phosphatased total-phosphate area from Experiment 2, Table XI. The outlined glucose area was defined by added carrier glucose on the paper.

Table VI

Series N. * 1% suspension in M/300 KH_2PO_4 . 5 ml suspension per experiment. Light intensity 9000 foot candles, temperature 17°C . After 10 min preillumination 0.5% CO_2 in air, 100 μC $\text{NaHC}^{14}\text{O}_3$ (0.036 M) injected. Alcohol conc. for extraction 80%.

Column 1: Normal alcohol killing after 10 sec photosynthesis in C^{14}O_2 .
 Column 2: Together with C^{14}O_2 add 1 ml alcohol, and after 10 sec PS in C^{14}O_2 , alcohol killing.
 Column 3: After 10 sec PS in C^{14}O_2 add KCN to M/50 and further 10 sec light; alcohol killing.

(all numbers in % of total fixation)

	1 (II)**	2 (VI)	3 (VII)
Total fixation	485000	362000	630000
Insoluble	1.45%	0.5%	3.6%
PGA	46.0	78	10.1
Phosphoglycolic + phosphoenolpyruvate	2.2	--	0.5
Diphosphate	18.0	6.7	31.0
Hexose + Heptose monophosphate	24.5	9.1	46.0
Pentose Monophosphate	2.2	--	1.5
Triose Monophosphate	2.8	--	2.6
Malic Acid	5.4	4.1	3.3
Organic Acids + Amino Acids	0.2	2.0	1.5

* Series: identifies group of chromatograms.

** Roman numerals in columns identify individual chromatogram (experiment) in a series.

Table VII

Series O: General conditions as in Table VI.

- Column 1: Preillumination in N_2 ; after 10 sec PS in $C^{14}O_2$, normal alcohol killing.
 Column 2: Preillumination in N_2 ; after 10 sec PS in $C^{14}O_2$, add KCN to M/30 and further 10 sec light, alcohol killing.
 Column 3: Preillumination in N_2 ; after 10 sec PS in $C^{14}O_2$, add KCN to M/30 and alcohol killing simultaneously.
 Column 4: Preillumination in 0.5% CO_2 in air; after 10 sec PS in $C^{14}O_2$ add KCN to M/30 and alcohol killing simultaneously.
 Column 5: Preillumination in .5% CO_2 then 30 sec N_2 , then 10 sec PS in $C^{14}O_2$, add KCN to M/30 and alcohol killing simultaneously.

(All numbers in % of total fixation)

	1 (I)	2 (II)	3 (III)	4 (V)	5 (VI)
Total fixation	440000	560000	450000	510000	580000
Insoluble	0.3%	1.1%	0.3%	1.3%	0.5%
PGA	49.5	3.9	64.0	38.0	52.0
Phosphoglycolic + phosphoenolpyruvate	3.5	1.2	5.2	1.3	1.8
Diphosphate	6.0	58	5.5	8.4	8.0
Hexose + Heptose monophosphate	23.0	29.0	11.7	49.5	37.0
Pentose monophosphate	1.5	1.0	--	0.4	0.4
Triose monophosphate	0.4	--	--	0.9	
Malic Acid	4.0	4.0	10.0	0.4	
Aspartic Acid	7.2	1.0	1.6		1.0
Alanine	2.5	1.0	0.3	0.4	
Organic Acids + Amino Acids	1.2	1.0	0.5	0.2	

SUMMARY

PGA	49.5	3.9	64.0	37.5	52.0
Sugar (I + II)	31.2	88	17.5	60.3	45.9
I + II	0.11	56.0	2.8	4.0	
Acids	18.4	8.2	16.6	2.3	2.8

% of Diphosphate

Glyceric Acid	7.0	0.27	7.1	3.9	
I + II	1.9	97.0	52.0	48.0	
Pentose	19.0	0.4	--	--	
Fructose	49.0	1.2	23.3	26.0	
Heptose + Glucose	21.0	1.1	17.3	22.0	

Table VIII

Series P: General conditions as in Table VI.

- Column 1: Preillumination in 0.5% CO₂ + air; after 10 sec PS in C¹⁴O₂ normal alcohol killing.
- Column 2: Preillumination in 0.5% CO₂ + air; after 10 sec PS in C¹⁴O₂ add KCN to M/100 and further 10 sec light; alcohol killing.
- Column 3: Preillumination in 0.5% CO₂ + air; with C¹⁴O₂ add KCN to 2·10⁻³M after 10 sec PS in C¹⁴O₂, alcohol killing.
- Column 4: Preillumination in 0.5% CO₂ + air; after 10 sec PS C¹⁴O₂ add KCN to M/100 and after 1 sec alcohol killing.
- Column 5: Preillumination in 0.5% CO₂ + air; with C¹⁴ add alcohol to 25%, after 10 sec PS in C¹⁴O₂, alcohol killing.

(all numbers in % of total fixation)

	1 (I)	2 (II)	3 (III)	4 (IV)	5 (V)
Total fixation	230000	390000	220000	970000	158000
Insoluble	0.65%	3.5%	0.68%	1.6%	~1.0
PGA	45.2	15.3	39.0	21.5	53.0
Phosphoglycolic + phosphoenolpyruvate	~1.0	1.5	--	3.6	1.6
Diphosphate	13.7	28.0	14.0	20.5	10.3
Hexose + Heptose monophosphate	35.0	48.0	43.0	39.0	30.0
Pentose monophosphate	3.4	1.65	3.1	3.7	4.0
Tiose monophosphate					
Organic acids + amino acids	~2.0	~2.0	--	10.9	2.2

SUMMARY

PGA	45.2	15.3	39.0	21.5	53.0
Sugars (I + II)	52.0	81.3	60.8	62.8	45.0
I + II	--	14.0	4.8	?	?
Acids	3.0	3.5		14.5	3.8

Table IX

Series R: General conditions as in Table VI.	
Column 1:	Preillumination in N ₂ ; after 10 sec PS in C ¹⁴ O ₂ add KCN to M/50 and further 10 sec light, alcohol killing.
Column 2:	Preillumination in N ₂ ; after 10 sec PS in C ¹⁴ O ₂ add KCN to M/50 and further 10 sec dark, alcohol killing.
Column 3:	Preillumination in N ₂ ; after 10 sec PS in C ¹⁴ O ₂ add KCN to M/50 and further 1.5 sec light, alcohol killing.
Column 4:	Preillumination in N ₂ ; after 10 sec PS in C ¹⁴ O ₂ add KCN to M/50, 10 sec dark and again 10 sec light before alcohol killing.

(all numbers in % of total fixation)

	1 (II)	2 (III)	3 (IV)	4 (V)
Total fixation	500000	520000	440000	650000
Insoluble	2.3%	1.0%	0.6%	3.1%
PGA	24.0	48.0	52.0	3.5
Phosphoglycolic + phosphoenolpyruvate	2.0	1.6	2.0	2.8
Diphosphate	22.0	6.1	13.0	18.0
Hexose + Heptose monophosphate	32.0	22.5	18.0	33.0
Pentose monophosphate	3.0	1.1	0.8	1.5
Triose monophosphate	4.0		4.8	
Malic acid	0.7	1.1	1.5	2.0
Aspartic Acid	0.6	0.7	0.5	2.0
Alanine	3.6	6.8	3.5	17.0
Organic acids + amino acids	~5.0	~11.0	~3.5	17.2

SUMMARY

PGA	24.0	48.0	52.0	3.5
Sugar (I + II)	64.0	30.7	37.2	55.6
I + II	2.4	0.3	0.15	10.0
Acids	11.9	21.2	11.0	41.0

% OF DIPHOSPHATE

Glyceric	1.3	6.5	3.0
I + II	6.7	6.5	1.8
Pentose	32.0	46.0	13.0
Fructose	38.0	19.0	61.0
Glucose + Heptose	21.0	22.0	15.0

Table X

Series T: In experiments 2, 4, and 6 injection of 8% alcohol (end conc.) after 10 min preillumination in 0.5% CO₂ and air and 2 min before adding C¹⁴O₂. Killing after 8, 16, or 30 sec in normal way with 80% alcohol.

Column 1: 8 sec PS
 Column 2: 8 sec PS, alcohol-poisoned
 Column 3: 16 sec PS
 Column 4: 16 sec PS, alcohol-poisoned
 Column 5: 30 sec PS
 Column 6: 30 sec PS, alcohol-poisoned

(All numbers in % of total fixation)

	1 (I)	2 (IV)	3 (II)	4 (V)	5 (III)	6 (VI)
Total fixation	260000	135000	530000	330000	1050000	640000
Insoluble	0.7%	1.65%	1.23%	2.7%	2.2%	4.25%
PGA	40.0	67.0	29.0	44.5	29.0	40.0
Phosphoglycolic + phosphoenolpyruvate	3.3	3.0	3.6	2.3	2.4	3.2
Diphosphate	6.8	7.0	6.1	10.0	5.8	10.2
Hexose + Heptose monophosphate	42.0	21.6	55.0	33.0	51.0	34.0
Pentose monophosphate	2.0	1.2	1.6	1.2	1.1	2.1
Triose monophosphate	4.3		1.85	4.7	1.6	2.5
UDPG	--		1.0	0.5	2.2	2.0
Sucrose	--		--		0.6	--
Malic Acid	0.8	0.25	0.8	0.3	0.5	0.7
Aspartic Acid	--	--		--	--	--
Alanine		--	0.9	--	1.0	--
Organic acids	~0.5	0.6	~0.5	0.2	1.0	~0.5
Amino acids	~1.0		~0.3	0.5	0.5	~0.5
% OF DIPHOSPHATES						
Glyceric	5.3	2.0	4.5	1.5	4.2	2.0
Pentose	57	67	44.0	72.0	62.0	64.0
Fructose	26	25	31.0	20.0	21.5	26.0
Heptose: approx.:	10.0	5.0	18.5	3.0	11.0	3.0
Glucose: approx.:	2.7	4.0	2.5	3.0	2.0	5.0

Table XI

Series S: Conditions as in Table VI. All samples preilluminated for 7 min under N_2 .

Column 1: After 10 sec PS in $C^{14}O_2$, normal alcohol killing.

Column 2: After 10 sec PS in $C^{14}O_2$ add KCN to M/80 and further 10 sec light, alcohol killing.

Column 3: After 10 sec PS in $C^{14}O_2$ add KCN to M/80 and further 10 sec dark, alcohol killing.

Column 4: After 10 sec PS in $C^{14}O_2$ add KCN to M/80 and further 1 sec dark, alcohol killing.

(all numbers in % of Total fixation)

	1 (I)	2 (II)	3 (III)	4 (V)
Total fixation	300000	360000	320000	320000
Insoluble	3.5%	8.5%	6.4%	5.0%
PGA	46	12.6	41.0	46.0
Phosphoglycolic + phosphoenolpyruvate	2.0	2.2	3.5	4.0
Diphosphate	11.5	28.0	12.0	12.5
Hexose + Heptose monophosphate	25.0	29.0	20.0	19.0
Pentose monophosphate	2.6	1.7	1.6	0.5
Triose monophosphate	4.5	1.8		1.3
UDPG	0.6	1.6	0.5	1.0
Malic Acid	3.0	9.2	9.5	7.5
Aspartic Acid	1.2	3.0	3.5	2.0
Alanine	0.4	2.4	1.6	0.5
Organic acids + amino acids	0.5	1.0	2.0	0.5
SUMMARY				
PGA	46	12.6	41.0	46.0
Sugar (I + II)	47.7	70.6	40.5	39.3
I + II	--	17.5	6.0	4.7
Acids	7.0	17.8	20.1	14.5
% OF DIPHOSPHATE				
Glyceric	10	0	6.0	0.8
I + II	--	62.3	50.0	39.3
Pentose	71	32	37.0	52.0
Hexose + Heptose	19	5.3	7.4	8.5

Table XII

Series U: General conditions as in Table VI; 8 min preillumination in 0.5% CO₂ in air.

- Column 1: After 7 sec PS in C¹⁴O₂, normal alcohol killing.
 Column 2: After 7 sec PS in C¹⁴O₂, add KCN to M/80 and further 30 sec dark, alcohol killing.
 Column 3: After 7 sec PS in C¹⁴O₂, add KCN to M/80 and further 30 sec light, alcohol killing.
 Column 4: After 7 sec PS in C¹⁴O₂, add KCN to M/80 and further 30 sec dark followed by 30 sec light, alcohol killing.
 Column 5: After 40 sec PS in C¹⁴O₂, normal alcohol killing.
 Column 6: After 40 sec PS in C¹⁴O₂, add KCN to M/80 and further 30 sec light, alcohol killing.
 Column 7: After 40 sec PS in C¹⁴O₂, add KCN to M/80 and further 30 sec dark, alcohol killing.
 Column 8: After 40 sec PS in C¹⁴O₂, add KCN to M/80 and further 30 sec dark, followed by 30 sec light, alcohol killing.

(all numbers in % of total fixation)

	1 (I)	2 (II)	3 (III)	4 (IV)	5 (V)	6 (VI)	7 (VII)	8 (VIII)
Total fixation	252000	325000	575000	420000	1280000	1570000	2150000	780000
Insoluble	2.0%	3.2%	8.3%	4.8%	3.5%	14%	8.3%	17.8%
PGA	60	40.0	13.5	4.2	24.0	5.8	13.0	7.2
Phosphoglycolic + phosphoenolpyruvate	1.5	1.5	0.8	0.4	2.0	0.65	1.4	1.0
Diphosphate	4.5	0.8	16.0	13.5	6.0	22.0	4.8	1.0
Hexose + Heptose monophosphate	30.5	17.5	40.5	15.0	56.0	34.0	40.0	17.3
Pentose monophosphate	0.8	0.5	0.7	0.4	1.0	1.2	0.8	0.7
Triose monophosphate	0.7	0.3	0.6	0.4	1.4	0.9	0.5	0.5
UDPG	0.1	0.6	4.2	2.0	3.1	4.0	2.7	5.5
Malic Acid	0.5	5.5	3.1	8.8	0.4	4.2	4.0	7.4
Aspartic Acid	0.1	4.70	2.5	5.1	0.7	3.2	3.2	4.1
Alanine	0.7	14.0	5.1	24.0	1.3	5.5	11.0	8.3
Organic Acids	0.2	9.0	3.3	20.0	0.2	3.5	6.5	6.0
Amino Acids	--	2.0	2.5	3.0	1.5	0.5	2.5	2.0
Sucrose	--	0.25	0.5	0.5	0.7	3.0	2.0	2.8
SUMMARY								
PGA	60.0	40.0	13.5	4.2	24.0	5.8	13.0	7.2
Sugar (I + II)	38.6	23.1	70.8	36.6	71.7	79.1	59.1	63.1
I + II	--	--	6.0	5.4	--	11.0	?	2.7
Acids	2.5	36.7	17.3	61.0	6.1	17.0	28.6	28.8

Table XIII

Series V: General conditions as in Table VI. Preillumination 10 min in 0.5% CO₂ in air.

Column 1: After 5 sec PS in C¹⁴O₂ normal alcohol killing.
 Column 2: After 5 sec PS in C¹⁴O₂ add KCN to M/50 and further 20 sec light, alcohol killing.
 Column 3: After 10 sec PS in C¹⁴O₂ normal alcohol killing.
 Column 4: After 10 sec PS in C¹⁴O₂ add KCN to M/50 and further 20 sec dark, alcohol killing.
 Column 5: After 10 sec PS in C¹⁴O₂ add KCN to M/50 and further 20 sec dark, alcohol killing.
 Column 6: After 10 sec PS in C¹⁴O₂ add KCN to M/50 and further 20 sec dark followed by 20 sec light, alcohol killing.
 Column 7: After 40 sec PS in C¹⁴O₂ normal alcohol killing.
 Column 8: After 40 sec PS in C¹⁴O₂ add KCN to M/50 and further 20 sec light, alcohol killing.
 Column 9: After 40 sec PS in C¹⁴O₂ add KCN to M/50 20:sec dark, alcohol killing.
 Column 10: After 40 sec PS in C¹⁴O₂ add KCN to M/50, 20 sec dark, 20 sec light, alcohol killing.

(all numbers in % of total fixation)

	1(I)	2(IV)	3(II)	4(V)	5(VII)	6(VIII)	7(III)	8(VI)	9(IX)	10(X)
Total fixation	310000	550000	720000	880000	830000	900000	1530000	1250000	1300000	1350000
Insoluble	0.5%	3.8%	0.8%	9%	1.8%	6.7%	5.7%	8.7%	7.1%	8.9%
PGA	66.0	11.0	49	4.8	47.5	9.8	28.5	14.3	30.0	6.9
Phosphoglycolic + phosphoenolpyruvate	1.5	2.1	2.9	1.4	5.0	3.0	3.3	3.0	3.5	2.0
Diphosphate	6.5	35.0	8.3	30.0	1.7	19.0	7.2	26.8	2.2	9.5
Hexose + Heptose monophosphate	24.0	31.0	35.0	35.0	27.0	36.3	47.0	30.5	42.0	32.0
Pentose monophosphate	0.7	1.2	1.5	1.7	0.5	0.9	1.1	1.9	0.4	0.9
Triose monophosphate	0.25	1.3	0.9	1.7	0.3	1.1	0.7	2.4	0.45	0.8
UDPG	0.1	2.1	0.7	3.6	1.1	3.0	3.0	2.7	2.9	5.5
Sucrose	--	0.5	0.2	1.2	0.4	1.2	0.8	1.0	1.4	3.7
Malic Acid	0.1	4.8	0.3	4.0	0.4	4.0	0.5	3.1	0.4	5.8
Aspartic Acid	--	1.5	0.15	1.1	0.4	--	0.3	1.1	0.4	2.2
Alanine	0.3	4.0	0.3	2.6	8.6	9.5	1.0	2.8	5.2	13.3
Organic Acids	~0.1	1.5	~0.2	~2.5	~4.0	~3.5	0.5	0.8	1.5	6.0
Amino Acids	~0.1	~0.3	~0.1	~1.5	~1.5	~1.5	1.5	2.0	0.5	2.5
SUMMARY										
PGA	66.0	11.0	49.0	4.8	47.5	9.8	28.5	14.3	30.0	6.9
Sugar (I + II)	32.0	74.9	47.4	82.2	32.8	69.2	65.5	74.0	56.4	61.3
I + II		25.0		26.0	0.6	20.0	--	4.3	1.25	5.2
Acids	2.1	14.2	3.9	13.1	19.9	21.5	7.1	12.8	11.5	31.8

RELATIVE RADIOACTIVITIES OF CHLOROPHYLL a
AND CHLOROPHYLL b FROM PHOTOSYNTHETIC STUDIES

Jan Anderson and Ulrich Blass

The study of the relative radioactivities of chlorophyll a and b from *Scenedesmus* following feeding of $C^{14}O_2$ has been continued. The methods of photosynthesis, extraction, and chromatography are similar to those previously described.¹

The visual separation of labeled chlorophyll a and b on paper chromatograms appeared satisfactory, but when the zones were counted and radioautographs taken to check the distribution of the radioactivity in comparison with the colored zones of chlorophyll a and b, the radioactivity showed one long streak, with no separation corresponding to the blank area on the paper separating the colored zones of a and b. Since chlorophyll a, or a degradation product of it, was tailing into b, no reliability could be placed on the specific activities obtained in earlier experiments.

To overcome this difficulty the experiment was done by separating chlorophyll a and b by column chromatography, checking the concentration of each fraction, and determining the activity of spectrophotometrically pure chlorophyll a and chlorophyll b, which possess distinct and characteristic visible spectra. The results indicated that the specific activities of a and b were similar.

Columns Used

Cellulose column (solvent: petroleum ether) resulted in elution of carotenoids, followed by chlorophyll a and later b. A reverse phase was obtained by using polyethylene columns (solvent: 85% methanol), in which chlorophyll b preceded a. Both columns were used in each experiment to cross-check the activities obtained.

Paper chromatograms of spectrophotometrically pure chlorophyll a and b were made. In the radioautographs obtained from chlorophyll a chromatograms, a long streak of radioactivity was obtained extending below the colored a zone (into the region where chlorophyll b would be located). Radioautographs from chlorophyll b chromatograms showed no activity corresponding to the colored b zone; all the activity was present at the origin. This means either that decomposition of the chlorophylls is occurring on the paper, or that the spectrophotometrically pure fractions of a and b obtained from columns may be contaminated by colorless degradation products; both seem to be true.

Further refinement of paper chromatography methods are being investigated, by use of nitrogen-filled chambers in the cold, and also by reverse-phase circular chromatography on paraffin-impregnated paper.²

¹ Jan Anderson, in Chemistry Division Quarterly Report, UCRL-3629, Jan. 1957, p. 39.

² Angkapindu, Kaplan, Silberman, and Tantivataa, Arch. Biochem. Biophys., in press.
Calvin

PHYSIOLOGY OF CHLORELLA GROWN IN HEAVY WATER

Vivian Moses and Osmund Holm-Hansen

As reported in the previous quarterly reports, attempts have been in progress to obtain *Chlorella* grown in deuterium oxide as the sole source of hydrogen. By use of techniques (described earlier) of serial subculture in media containing increasing concentrations of heavy water, cells have now been obtained which grow well in 60% D₂O.

Growth as a Function of D₂O Concentration

Cells were taken from one of the tube cultures in progress in the laboratory, passed through a medium containing 35% D₂O, and then subcultured four times in media containing 60% D₂O; The media had otherwise the same chemical constitution as in earlier work. Such cells were used to inoculate media having a graded D₂O content ranging from 2.3% to 98.5% D₂O. A 2-ml sample of cell suspension was used to inoculate 50 ml of medium. The cells were shaken at 25°C for 4 days and aerated in series with air containing 4% CO₂, the gas mixture entering the series at the flask containing the highest D₂O concentration and emerging at that with the lowest.

The 2 ml of inoculum contained 4.9 mg dry weight of cells having a packed-cell volume of 20 μ l, and containing 16.1×10^6 cells. The optical density of the media immediately after inoculation was 0.085. After growth, measurements were made of the packed-cell volume, dry weight, optical density, cell number, and average cell volume (Table XIV).

Table XIV

Growth of <i>Chlorella</i> in D ₂ O					
% D ₂ O	Packed-cell volume (μ l)	Optical density	Dry wt (mg)	Total number of cells ($\times 10^{-6}$)	Cell volume (μ l/ 10^8 cells)
2.3	234	0.360	49.0	4310	5.4
10.0	273	0.375	46.9	4390	6.2
20.0	221	0.350	43.0	4230	5.2
30.0	195	0.350	42.8	3860	5.1
40.0	221	0.325	39.9	3450	6.4
50.0	169	0.285	33.2	2350	7.2
60.0	130	0.215	40.6	1850	7.0
70.0	104	0.175	22.5	750	13.9
80.0	91	0.110	15.3	160	56.9
90.0	63	0.075	9.4	140	45.0
98.5	78	0.070	20.2	150	52.0

Comparison can be made with a similar curve constructed earlier, using as inoculum cells grown in H₂O. It can be seen that previously (with H₂O-grown cells) growth declined slowly up to 33% D₂O, followed by a precipitate drop at higher D₂O concentrations. In the series reported here, however, the fall in rate of growth was more gradual over the whole range.

Calvin

The cell volume, which previously rose rapidly at 44% and higher D₂O concentrations, has remained low and fairly constant until 70% D₂O. Thus serial growth in D₂O had rendered the cells more immune to the toxic action of heavy water exhibited earlier, but had not impaired their ability to grow when they were returned to H₂O containing no deuterium.

Photosynthesis

Replicate flasks were set up in the above experiment for growing cells in 2.3%, 20%, 40%, and 60% D₂O. These cells were washed and re-suspended in their corresponding D₂O/H₂O mixtures at a cell concentration of 0.17 ml of packed cells in 10 ml of water. The cells were flushed with air + 0.6% CO₂ in the light for 30 min and were then allowed to photosynthesize in the presence of C¹⁴O₂ (7.5 x 10⁶ cpm) for 6 min. The cells were killed and extracted with hot ethanol by standard procedures; aliquots of the extracts were assayed for total fixed radioactivity and others were chromatographed. The total fixation of C¹⁴O₂ for cells grown and suspended in 2.3%, 20%, 40%, and 60% D₂O were 415,000, 1,108,000, 348,000, and 67,000 cpm respectively. Counts were made on the paper chromatograms of the relative activities in certain compounds (Table XV).

Table XV

Influence of D₂O concentration on plant biochemistry

Compound	D ₂ O Concentration			
	2.3%	20%	40%	60%
	cpm in each compound			
Fumaric acid	450	2,400	--	--
Glycolic acid	100	550	--	--
Malic acid	2,160	10,750	6,500	3,200
Citric acid	140	2,475	1,560	615
Alanine	2,355	6,700	875	285
Glutamic acid	700	8,700	5,775	865
Aspartic acid	3,720	6,000	4,800	1,170
Glycine and serine	535	1,035	--	--
Sucrose	2,635	1,070	--	--
Phosphoglyceric acid	3,700	650	100	70
Monophosphates	4,900	915	175	100
Diphosphates	1,850	825	--	--
Glutamine	--	17,500	3,225	490
Citrulline	--	12,460	2,600	400
Unidentified 1	--	10,963	1,470	--
Unidentified 2	--	2,390	--	--
Unidentified 3	--	2,575	825	185

Positions of unidentified spots:

1. Level with glutamate in phenol; level with sucrose in butanol-propionic acid.
2. Behind leucine in phenol; level with leucine in butanol-propionic acid.
3. Level with glutamine in phenol; behind glutamine in butanol-propionic acid.

Calvin

In general, cells grown in D_2O showed lower activity than H_2O -grown cells in sucrose and sugar phosphates, and higher activities in amino and organic acids. Cells grown in D_2O also showed activity in three unidentified substances (one heavily labeled) and heavy activity in glutamine and citrulline; none of these substances was visible in cells grown in H_2O . This pattern of $C^{14}O_2$ incorporation suggests that cells grown in D_2O have an impaired photosynthetic CO_2 fixation mechanism, but can assimilate CO_2 rapidly in dark-reaction mechanisms.

Deuterium Content of Algae Grown in Heavy Water

One liter of medium containing 60% D_2O was inoculated with 110 ml of cell suspension containing cells with a previous history of several passages through 60% D_2O media. The flask was flushed with air + 4% CO_2 for 6 days on a shaker assembly.

The cells were centrifuged to form a stiff paste. A sample of the supernatant was distilled in vacuo and the water condensed in a receiver chilled in liquid nitrogen for determination of the D_2O content. The packed cells were lyophilized; the water distilling off again was trapped in a chilled receiver. The dried cells (1.85 g) were combusted and the resultant water collected. Measurements of the hydrogen content of these three samples were performed on the nuclear magnetic resonance machine (Table XVI).

Table XVI

Deuterium concentration in cells grown in D_2O		
Sample	H_2O concentration (%)	D_2O concentration (%)
Medium (extracellular water)	36.3	63.7
Intracellular water	36.6	63.4
Combusted cells	30.2	69.8

These results show that the intracellular water is in equilibrium with the extracellular water, but the cells tend to some extent to bind deuterium in preference to hydrogen.

Work is presently in progress:

1. To compare in detail the photosynthetic patterns on cells grown and suspended in various H_2O - D_2O mixtures.
2. To attempt to adapt the cells to grow in concentrations of D_2O higher than 60%.

At present it has been found that cells transferred from 60% D_2O to 90% D_2O will grow for one subculture but not in the second subculture. However, there is some evidence that growth might be possible for several transfers through 80% D_2O . At present, although such cells show an unhealthy appearance

(turbidity and yellowish color), growth is nevertheless taking place. By use of heavy inocula to transfer from one culture to the next it may prove possible to select strains capable of growing in the presence of still more deuterium and less hydrogen.

EFFECT OF MANGANESE DEFICIENCY ON CO₂ METABOLISM IN NOSTOC

Osmund Holm-Hansen

A promising approach to the study of the metabolic function of microelements in algal physiology is afforded by following the pathway of radioactive substances in normal and deficient algae. A deficiency of manganese would be expected to be reflected by profound alterations in the CO₂ metabolism, as Mn is known to activate many reactions involved in glycolysis and organic acid metabolism.¹ A deficiency of molybdenum, on the other hand, would be expected to show more changes in the amino acid composition rather than in the carbohydrate metabolism.² The extent of the metabolic changes brought about by a deficiency of an essential microelement is strongly correlated to the degree of deficiency of the element in question. It is therefore important in interpreting results to indicate whether the deficiency was slight or marked, as reflected by the centrifuged cell pack or dry weight. Representative data (Table XVII) indicate the over-all growth effects of Mo and Mn deficiency in Nostoc and Scenedesmus; it is to be noted that no requirement has been shown for Zn or Cu, while the Co deficiency for Nostoc (Exp. II) is questionable.

The Mn-deficient and the control Nostoc from Exp. I were allowed to photosynthesize for 6 minutes with radioactive bicarbonate, by the standard procedures of the laboratory. The results are shown in Table XVIII. The most striking results were, as expected, in the marked lowering of the activity incorporated into the organic phosphate compounds.

A problem closely related to this is the demonstration by Pirson and Bergmann³ that Mn-deficient Scenedesmus was not able to utilize glucose efficiently in the light, while it was able to do so in darkness. This has been tested with Scenedesmus, by use of C¹⁴-labeled glucose; the results are shown in Table XIX. In both the light and the dark experiments, the algae were shaken with the glucose for 4 minutes before being killed with ethanol. It does appear that in the presence of light, Mn-deficient Scenedesmus was less able to utilize glucose than when in complete darkness, but this will have to be further tested in more experiments.

Some work has been done on the effect of Mo deficiency on CO₂ incorporation, but these experiments require further verification. At the present time efforts are being made to obtain more marked deficiencies of Mo and Mn in Nostoc and Scenedesmus, with the expectation that clearer differences in carbon metabolism will be noted with increasing severity of the microelement deficiency.

¹W. D. McElroy and A. Nason, *Ann. Rev. Plant Physiol.* 5, 1 (1954).

²E. J. Hewitt, *ibid* 2, 25 (1951).

³A. Pirson and L. Bergmann, *Nature* 176, 209 (1955).
Calvin

Table XVII

Effect of Mn and Mo deficiency on the growth of <u>Nostoc</u> and <u>Scenedesmus</u>						
Micro-element omitted	Experiment I <u>Nostoc</u>		Experiment II <u>Nostoc</u>		Experiment III <u>Scenedesmus</u>	
	Centrifuged cell pack (ml)	Dry wt (mg)	Centrifuged cell pack (ml)	Dry wt (mg)	Centrifuged cell pack (ml)	Dry wt (mg)
Mn	0.08	---	0.88	---	0.02	---
Mo	0.20	19.6	0.18	16.4	0.37	73.5
Co	0.24	29.2	0.20	28.2	---	---
Cu	0.20	29.7	0.29	29.7	---	---
Zn	0.22	27.4	0.33	25.9	---	---
Mn, Mo, Co, Cu and Zn	0.07	4.7	0.07	4.0	---	---
Control	0.25	29.4	0.31	23.6	0.45	89.5

Table XVIII

Effect of Mn deficiency on photosynthesis on <u>Nostoc</u>		
	Control	Mn-deficient
Total activity fixed per ml cells (cpm)	5,150,000	240,000
% of activity in solution	33%	95%
Total cpm per ml cells found in:		
Aspartic acid	45,000	20,700
Malic acid	30,200	6,900
Phosphates	790,000	78,300
Sucrose	74,000	21,600
Alanine	18,800	6,970
Citrulline	53,800	25,500
Glucose cyclic phosphate	88,700	4,280

Table XIX

Effect of Mn deficiency on the ability of *Scenedesmus* to utilize glucose in light and in dark (expressed in cpm per ml cells).

Compound	Light		Dark	
	+Mn	-Mn	+Mn	-Mn
UDPG	128,000	---	400,000	1,120,000
Hexose-Mono-P	203,000	44,800	603,000	1,800,000
PGA	136,000	11,700	213,000	524,000
PEP	15,300	---	17,900	62,300
Aspartic acid	64,800	59,600	54,600	87,700
Unknown A	123,000	53,800	130,000	51,600
Unknown B	---	---	29,200	101,000
Glutamic acid	---	---	---	62,500
Malic acid	10,300	---	---	15,600
Citric acid	8,300	---	---	30,200
Alanine	---	---	---	57,200
Unknown C	present	present	present	101,000

CAROTENOIDS IN ALGAE IN LIGHT AND DARK

Ulrich Blass

We continued the comparison of carotenoid concentrations in algae that were exposed to light and dark, respectively.¹ Earlier experiments of this kind showed that in the dark all the carotenoid concentrations in Chlorella are higher than in the light, especially for violaxanthine. In these earlier investigations, we always used exposure times of 30 min to light and to dark. The results led to suggestions concerning the role of the carotenoids as oxygen carriers in photosynthesis and called for further examination.

New experiments were for the following purposes: (a) to find a better separation method for determination of concentration of the carotenoids in algae, especially separation of the pairs $\alpha + \beta$ -carotene and lutein + zeaxanthine; (b) to compare the data from Chlorella with those from Scenedesmus; and (c) to find the shortest exposure time in which the carotenoid concentrations yield distinct differences in light and dark.

To solve these problems we used essentially the same methods as described formerly. The better separation proved to be the most difficult to achieve. A better chromatographic separation can be made with stronger adsorbents; with longer chromatographic columns (i. e., more adsorbent); and by a slower movement of the solvent. The sensitivity and instability of the algae pigments, to the contrary, call for a very fast separation, i. e., less and weaker adsorbents, a faster-moving solvent. In this respect all attempts to separate the pairs of the carotenes and xanthophylls proved to be too slow; e. g., a separation of the carotenes on calcium hydroxide in petroleum ether gave much smaller over-all concentration figures than on weaker adsorbents (polyethylene), where the α -carotene cannot be separated from β -carotene. This shows that the pigments are partly destroyed on calcium hydroxide. For similar reasons we have not yet succeeded in a sufficient separation of zeaxanthine from lutein.

First experiments to attack Points 2 and 3 together were concerned with a comparison of the pigments in Scenedesmus algae that had been exposed for 15 minutes to light and dark, respectively. Unfortunately, the algae samples already showed qualitatively very different pigments, depending on whether their origin was in the shaker flask or the continuous-culture tube (the latter algae show some odd pigments of pink and green color). Data from these experiments are not, therefore, conclusive.

Recent checking tests showed that the main difficulties can be overcome by washing the polyethylene with EDTA. It should now be possible to get the desired information and to extend the investigations on radioactive pigments.

¹Ulrich Blass, in Chemistry Division Quarterly Report, UCRL-3629, Jan., 1957, p. 34.

STUDY OF THE INHIBITION
OF AZASERINE AND DIAZA-OXO-NORLEUCINE (DON)
ON THE ALGAE SCENEDESMUS AND CHLORELLA

Petronella Y. F. van der Meulen

Introduction

In experiments on azaserine inhibition on Scenedesmus during photosynthesis with $C^{14}O_2$,¹ the inhibitor was found to effect many changes in the metabolic intermediates. The transamination reactions were given as a possible site of inhibition. The work has been extended, and this report presents a study on the inhibition of both azaserine and diaza-oxo-norleucine (DON) on the algae Scenedesmus and Chlorella.

Discussion

Four combinations have been investigated:

Scenedesmus and azaserine inhibition,

Scenedesmus and DON inhibition,

Chlorella and azaserine inhibition,

Chlorella and DON inhibition.

On Scenedesmus the effects of azaserine and DON are largely the same: a decrease of amino acids (e. g., aspartic acid, glutamic acid, alanine, and serine), and a build-up of glutamine and of α -ketoglutaric, citric, malic, lactic, fumaric, and succinic acids.

Lower activity was found in the diphosphate area (mainly ribulose diphosphate) of the DON-inhibited Scenedesmus than in the control and azaserine-inhibition experiments (see below).

<u>Inhibitor</u>	<u>cpm on paper of diphosphate area</u>
Azaserine (60 min)	3020
DON (60 min)	1870
Control	2875

This decrease was found in all DON-inhibited Scenedesmus experiments.

With both inhibitors a spot was found upon phosphatasing of the glucose cyclic, 1,2-phosphate area, which moved a little faster than ribose in phenol-water and a little slower in butanol-propionic acid, and which was absent in the control. This spot exactly cochromatographed with a phosphatased sample of formylglycinamide ribotide, which Professor John M. Buchanan kindly provided.²

¹Barker, Bassham, Calvin, and Quarck, J. Am. Chem. Soc. 78, 4632 (1956).

²Dr. J. M. Buchanan, Dept. of Biochemistry, Massachusetts Institute of Technology, Boston.

No inhibition was found with azaserine on Chlorella.¹ Very likely the azaserine cannot penetrate the cells. The DON penetrates only slowly into the cells of Chlorella, and it takes some time, depending on the outside concentration, before a sufficiently high level of DON within the cells is reached to effect the inhibition. At very low concentrations of inhibitor within the cells--that is, with low concentrations of inhibitor outside, or with short-time exposure to a higher concentration outside--an increased activity was found in glutamic acid. This is discussed below.

The effect of DON on Chlorella is in general the same as that in both inhibitors except that FGAR could not be detected. In some experiments two compounds in the phosphate area build up, which after phosphatasing moved into the neighborhood of dihydroxyacetone. However, they appeared in only some of the experiments and may be the result of a slower destruction of certain enzymes.

Azaserine has been shown to inhibit the formation of α -N-formylglycinamide ribotide (FGAM) from α -N-formylglycinamide ribotide (FGAR),³ in which reaction glutamine supplies the nitrogen. DON appears to inhibit the same reaction, as with both inhibitors FGAR has been found, although it is absent from the control experiments, and with both inhibitors glutamine builds up.

Besides inhibition of this reaction and possibly other transamidations,^{4,5} the inhibitors affect the metabolism in other points. The effects found can be explained by either of these mechanisms:

(a) A general inhibition of transamination reactions.¹ This would account for decreased synthesis of amino acids and build-up of Krebs-cycle intermediates. It is difficult, however, in this picture to explain the simultaneous decrease in amount of glutamic acid--which is the donor of amino groups in the transamination reactions--and the rise of its specific activity. At least a partial inhibition of the synthesis of glutamic acid from α -ketoglutaric acid also has to be assumed.

(b) A partial inhibition of the synthesis of glutamic acid from α -ketoglutaric acid. The resulting decrease in amount, the "using up" of glutamic acid, would bring about as a secondary effect the decrease in transamination reactions.

After 40 minutes' photosynthesis with $C^{14}O_2$ the glutamic acid is still gaining in radioactivity and is of low specific activity. This indicates that a great part of the fairly large glutamic acid pool (6 μ /ml wet packed cells) is still unlabeled.

If the amount of glutamic acid formed and used per minute is small in comparison with the pool size, and the α -ketoglutaric acid from which it is formed is of much higher specific activity, then upon partial inhibition of the glutamic acid synthesis the amount of glutamic acid will decrease, unlabeled glutamic acid will be used, its specific activity will increase, and the α -ketoglutaric acid building up will contain much radioactivity, as found.

³B. Levenberg and J. M. Buchanan, J. Am. Chem. Soc. 78, 504 (1956).

⁴M. Bentley and R. Abrams, Fed. Proc. 15, 218 (1956).

⁵L. Kaplan and C. C. Stock, Fed. Proc. 13, 239 (1954).

If the turnover rate of glutamic acid is fairly high in comparison with the pool size, but the newly formed labeled glutamic acid is used, preferentially then upon inhibition the same results will be found, but the α -ketoglutaric acid can be of any specific activity, if not lower than that of the glutamic acid. In view of the rate at which the glutamic acid disappears, the latter hypothesis seems the more likely.

However, neither of the two explains the initial increase in labeling of glutamic acid. As in this period the transamination reactions still go on, it cannot be explained by a decrease in the preferential use of labeled glutamic acid, nor by a decreased dilution of activity of the α -ketoglutaric acid, when it is no longer formed in the transamination reaction. It may be that the specific activity of α -ketoglutaric acid increases through the action of the inhibitor, for instance through an increased "leakage" of radioactivity into the Krebs cycle; but as the specific activity of the acids could not be determined on the papers, this had to remain a suggestion.

The inhibitors must affect the metabolism in still other points, as a decrease in the labeling of diphosphates and an increase in labeling of some compounds in the phosphate area have been found, but from these experiments no evidence can be found on where this interference may be, and whether they are primary or secondary effects.

The specific activity curves of glutamine and glutamic acid, from which glutamine seems to have a higher specific activity at some moments than glutamic acid, the unrelatedness of the two curves and the constant high rate of formation of glutamine, even after the amount of glutamic acid has fallen from 6γ to below 0.2γ /ml wet packed cells, almost leads one to suspect that there must be another way by which glutamine can be formed.

In keeping to the known way of synthesis of glutamine from glutamic acid only, we have to assume a separation of phases of glutamic acid,⁶ glutamine being formed from the more active (newly synthesized) phase. After 30 minutes of inhibitor in steady-state experiment No. II, the amount of glutamic acid is 1.4γ , and the increase in amount of glutamine in the next 10 minutes is 1.2γ . The specific activities of the two compounds should be more comparable, unless glutamine of very low or zero activity is formed in that period by, for instance, degradation of protein.

⁶Steward, Bidwell, and Yemm, *Nature* 178, 734 (1956).

RADIATION SENSITIVITY IN CHLORELLA

Chris van Sumere and Osmund Holm-Hansen

Although many studies have been made on radiation damage to biological systems, most of the work has been done either with animal tissue or with fungi. The algae have received very little attention in this regard. As algae offer many advantages such as ease of handling, unicellular suspensions, ease of studying carbon metabolism by use of radioactive CO₂, etc., a project utilizing algae has been undertaken to determine the radiation doses necessary to cause a complete cessation of growth, and to study at what stage in the metabolism of the cell the radiation has its primary effect.

In the first experiment, fresh *Chlorella* cells were irradiated by Co⁶⁰ sources (one giving a maximum of 2.5×10^5 rep/hr and the other 10⁷ rep/hr) with doses of 0, 900, 1800, 4500, 8500, 17,000, 42,000, 100,000, 200,000, and 500,000 rep. The irradiation was carried on in small test tubes containing 2 ml of the *Chlorella* suspension (about 1.15 ml of packed cells). Immediately after removal from the source, a sample of the algae was streaked on an agar nutrient plate and allowed to incubate for two weeks, at the end of which the resulting growth was examined under the microscope. The plates inoculated with algae that had received 0, 900, 1800, and 4500 rep showed a large amount of normal-appearing growth; plates of algae that had received 8500, 17,000, and 42,000 rep showed a very small amount of growth; and those which had received 100,000, 200,000, and 500,000 rep showed no increase in cell number. There were no differences in appearance of cells noted among the various treatments. The sample receiving no radiation and that receiving 500,000 rep were used to measure the CO₂-fixing ability and the resulting fixation pattern. The usual laboratory procedures were employed in this photosynthesis test. The results are shown in Table XX. The radioautograms of the two ethanol extracts showed no significant differences. Further experiments along this same line are now in progress.

Table XX

Effect of radiation on CO ₂ fixation in <u>Chlorella</u>				
Sample	Total counts fixed	cpm in 80% ethanol ext.	cpm in 20% ethanol ext.	cpm in insoluble portion
Blank	659,086	173,800	9,486	475,800
500,000 rep	410,856	45,068	7,068	358,880

A MODIFIED METHOD FOR PREPARATION OF
CARBOXYDISMUTASE

Ning G. Pon and Brian R. Rabin

In previous experiments, carboxydismutase was obtained by ammonium sulfate fractionation of homogenates of *Tetragonia expansa* leaves.¹ The precipitate obtained between 35% and 39% saturated ammonium sulfate (SAS) was designated as carboxydismutase. However, this precipitate was often intensely brown and contained a small amount of nucleic acid.² Under further treatment, such as heating at 60°C and precipitation with cold ethanol, this color still persisted. Wildman's group has found that the brown color, which was caused by the polyphenoloxidase system, produced a marked change in the properties of the soluble proteins in tobacco-leaf extracts.³ Thus, the pellet obtained after prolonged centrifugation at high speeds was very difficult to redissolve. Also, the intense color often seriously hampered observations of the proteins during electrophoresis and ultracentrifugation. When proteins were obtained from extracts prepared under 99.99% nitrogen atmosphere, all these difficulties were avoided.

It is known that the carboxylation enzyme is present in the water extract of chloroplast.⁴ Furthermore, this colorless extract contains a large portion of this enzyme, and it was found to be free of nucleic acids.⁵ Accordingly, the best way to prepare this enzyme was to proceed via the chloroplast. A typical experiment for the preparation of the chloroplast extract is given in the flow diagram, Fig. 2.

The amount of protein in the chloroplast extract ranged from 90 mg to 140 mg per 500 g leaves. The wet packed volume of the chloroplast fragments was from 3 to 7 ml. On the average, the yield was about 20 mg of protein per ml of wet packed chloroplast fragments. Protein content was determined by the method of Lowry et al.⁶ Volume of chloroplast fragments was determined by measuring the volume of the centrifuged chloroplast fragments packed at 10,000 x g for 10 min in 0.05 M pH 6.8 phosphate buffer. A diluted chloroplast extract (0.6 mg of protein per ml) gave an optical density of about 1.2 at its absorption maximum, $\lambda = 270 \text{ m}\mu$. This indicated that a small amount of nucleic acid may still be present. (The 35 to 39% SAS precipitate, in previous experiments, usually has absorption maximums at $\lambda = 265 \text{ m}\mu$. To prepare the enzyme from the chloroplast extract, the latter is subjected to ammonium sulfate fractionation as shown in the flow diagram, Fig. 3. The distribution of material and carboxydismutase activity in the various ammonium sulfate fractions has been obtained from another experiment. The results are shown in Table XXI.

¹Ning G. Pon, in Chemistry Division Quarterly Report, UCRL-3157, Sept. 1955, p. 18.

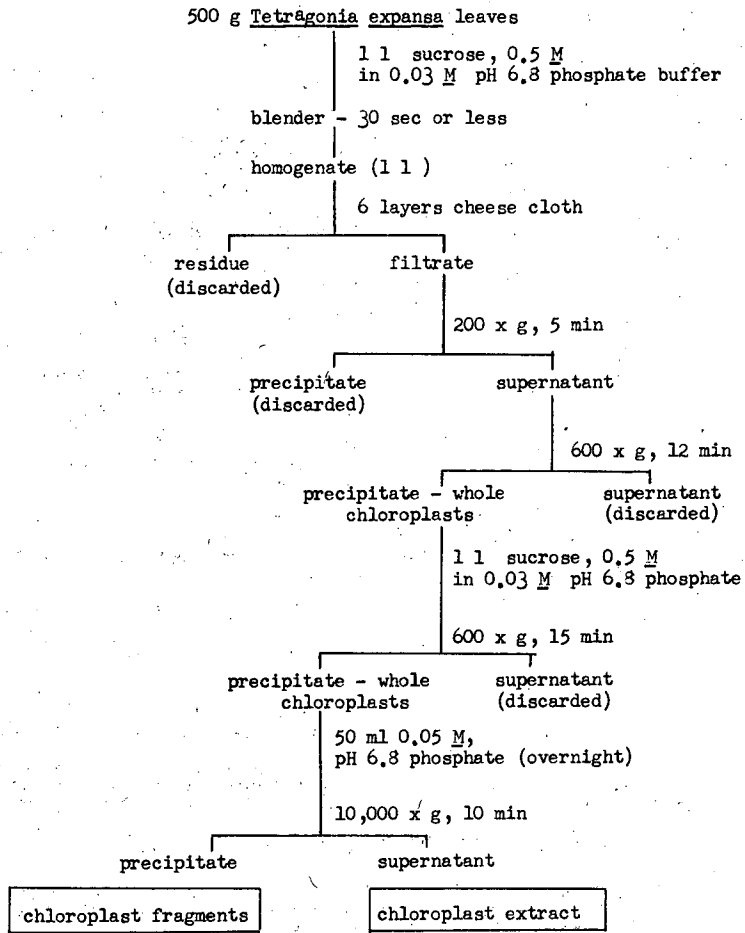
²J. Mayaudon, A. A. Benson, and M. Calvin, unpublished results.

³Cohen, Ginoza, Dorner, Hudson, and Wildman, *Science* 124, 1081 (1956).

⁴R. C. Fuller, in Chemistry Division Quarterly Report, UCRL-2932; March 1955, p. 32.

⁵J. W. Lyttleton, personal communication.

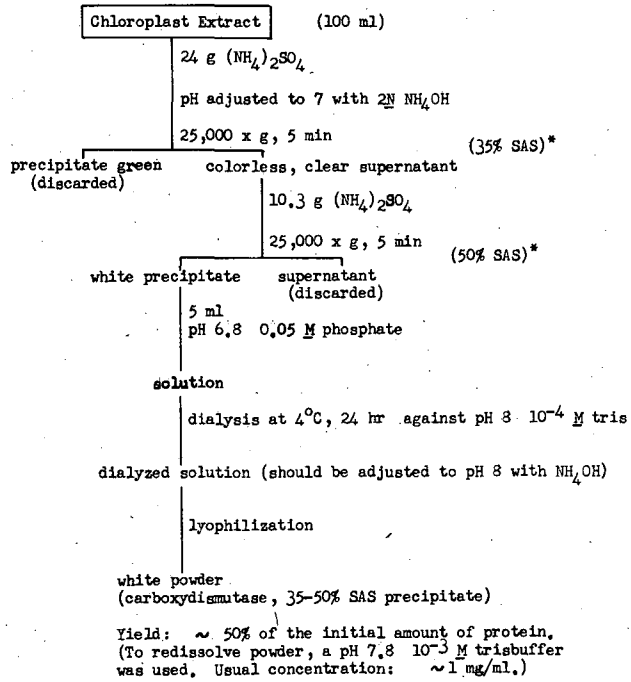
⁶Lowry, Rosebrough, Farr, and Randall, *J. Biol. Chem.* 193, 265 (1951).
Calvin



All operations were carried out at or near 0°C.

MU-13012

Fig. 2. Preparation of chloroplast extract.



All operations were carried out at 0°C.

* Saturated ammonium sulfate is considered to be 63.5 g of $(\text{NH}_4)_2\text{SO}_4$ for each 100 ml initial volume of solution.

MU-13013

Fig. 3. Fractionation of the chloroplast extract.

Table XXI

Distribution of material and activity		
Ammonium sulfate fraction	% by wt of starting material ^a	Activity in cpm ^b
0-35% SAS precipitate	15	1100
35-39% SAS precipitate	19	9300
39-70% SAS precipitate	40	6800

^aBased on the method of Lowry et al⁶ for protein determination

^bAssay mixture: NaHC¹⁴O₃, 1.3 μmole at 20 μC
 NiCl₂ 0.4 μmole
 HCl 1.2 μmole
 Ribulose-1,5-diphosphate (RuDP) ~0.1 μmole
 Enzyme fraction, ~30 μg
 H₂O added to make 200 μl final volume
 pH = 7.0

Assay conditions: The enzyme was preincubated at 0°C for 10 min with HC¹⁴O₃⁻, NiCl₂, and HCl. After this period the reaction was started by the addition of RuDP and allowed to stand at 25°C for 10 min. The reaction was stopped with steam heat for 40 sec and then 50 μl of 6N HCl was added; 1/10 of the total mixture was counted.

From the results in Table XXI it is evident that the precipitate obtained between 35% and 70% SAS contains the bulk of the activity. In large-scale preparations, in general, little precipitate was formed in the region between 35% and 39% SAS; therefore, the 35-50% SAS precipitate was prepared instead. In the 50-70% SAS region, only a small amount of precipitate was formed--usually not sufficient to warrant further work--so that this fraction was discarded. It is interesting to note that the 35-39% SAS precipitate showed no signs of nucleic acid: the optical density of 0.62 mg/ml solution (pH 6.8 0.05 M phosphate buffer) was about 1.0 with an absorption maximum at 278 mμ.

In preliminary experiments, many conditions have been tried in the effort to increase the yield of the final product. For example, a variety of conditions were used to rupture the leaf cells and to prepare the chloroplast. These are indicated below:

1. Leaves were ground with a mortar and pestle, either with or without sand.

2. Centrifugation speeds were varied in the chloroplast preparation.
3. Leaves were ground in a blender for different time periods.
4. Leaves frozen in liquid N₂ were ground in blender at dry ice temperatures.
5. Chloroplasts were prepared by the method of Commoner et al.⁷ This is a method in which the chloroplasts are separated from the rest of the debris and fragments by flotation of the chloroplasts in a hypertonic sugar solution.
6. Chloroplasts were prepared in isotonic salt solution (0.35 M NaCl) instead of sugar solution.

The results are summarized Tables XXII, XXIII, and XXIV. From these results it appears that the best method for the preparation of the chloroplast is as shown in Fig. 2. No further work is being done to improve the chloroplast or protein yield.

Table XXI

Effect of method of grinding on yield of protein in the chloroplast extract		
Grinding Method	Chloroplast centrifugation conditions	Yield: mg protein per 500 g leaves
Mortar--no sand	400 x g, 10 min	100 ^a
Blender ^c	400 x g, 10 min	100 ^a
Mortar plus sand	1000 x g, 7 min	240, ^a 100 ^b
Blender ^c	{ 600 x g, 12 min 1000 x g, 7 min	110 ^b
Blender, dry ice temp.	1000 x g, 7 min	< 1 mg

^aCalculated from small-scale preparations; i. e., 50 leaves.

^bCalculated from large-scale preparations; i. e., >250 leaves.

^cGrinding time: 30 sec.

⁷Commoner, Heise, and Townsend, Proc. Natl. Acad. Sci. U.S. 42, 710 (1956).

Table XXIII

Yields of protein by various methods		
Method	Volume of packed chloroplast fragments per 500 g leaves	Mg protein per 500 g leaves
Commoner et al. ⁷	6 to 17 ml	20
NaCl, 0.35 <u>M</u>	7 ml	60
Sucrose, 0.5 <u>M</u>	3 to 7 ml	90 to 140

Table XXIV

Grinding time in blender vs protein yield in the chloroplast extract		
Grinding time	Volume of packed chloroplast fragments per 500 g leaves (ml)	Mg protein per 500 g leaves
15 sec	3.5	90
22.5 sec	4	80
30 sec	3.5	80
1 min	2	60
2 min	1	30

LARGE-SCALE PREPARATION OF RIBULOSE DIPHOSPHATE (RuDP)

Ning G. Pon and Brian R. Rabin

The phosphoriboisomerase-phosphoribulokinase mixture used was prepared essentially as described by Horecker et al.¹ The steps are illustrated in the accompanying flow diagram, Fig. 4. It is essential that all operations be carried out at 0°C.

The preparation was assayed by use of a pH-stat in the following manner. The test solution contained 11 μ moles adenosine triphosphate (ATP), 10 μ moles ribose-5-phosphate, 10 μ moles $MgCl_2$, and 5 μ moles cysteine in 10 ml. The pH was adjusted to 7.40 and held constant during the reaction by addition of 0.1 M NaOH. At zero time the enzyme preparation (150 λ) was added. In a typical assay 7.14 μ moles NaOH were consumed in 25 min; the alkali uptake had slowed down considerably after 10 min. A control without ribose-5-phosphate showed the preparation to contain very little ATPase activity (alkali consumption ceased after 10 min; a total of 1.5 μ moles was consumed).

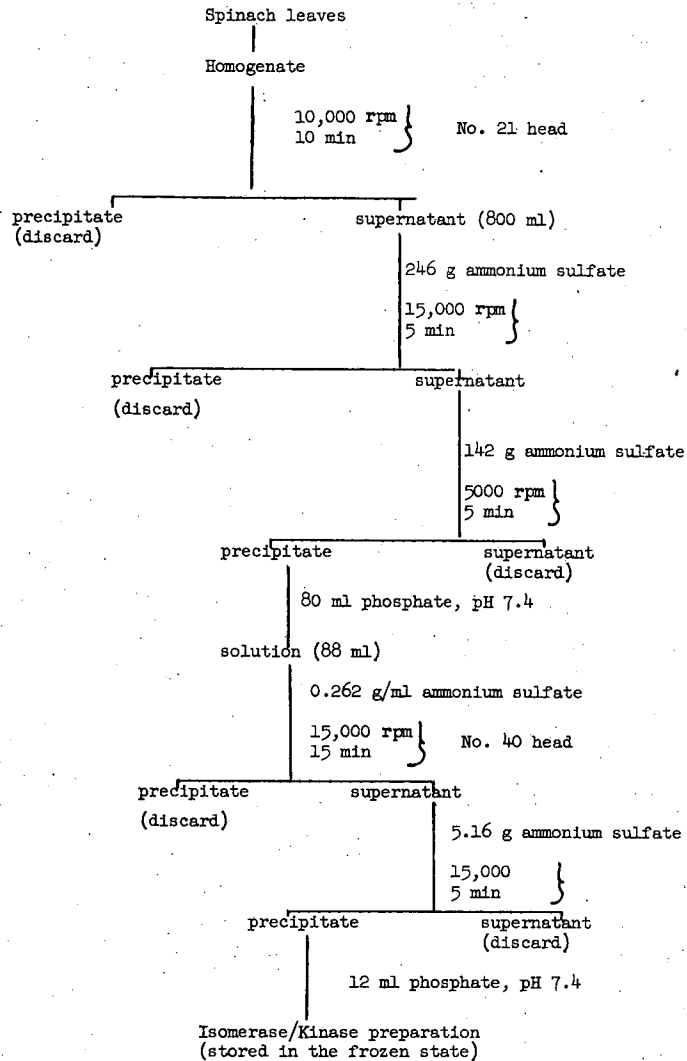
Preparation of RuDP IV

Four mmoles of ribose-5-phosphate (barium salt) was dissolved in water (40 ml), and potassium sulfate (40 ml of 0.15 M) was added. The mixture was centrifuged and the residue washed with water (20 ml). To the combined washings and supernatant, 6 mmoles ATP, 0.4 mmole cysteine, and 4 mmoles $MgCl_2$ were added, and the volume was made up to 300 ml. The reaction was carried out in an automatic titration apparatus at room temperature under an atmosphere of N_2 gas; the pH was adjusted to 7.40 and held constant by the addition of CO_2 -free NaOH (1.8 N). The reaction was started by the addition of the kinase-isomerase preparation (5 ml) and stopped after 37 min, when the uptake of alkali had slowed down, by the addition of trichloroacetic acid (20 ml); 1.5 ml of alkali was used. The nucleotides were removed¹ by the addition of acid-washed Norite A (120 g). The solution was centrifuged (2000 rpm for 10 min) and the residue washed successively with four 200-ml increments of water. It was found essential to layer the solution with alcohol to facilitate centrifugation. To the combined supernatant and washings, barium acetate (4 ml of 1 M) was added and the pH adjusted to 6.4 with saturated barium hydroxide. The precipitate was removed by centrifugation and washed with water (50 ml). An equal volume of ethanol was added to the combined supernatant and washings. The RuDP precipitates in a gelatinous form; it was collected by centrifugation, washed with 80% ethanol and dried in vacuo over P_2O_5 . Yield: 1.75 g.

Analysis of the preparation showed it to contain 0.4 μ mole of inorganic phosphate and 2.31 μ moles of organic phosphate per mg. These analytical figures must be regarded as approximate only. If, as assumed, the only phosphate ester present is the dibarium salt of RuDP, the product is 69% pure.

Purification by fractional alcohol precipitation was attempted. In a typical experiment, RuDP (46 mg) was titrated with water (20 ml) and the solution centrifuged to remove insoluble material. The insoluble fraction

¹Horecker, Hurwitz, and Weissbach, J. Biol. Chem. 218, 785 (1956).
Calvin



All centrifugations were done with Spinco Model L.

MU-13014

Fig. 4. Flow Diagram for Preparation of Isomerase/Kinase.

(11 mg) was washed with 50% alcohol (5 ml) and dried in vacuo over P_2O_5 ; it consisted mainly of inorganic phosphate. The addition of ethanol (5 ml) to the supernatant precipitated 22 mg of material, which gave on analysis 0.55 μ mole of inorganic phosphate and 2.63 μ moles of organic phosphate per mg. This corresponds to 76% purity on the basis of organic phosphate. In view of the large amount of inorganic phosphate still present, fractional alcohol precipitation was abandoned in favor of column chromatography.

Column Chromatography of RuDP

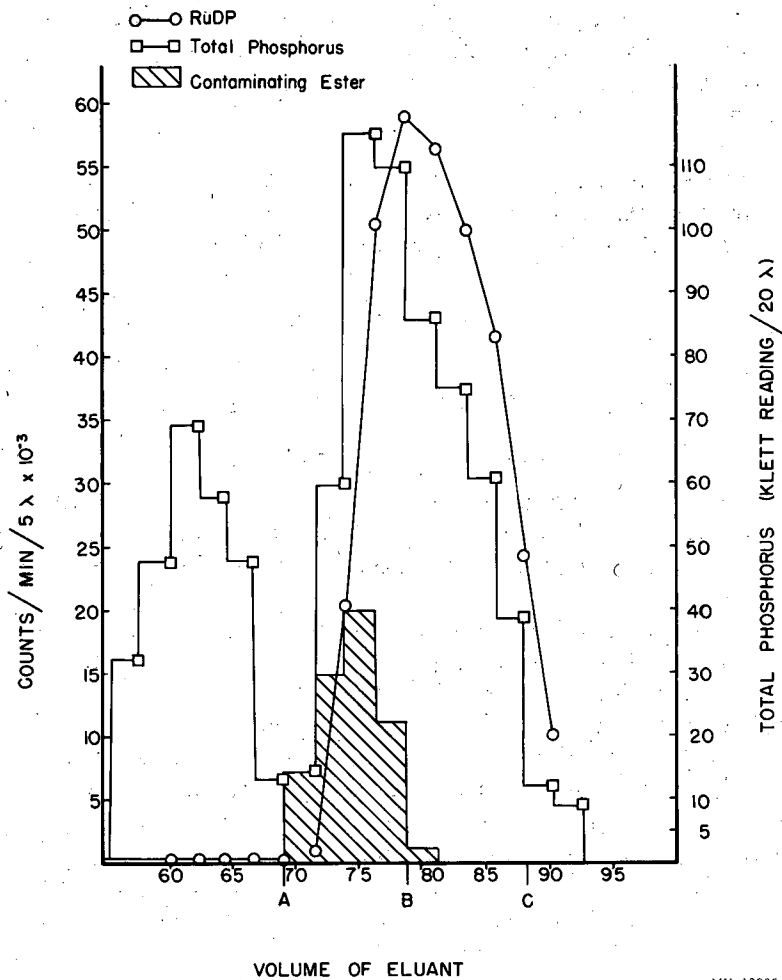
The column employed was 0.8 cm (diameter) x 27 cm. The resin used was Dowex-1 formate; it was freed from fines by decantation and converted from the chloride to the formate form with 2 N formic acid.

The elution apparatus consisted of two vessels of equal size and shape. One, the mixing vessel, was provided with a stirrer and had an outlet to the top of the column; water (100 ml) was placed in this vessel. Ammonium formate (100 ml, 2 M) was placed in the other vessel and the two vessels connected together by means of a siphon tube. This system provides a linear gradient of ammonium formate at the outlet of the mixing vessel.

RuDP (100 mg) was dissolved in water (30 ml) with the aid of a little Dowex 50, H^+ form, and the pH adjusted to 6.0 with KOH. The solution was centrifuged and run through the column. The column was washed with water and subjected to gradient elution; fractions were collected every 5 min by use of an automatic device. The flow rate was 0.44 ml/min. The fractions found to contain phosphorus by a qualitative test were assayed for total phosphate and RuDP. Twenty λ was taken for phosphate determination; the technique previously described² for aliquots containing 0 to 35 g phosphorus was used. The method used for the determination of RuDP is based on the fixation of $C^{14}O_2$ by RuDP in the presence of carboxydismutase. The reagent solution was prepared by mixing $NaHC^{14}O_3$ (200 λ of 0.036 N, 400 μ C/ml), $MgCl_2$ (80 λ of 0.01 M in 0.04 N HCl), tris buffer (20 λ , pH 7.83, 1 M with respect to tris), and carboxydismutase (50 λ of a spinach preparation fractionated between 35% and 39% saturated ammonium sulfate containing 6 mg of protein per ml). An aliquot from each fraction (5 λ) was placed on a planchet and the enzyme reagent (15 λ) added. The planchet was placed on moist filter paper in a covered vessel, to reduce evaporation, and allowed to incubate at room temperature. After two hours the reaction was stopped by the addition of acetic acid (10 λ of 6 N) and the planchet prepared for counting in the usual manner. The elution pattern obtained is shown in Fig. 5. Under the conditions employed, a Klett reading of 230 corresponds to 0.5 μ mole of phosphate.

Two well-separated phosphorus-containing peaks are observed. The first to emerge contains inorganic phosphate; the second peak is in the position expected for a diphosphate ester, and the enzyme assay shows it to contain essentially all the RuDP emerging from the column. It is noteworthy that the RuDP and phosphate peaks do not coincide, suggesting the presence of at least one phosphate ester additional RuDP; this contaminant emerges from the column slightly ahead of RuCP. From the ratio RuDP/organic phosphate,

²J. R. Quayle, Preparation and Some Properties of Ribulose-1,5-Diphosphate, UCRL-3017, Jan. 1956.



MU-12905

Fig. 5. Elution pattern of RuDP IV.

the quantity of this contaminant can be calculated: this constitutes the shaded area on the graph. The fractions emerging between A and B (Sample a) and B and C (Sample b) were bulked. To each of these, barium acetate (500 λ of 1 M) and an equal volume of 95% ethanol were added. The solutions were cooled in ice and the precipitate collected by centrifugation. The precipitates were washed with 50% ethanol (20 ml), 95% ethanol (10 ml), and absolute ethanol (10 ml), and dried in vacuo over P₂O₅. Material recovered: Sample a, 22 mg; Sample b, 23 mg.

Both samples contained a small quantity of inorganic phosphate, though very much less than the starting material. The constitution of these separated column extracts is under investigation.

GLUCOSE DISSIMILATION IN A FREE-CELL NEOPLASM

Karl K. Lonberg-Holm

There are further developments in the investigation of the kinetics of glucose dissimilation by whole living cells.¹ The "automatic rapid sampler," which was reported earlier,² has been employed in these studies.

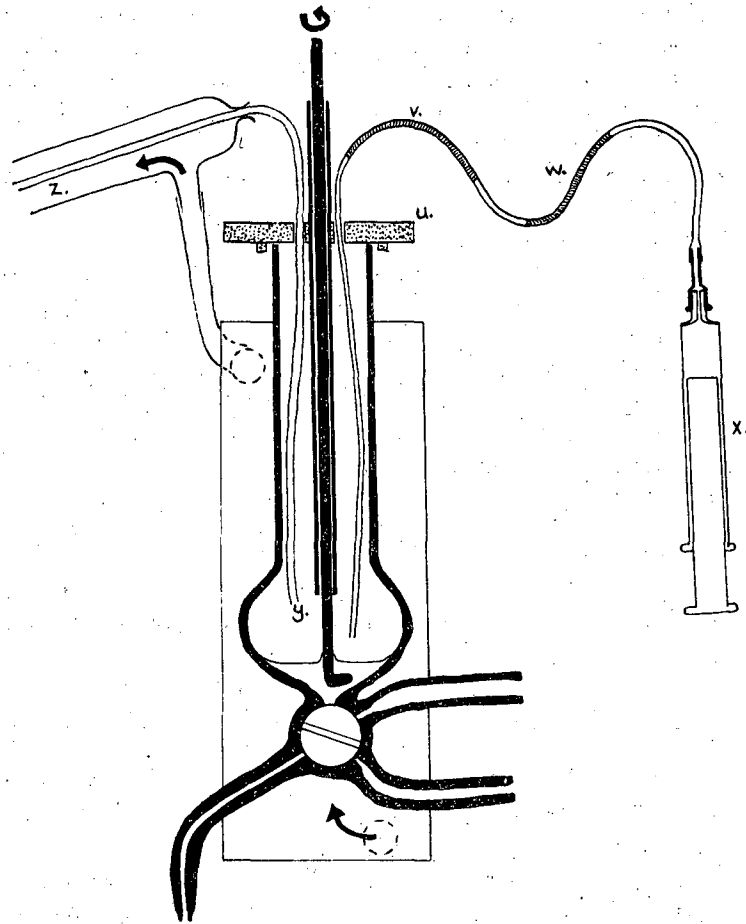
The conditions of short-exposure experiments using the automatic rapid sampler previously described are as follows: The Ehrlich mouse ascites carcinoma cells used are washed twice in ten volumes of ice-cold NaSM PO₄ Lockes buffer³ by centrifuging for 40 sec and then resuspended to give approximately a 10% suspension (as measured by spinning an aliquot 15 min in hematocrit tube). The cell suspension is drawn up into a syringe equipped with a thin plastic tube (approx. 1 mm i. d.) long enough to be inserted into the reaction vessel through a small hole in the plastic lid (see Fig. 6), and 1.0 ml is injected. The lid also has holes for other tubes, one of which can be used for the introduction of nonradioactive substrate, one for radioactive substrate, and one for gas flushing. The substrates, radioactive or nonradioactive, are inserted ahead of time into tubes together with 20 to 30 μ l of isotonic buffer for flushing (see arrangement in Fig. 6). These tubes are inserted into the sampler beforehand and are attached to gas-filled syringes for ejecting their contents.

After the cells have been stirred for a few minutes at bath temperature, 72 μ g nonradioactive glucose is injected. This is enough to last about 2 min at 37°C and is given to keep the cells in an active condition. After almost 3 min the radioactive substrate is added, and simultaneously a marker switch is thrown recording the time on an Esterline-Angus recorder along with the recorded times of the sample ejections. A maximum of 15 samples are automatically discharged into 2 ml aliquots of hot 95% ethanol.

¹K. K. Lonberg-Holm, in Chemistry Division Quarterly Report, UCRL-3351, March 1956, p. 32.

²K. K. Lonberg-Holm, in Chemistry Division Quarterly Reports, UCRL-3415, June 1956, p. 36.

³R. W. McKee and A. J. Walker, *Science* 118, 133 (1953).



MU-13015

Fig. 6. Automatic rapid sampler equipped with gassing system and substrate injection tube. U is the plastic lid with holes for four tubes and is attached to the stirrer-bearing tube. V and W are substrate and rinse to be injected by pressing syringe X. Y is outlet for water-saturated (when reached) gas brought from bubbler in the temperature bath by a tube running up the temperature-jacket water return Z.

Each sample is centrifuged and re-extracted with hot 20% ethanol, and the combined extracts are evaporated to dryness in vacuo; this results in less than 2% total activity loss from volatilization. The residue is removed from the flask, with four rinses of live steam, which condenses on the flask walls, and is transferred to a depression in a glass spot-test dish and evaporated over P_2O_5 in vacuo. The residue is transferred to the origin of a paper chromatogram with four 15- μ l rinses. For determining the total activity in each sample, an aliquot may be removed before the first evaporation, or 1.00 ml water may be added to the residue in the pear-shaped flask and swirled for 1 min and an aliquot removed, followed by re-evaporation to dryness. The losses of organic phosphates, as a result of sticking or incomplete rinse, in either the flask or spot-dish evaporation, are less than 1%.

The sample extracts are then chromatographed in the usual manner and radioautographs prepared and counted. A schematic map of the results is shown in Fig. 7. The spots are identified by enzymatic hydrolysis followed by cochromatography with nonradioactive carrier, and the evidence presented comes from earlier experiments made without the rapid sampler and under somewhat different conditions from the experiments reported above. The enzyme used is ammonium-sulfate-fractionated⁴ Poldase S that has been dialyzed against water and lyophilized. The separation of mannose and sedoheptulose is poor; the sugars may be a mixture of both, or even confused.

Spot 1 is the sugar diphosphate region and contains mostly fructose 1,6-diphosphate; 3% and 8% of its activity can be accounted for as glucose in 20 and 36 sec, respectively. Also, "sedoheptulose" is present as well as a little ribose. Spot 2 appeared after 1 or 2 min, and upon phosphatasing yields glucose, "mannose," galactose, and ribose, and maybe the UDP derivatives of these sugars.

Spots 3a, 3b, and 3c contain glucose, fructose, and ribose, respectively. Spot 3a may also contain "sedoheptulose." Spot 3b contains some "mannose." In one earlier experiment, taking Spots 3 as a whole, glucose accounted for 66%, 73%, and 63%, at 12, 20, and 36 sec; fructose for 23%, 17%, and 14%; and "mannose" for 11%, 9.4%, and 17%, respectively. Ribose was present in concentrations up to 4.2% at 36 sec after hot glucose was fed.

Spot 4b, found occasionally, was identified as phosphoglyceric acid. Spot 5 may be phosphoglycolic acid. Spots in the area of 6 and 7 have given ribose upon phosphatasing, but these have been in relatively long exposures; possibly in shorter exposures other compounds, such as tetrose or triose phosphates, may be present.

Figure 8 gives the results of a short-exposure experiment with the automatic rapid sampler. About 95 μ l (packed volume) of ascites tumor cells at 37°C were given 300 μ g of high-activity glucose (224 μ C/mg), as has already been described. The values given should be precise to within 5%, except for 3c, 6, and 7, where less than 10,000 counts could be made in 10 min of counting.

⁴S. S. Cohen, J. Biol. Chem. 201, 71 (1953).

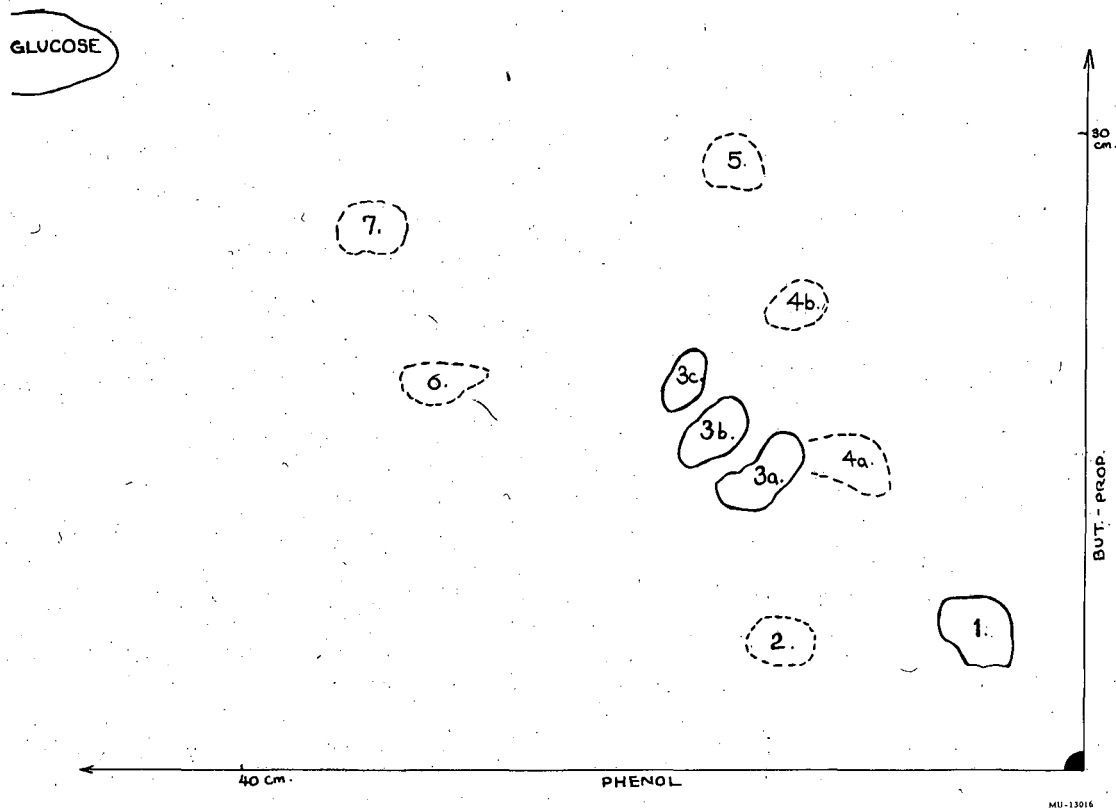


Fig. 7. Relative positions of radioactive compounds following short exposure to radioactive glucose. Developed 20 and 30 hours.

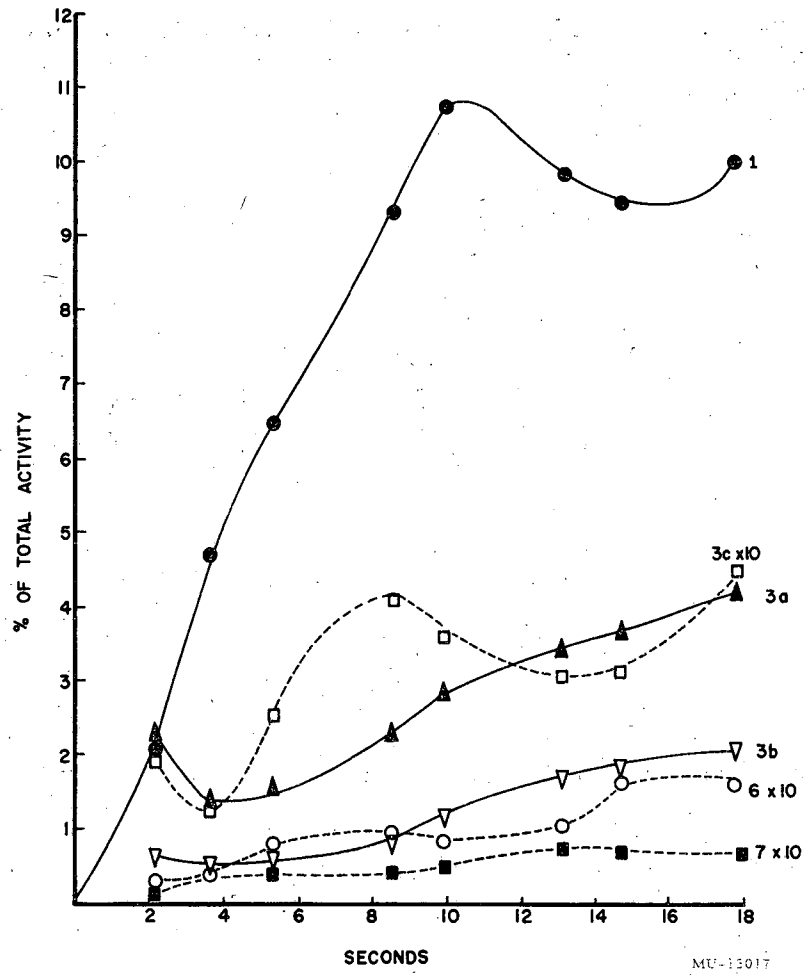
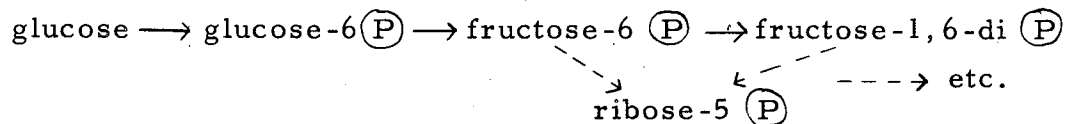


Fig. 8. Short exposure of Ehrlich's mouse ascites carcinoma cells radioactive glucose at 37°C.

Figure 9 shows a similar experiment in which, however, the cells are at 21.4°C. In this case, the cells are given 10 min to utilize the added 72 µg of nonradioactive glucose before the 300 µg of radioactive glucose is added. This is the only experiment performed so far at less than 37°C. In the experiment at 37°C we have not been able to get into short enough time ranges to catch all components in the ascending slope. Thus the monophosphates are decreasing in radioactivity during the first 4 sec. For this reason we have had to resort to making a run at lower than physiological temperatures. At the lower temperature, the dip after the first peaks of the monophosphate, 3a and 3b, comes about 10 sec later than at 37°C. The change in temperature produces qualitative differences; it can be seen that the 3c curve is different in shape and that the final concentrations seem to be little more than one-third of those in the cells at physiological temperature.

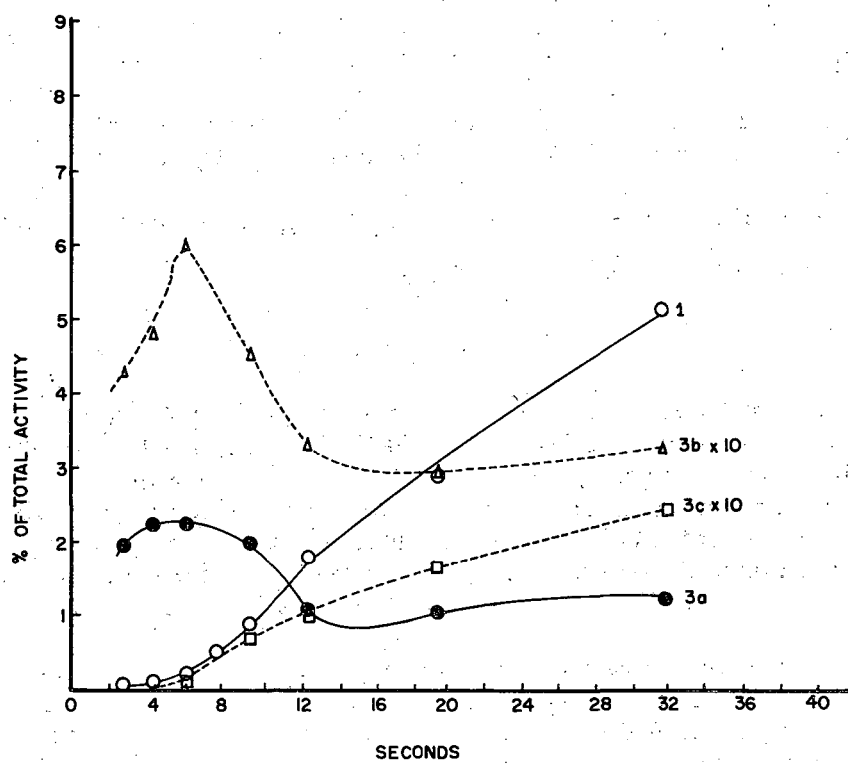
The results agree with a scheme for glucose dissimilation as follows:⁴



The first transient peak seems to be glucose-6-phosphate, and only slightly later fructose-6-phosphate reaches a peak. Fructose-1,6-diphosphate increases rapidly as the monophosphates fall, and--in Fig. 9 at least--the pentose- (P) increases. This does not rule out a major contribution to ribose synthesis by the direct oxidation of the No. 1 carbon of glucose-6- (P) if--as it may in this nonsteady-state type experiment--an abnormal transient state exists in which the normally present pathway is blocked.

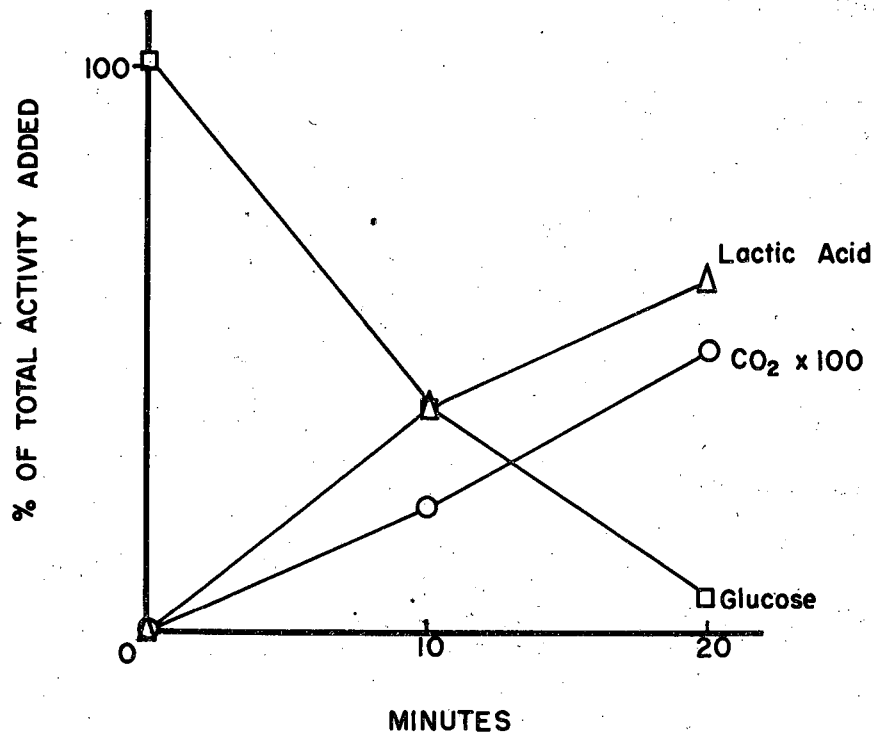
The peaks observed are transient states of the metabolic system that is seeking to establish a steady state. The observed behavior could be explained if the supply of ATP is the limiting factor in this system: ATP is used to phosphorylate glucose, and not only is it drained off in that way but also by its further utilization to phosphorylate the newly formed fructose-6- (P). As a result, ATP decreases concentration, glucose phosphorylation slows down, and hexose phosphate pools decrease. As more fructose-di (P) is formed, some is utilized to speed the formation of ATP, and the hexose monophosphates again increase in concentration. It would be interesting to follow the concentration of ATP as a function of time following the introduction of glucose. P³² experiments are being done for this purpose and will be reported elsewhere.

Another aspect of this problem that requires investigation is the amount of glucose destroyed and the amount of lactic acid produced in short exposure periods. Although glucose utilization is roughly linear over periods of an hour or so, there is evidence that the utilization may be rapid for a few seconds initially and then slope off. Although as yet no successful rapid-sampling "balance" experiment has been completed, a start has been made with a moderately long-exposure-period balance experiment (Fig. 10). In the first 10 min, 60% of the glucose (4.5 µmoles) was destroyed, while 0.91 µmole of oxygen was consumed. In this same period only 0.22% of the radioactivity of the glucose appears in CO₂. In this period also, assuming a R.Q. of about one, 1 mole in 9 of the CO₂ produced was derived from the added glucose.



MC-33013

Fig. 9. Short exposure of Ehrlich's mouse ascites carcinoma cells to radioactive glucose at 21.4°C.



MU-13019

Fig. 10. A balance experiment on the dissimilation of radioactive glucose by Ehrlich's mouse ascites carcinoma cells. 100 μ l of cells given 1.34 mg glucose- C^{14} (5.5×10^6 cpm) at zero time. The cells are in 1.5 ml of NaSMPO₄ buffer at 37°C and in the presence of 3.8 moles of nonactive lactic acid. Oxygen consumption is linear and equals 1.8 μ l/min as measured in the standard Warburg apparatus. Glucose is determined by running duplicate aliquots chromatographically in two dimensions and eluting and counting the glucose spot. Lactic acid was determined by continuous ether extraction and checked for radiopurity by chromatography. CO₂ was determined by counting aliquots from the centerwells of Warburg flasks the contents of which were killed at the times indicated by tipping in sulfuric acid.

Addendum

The micro titration of sugar by Hirst and Jones⁵ has been modified to smaller quantities. The principle of the determination involves the periodate oxidation of glucose or fructose to formic acid (theoretical yield is 5 and 3 moles per mole, respectively), and the direct titration of the formic acid liberated. About 4.5 moles of formic acid are liberated from each mole of glucose.

A 10- to 60- λ sample in a 4-mm id test tube containing about 10 μ g or more of glucose is adjusted to a yellow-orange color in the presence of 10 μ l of methyl red indicator (0.1 mg ml), and 150 μ l of 0.04 N sodium periodate is added which contains a predetermined amount of HCl to give a slightly positive blank titration value. The titration value is determined with a reagent blank oxidized in the same way as the unknown (20 μ l of 0.1 N HCl per 10 ml periodate on the day of the titration, in our case). The sample is heated 15 min in a beaker of water on a steam bath, and then removed to an ice bath. Then 10 μ l of ethylene glycol is added, and the solution is mixed and transferred to a spot-test dish to be titrated with 0.05 to 0.02 N NaOH from a Kirk microburet in the presence of 10 μ l of methyl red indicator. Standards and blanks are run simultaneously to a yellow end point. With duplicates, less than 2% error can be achieved.

Sucrose can be determined in the same manner, but the yield is only 1 mole/mole formic acid. The analysis is also subject to large error if the sample is partially hydrolyzed. Therefore, the following modification has been made: After the pH of the sample is adjusted, as above, 25 μ l of invertase⁶ solution is added (enough for a two- to threefold excess; equivalent to 1 μ g of scales in our case). After 70 min the sample is oxidized as above, but no acid should be added to the periodate as the blank will now be positive as a result of the added invertase preparation. The titration is performed as above; the precision does not seem to be quite so good.

⁵E. L. Hirst and J. K. N. Jones, J. Chem. Soc. 1949, 1659.

⁶Wallerstein Blue Label (yeast) Invertase Scales, Wallerstein Laboratories, 180 Madison Avenue, New York, N. Y.

GLUCOSE METABOLISM IN DEPANCREATIZED RATS

Martha R. Kirk and B. M. Tolbert

The metabolism of glucose in normal and alloxan-diabetic rats, and the effects of insulin, tolbutamide (N-n-butyl-N'-tolylsulfonylurea), and carbutamide (N'-(n-butyl-carbamyl)-sulfanilamide) on this metabolism have been previously reported.¹ Using the same carbon-14 respiration pattern technique,² we have extended this study to include the effect of pancreatectomy³ on glucose metabolism, with and without insulin, tolbutamide, or glucagon.

Experimental

Animals. Four depancreatized Sprague-Dawley female rats were obtained from the Oregon Medical School through the courtesy of Dr. Clarissa Beatty and Dr. C. N. Rice. When shipped, about one week postoperative, the rats all had blood sugar levels about 350 mg%. Periodic checks on urine sugar consistently showed levels of 2% or over. For the first week after the operation, the rats were fed powdered Purina chow plus 3% pancreatin. After this they were kept on powdered food for several weeks, when they were put on the standard food pellets.

Testing Conditions. Determination of glucose-C₆¹⁴ respiration patterns was begun about 25 days after pancreatectomy. Measurements were made under the following conditions: (a) no pretreatment, (b) 1 or 2 units of insulin injected 1 hour before the glucose, (c) 250 mg/kg tolbutamide by stomach tube 1 hour before glucose, (d) 2 µg/kg or 10 µg/kg glucagon intraperitoneally at the time of glucose injection, (e) 2 units of insulin 1 hour before, plus 10 µg/kg glucagon at the time of glucose administration, and (f) 250 mg/kg tolbutamide 1 hour before plus 10 µg/kg glucagon at the time of glucose injection.

Results and Discussion

In Table XXV is given the percent injected glucose-C₆¹⁴ oxidized to C¹⁴O₂ by each rat at various times after pancreatectomy. As may be observed, rats designated DP₁ and DP₂ were still able to oxidize somewhat more glucose than the more severely diabetic rats on the twenty-fifth day postpancreatectomy, but were down to the average by the fortieth day. DP₃ was quite low and died very shortly. Results show that these rats become quite stable in their glucose oxidation rate and are able to maintain the level over a long period of time. In general, the residual glucose oxidation rate in these depancreatized rats was much higher than in the alloxan-diabetic rats studied earlier; the difference is more than 50%.

¹B. M. Tolbert and M. R. Kirk, Experiments with Normal and Diabetic Rats Using Carbon-14 Respiration Patterns, UCRL-3503, Sept. 1956.

²Tolbert, Kirk, and Baker, Am. J. Physiol. 185, 269 (1956).

³Crystalline glucagon (hyperglycemic-glycogenolytic factor, insulin content less than 0.05 U. per mg) and the tolbutamide were supplied by the Eli Lilly Research Laboratories, Indianapolis, Indiana, through the courtesy of Dr. C. N. Rice.

Table XXV

% C ¹⁴ as C ¹⁴ O ₂ from rats injected with glucose-C ₆ ¹⁴					
Rat No.	Day after operation	Cumulative % Minutes after injection			
		0-20	0-40	0-60	0-120
DP ₁	25	1.60	5.33	8.64	15.88
	40	0.41	2.06	4.75	11.95
DP ₂	25	0.57	2.99	6.01	14.32
	40	0.34	2.03	4.54	11.78
DP ₃	25	0.14	0.90	2.13	6.38
DP ₄	25	0.35	2.43	4.88	12.48
	60	0.32	1.86	4.05	10.17
	104	0.45	2.14	4.75	12.11

The nature of the residual oxidation mechanism for the glucose would be interesting to know. It might be due to insulin from a few residual β cells, but we think that after 40 days they should be noneffective. Depancreatized rats are more sensitive to insulin than are alloxan-diabetic rats. A dose of insulin easily tolerated by the latter would kill the former. This same increase in insulin sensitivity can be induced by hypophysectomy of alloxan-diabetic rats, although these Houssay animals can have a nearly normal blood-sugar level. We presume that such Houssay animals will have a near-normal glucose oxidation rate, although we have not yet measured them.

Table XXVI shows the response of depancreatized rats to various treatments as reflected in the changes in glucose oxidation rate. Each result is the average of several determinations. There was no consistent difference in response between 1 and 2 units of insulin. The lack of response to tolbutamide would seem to indicate that no insulin-producing mechanism remained. Two $\mu\text{g}/\text{kg}$ of glucagon made no change in the glucose oxidation pattern, but 10 $\mu\text{g}/\text{kg}$ produced a decided lowering of the percent of injected glucose appearing as C¹⁴O₂. This is probably simply a reflection of an elevated blood-sugar level, rather than any change in the amount of glucose being oxidized to CO₂ in a given time. It is an interesting observation that this effect is absent, or is masked, in the presence of exogenous insulin, but is still quite apparent in the presence of tolbutamide, even though tolbutamide is known to raise liver glycogen.^{4,5} These same results are represented graphically in Figs. 11 and 12.

⁴M. Vaughan, Science 123, 885 (1956).

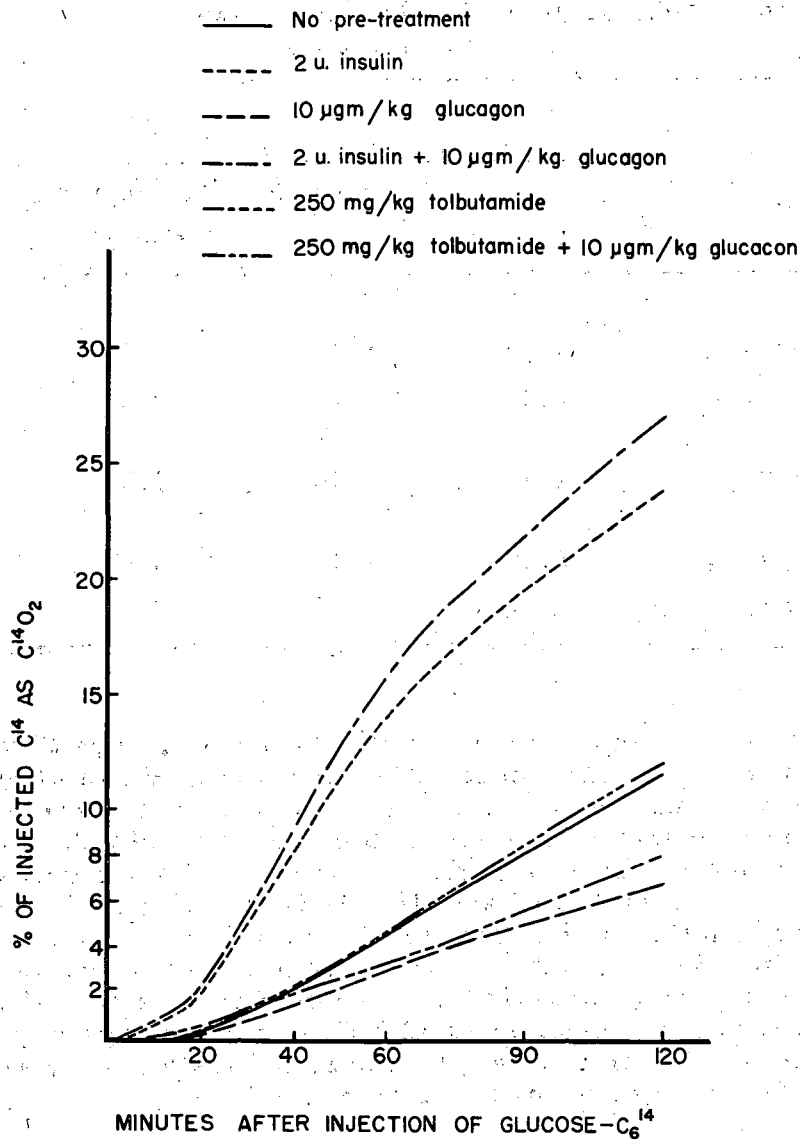
⁵W. L. Miller, Jr. and W. E. Dulin, Science 123, 584 (1956).

Table XXVI

Drugs	% C ¹⁴ as C ¹⁴ O ₂			
	Minutes after injection			
	0-20	0-40	0-60	0-120
None	0.37	2.10	4.59	11.70
Insulin (1 or 2 units)	1.95	8.20	14.32	23.91
Tolbutamide (250 mg/kg)	0.35	2.13	4.53	12.05
Glucagon (10 µg/kg)	0.35	1.55	3.03	6.75
Insulin and glucagon	2.18	9.31	15.88	27.11
Tolbutamide and glucagon	0.54	2.20	4.02	8.08

Preliminary experiments on the duration of crystalline insulin action in vivo have shown that this duration is about the same in alloxan-diabetic and in depancreatized rats. The nature of this duration-of-action curve is interesting and presents a difficult problem to understand. In an alloxan-diabetic rat, 8 units of insulin permits a normal glucose oxidation rate for 10 to 12 hours, and then the effect sharply terminates in 2 to 4 hours. Such a straight-line function with sharp cutoff would infer a nonlinear response of the animal to insulin, a great sensitivity at low insulin levels, and a limited response at normal concentrations. We might then deduce that the Houssay, or depancreatized, rats have an insulin only in the sensitive region, and that removal of the α cells or pituitary removes a substance (or substances) that limit(s) the effectiveness of insulin action.

An alternative to the above proposal would be that insulin has a finite life time in vivo and then is destroyed via a logarithmic process. Although possible, such a theory would not easily fit the duration-of-action data for small insulin doses.



MU-12914

Fig. 11. Glucose-C₆¹⁴ respiration patterns: effect of various drugs on the diabetes of depancreatized rats.

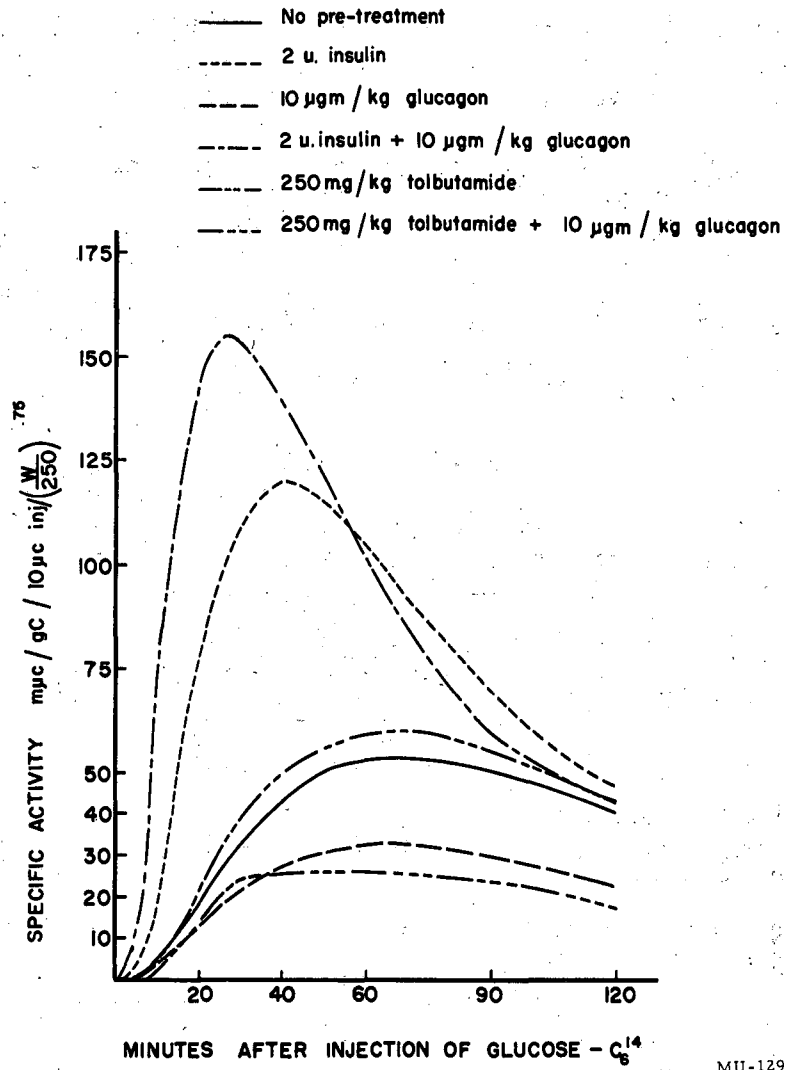


Fig. 12. Glucose-C¹⁴ respiration patterns: effect of various drugs on the diabetes of depancreatized rats.

EFFECT OF DIISOPROPYLFLUOROPHOSPHONATE (DFP)
UPON BRAIN CHOLINESTERASE

Edward L. Bennett, Joy Loe, and Hilda M. Karlsson

(In collaboration with Professors Mark R. Rosenzweig and David Krech, Department of Psychology, University of California, Berkeley, California; supported in part by grants from the National Science Foundation.)

We have continued to investigate the effects of injections of diisopropyl-fluorophosphonate (DFP) upon the behavior of the rat in the multiple-unit T maze described in the preceding quarterly report.¹ We have repeated our earlier observations that DFP reduces the cholinesterase (ChE) level by a greater amount in the cerebral cortex than in the rest of the brain. Table XXVII presents data on three groups of rats analyzed recently. In each case, the cortex shows a slightly greater inhibition of ChE due to the injected DFP than does the rest of the brain.

Table XXVII

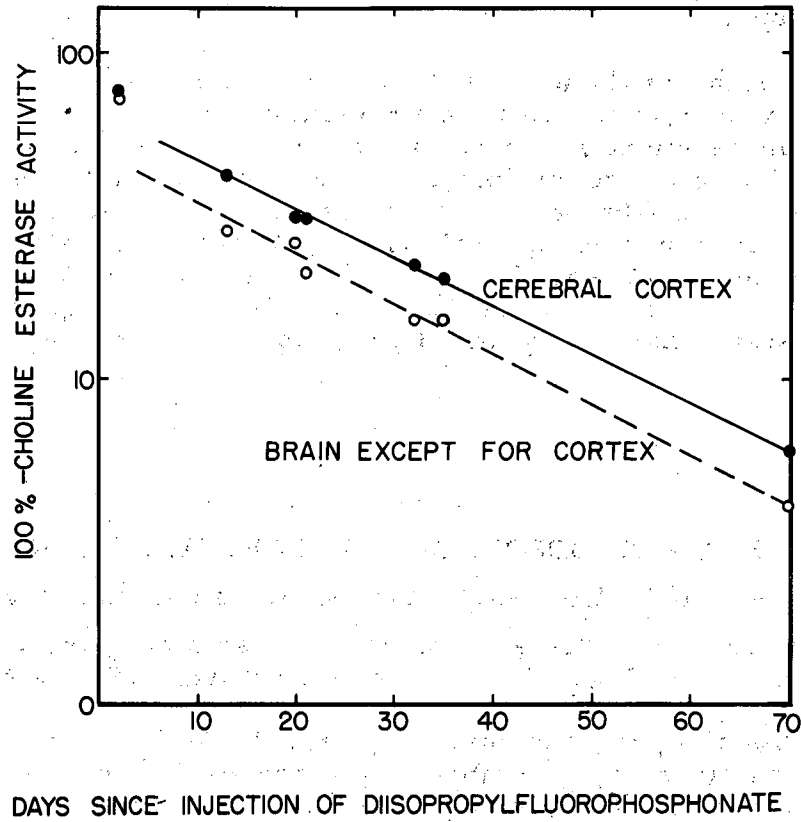
Influence of DFP on brain cholinesterase levels
(Male rats, injected with 1.0 mg/kg DFP at about 75 days of age)

		Mean ChE in injected Mean ChE in control		Time between injection and analysis (days)
		Cortex	Brain	
Group I	10 noninjected, control 13 DFP-injected	0.80	0.86	35
Group II	9 control 13 injected	0.78	0.86	32
Group III	3 control 9 injected	0.94	0.96	70

This table extends the lengths of time after injection beyond those presented in UCRL-3629, page 47, Table XVIII. Putting the data from both tables together, we obtain the function of recovery of ChE activity vs time after injection. Log (100-percent ChE activity) vs time gives a linear plot, as shown in Fig. 13. The half time of recovery of ChE is estimated to be about 20 days, from the 13- to 70-day data. This is somewhat longer than given in the last report, in which data from 2 to 21 days were used. A value of about 22 to 25 days was calculated for female rats from data obtained by Koelle and Gilman.²

¹E. L. Bennett and Hilda Karlsson, in Chemistry Division Quarterly Report, UCRL-3629 Jan. 1957, page 46; J. L. McGaugh and E. L. Bennett, *ibid.*, page 48.

²G. B. Koelle and G. Gilman, *J. Pharmacol.* 87, 421 (1946).
Calvin



MU-12908

Fig. 13. Cholinesterase activity in brain and cortex of rats after injection of DFP.

The first points in Fig. 13 at 2 days, do not fit the curves well. There are two possible reasons for this. These points are based on the smallest number of animals of any of the points--only 4 cases. Furthermore, many animals die from the injection during the first several days, so that there is probably a selective factor involved; that is, some of the rats tested at 2 days may have been so strongly affected by the DFP that they would not have survived to the later periods of analysis. Such rats would, then, not appear in the later groups.

The behavioral data and their relations to the chemical data are not yet completely analyzed. We have previously reported that DFP-injected animals run more quickly than control animals in the Krech Hypothesis Apparatus. A similar result has now been observed in the multiple-unit maze. Here, again, the behavioral measure is more sensitive than previously used physiological measures, with which no effect was detected unless ChE had been reduced by at least 50%. There appear also to be effects of the DFP injection on the error scores in the maze. Two further groups of animals have been tested behaviorally and the brains are now being analyzed.

DISTRIBUTION OF DIISOPROPYLFLUOROPHOSPHONATE IN RATS

Edward L. Bennett, Hilda M. Karlsson, and Joy Loe

(In collaboration with Professors Mark R. Rosenzweig and David Krech, Department of Psychology, University of California, Berkeley, California.)

In this and previous quarterly reports we have described experiments in which the cholinesterase inhibitor, diisopropylfluorophosphonate (DFP), has been administered to rats and the subsequent effects upon behavior and cholinesterase levels in several portions of the brain have been studied. DFP reacts with proteins to form a diisopropylphosphonated (DIP)-protein. Little information has been found in the literature indicating the quantities and distribution of the reacted DFP after administration to rats. The availability of DFP labeled with phosphorus-32 (DFP³²) (courtesy of Dr. Myron Pollycove, Division of Medical Physics) has enabled us to make some preliminary semi-quantitative investigations of this problem.

The first experiment was designed to determine the approximate distribution of the label from the DFP³² in the cortex, brain, serum, and cells of rats of similar strain (S₁) and age (75 days) to those used in our behavioral experiments, and, in particular, to determine the order of magnitude of P³² activity found in the various fractions, in order to plan how much P³² activity should be used for future experiments. Four male rats (littermates) were injected with DFP³² (1 mg/kg). The DFP³² was prepared by diluting 0.25 mg of DFP³² in 0.25 ml of propylene glycol with 1.0 mg of inactive DFP in 1.0 ml of ethanol; it was calculated to contain 7.7×10^7 dis/min/mg at the time of injection. Atropine (1 mg/kg) was administered shortly before DFP administration and 1 day after DFP administration.

Calvin

A control animal was sacrificed at 1 day and another at 18 days, and DFP³²-injected animals were sacrificed at 1, 4, 11, and 18 days after injection. The animals were placed under light ether anesthesia and approximately 5 ml of blood was removed by heart puncture into a heparinized syringe. The cells and serum were separated by centrifugation; the cells were washed with saline several times and lysed with distilled water. The entire cortex and the brain were removed, weighed, and homogenized in saline.

Determination of the cholinesterase (ChE) activity of the various fractions was made under the same conditions as used for our routine ChE assays of brain and cortex. Rather erratic curves were obtained in several instances with the lysed cells, perhaps owing to the relatively low ChE activity and the consequent large sample, with corresponding large buffer capacity, that had to be used. Thus any small variation in apparent pH due to meter drift during the analysis would greatly affect the results. The ChE values for the inhibited animals were compared with the two littermate control animals.

Radioactivity determinations were made by direct plating of aliquot portions of the brain and cortex homogenates, serum, and lysed cells. The samples were counted in the Nuclear D-40 automatic windowless flow counter. As subsequent results indicated, the P³² activity in the fractions--particularly the cortex, brain and serum--was very low, so that rather large aliquot portions had to be plated. In addition, considerable difficulty was experienced in plating the lysed cells, owing to flaking of the cells after drying. Consequently, the results presented are semiquantitative and serve only to indicate the order of magnitude of P³² to be found in the various tissue fractions.

In Table XXVIII we have summarized the results obtained in terms of total disintegrations of P³² found in the cortex, brain, serum, and cells (corrected for P³² decay, percent equivalent of injected DFP, equivalent gamma of DFP, and equivalent gamma DFP per gram tissue or per ml whole blood. In the fractions examined, the largest amount of P³² activity was found in the cells (a maximum of 1.2% at 1 day), while approximately 0.07% or about 0.2γ was found in the entire brain (including cortex).

Using the data obtained for the amount of P³² activity and the inhibition of ChE activity in the several fractions, one can calculate a "minimum turnover number" for ChE. Several assumptions must be made to calculate this turnover number. Among them are (a) that the ChE of the control and experimental animals would have been the same in the absence of DFP, (b) that one molecule of DFP is reacting with the enzymatically active site of ChE; and (c) that DFP is reacting only with ChE. The first assumption, at least for brain and cortex, is supported by considerable data that we have obtained in other experiments, particularly for littermates.

There is evidence in the literature that DFP reacts primarily with the enzymatically active site of ChE. In regard to the third assumption, it seems reasonable to assume that DFP would react with materials other than ChE that are present, as it is known to react with other proteins. However, the values obtained for the various fractions are reasonably constant as a

Table XXVIII

P³² Distribution and ChE Activity of Rats Following DFP³² Administration*

Time after injection (days)	Fraction	Total activity (dis/min)	Percent of injected DFP ³²	DFP	γ DFP per gram tissue or ml whole blood	Moles	ChE Activity** (moles per gram tissue or ml of whole blood)	Percent Control	Turnover Number
1	Cortex	3.7×10^3	0.02	0.05	0.14	7.6×10^{-10}	35×10^{-7}	45	5,700
	Brain	1.0×10^4	0.05	0.13	0.11	6.0×10^{-10}	74×10^{-7}	39	18,500
	Serum	1.4×10^5	0.7	1.8	0.15	7.1×10^{-10}	3.3×10^{-8}	14	280
	Cells	2.6×10^5	1.2	3.4	0.25	1.4×10^{-9}	19×10^{-8}	26	390
4	Cortex	3.6×10^3	0.02	0.05	0.14	7.6×10^{-10}	42×10^{-7}	54	4,800
	Brain	6.0×10^3	0.03	0.09	0.08	4.3×10^{-10}	118×10^{-7}	64	15,600
	Serum	2.3×10^4	0.12	0.3	0.023	1.3×10^{-10}	14×10^{-8}	61	720
	Cells	4.8×10^4	0.63	0.63	0.048	2.6×10^{-10}	38×10^{-8}	52	1,300
11	Cortex	2.0×10^3	0.01	0.026	0.08	4.3×10^{-10}	65×10^{-7}	83	3,100
	Brain	3.8×10^3	0.02	0.05	0.044	2.4×10^{-10}	161×10^{-7}	87	10,000
	Serum	3.8×10^3	0.02	0.05	0.004	2.2×10^{-11}	21.2×10^{-8}	92	820
	Cells	2.0×10^4	0.1	0.25	0.020	1.1×10^{-10}	35×10^{-8}	49	3,400
18	Cortex	2.4×10^3	0.012	0.03	0.096	5.2×10^{-10}	45×10^{-7}	57	6,400
	Brain	6.3×10^3	0.03	0.08	0.064	3.5×10^{-10}	136×10^{-7}	73	14,000
	Serum	2.9×10^3	0.014	0.04	0.0026	1.4×10^{-11}	21.6×10^{-8}	96	1,000
	Cells	3.0×10^4	0.15	0.39	0.027	1.5×10^{-10}	52×10^{-8}	71	1,330

* The rats (approx. wt. = 250 g) were administered 1 mg DFP³² in ethanol-propylene glycol/kg of body weight by intraperitoneal injection. The DFP³² had an activity of 7.7×10^7 dis/min/mg at the time of injection. All values have been corrected for radioactive decay. It was assumed that the blood volume was 2.5 ml/100 g body weight to calculate total activity in cells and serum.

** The ChE activities of two control rats were as follows: Cortex: $80,77 \times 10^{-7}$; brain: $187,182 \times 10^{-7}$; serum: $22,24 \times 10^{-8}$; cells: $67,77 \times 10^{-8}$.

function of time (excluding the values obtained for serum and cells at 1 day, and for cortex and brain at 11 days), indicating that if DIP is attached to other compounds, either they are resynthesized, or the DIP is removed, at a rate similar to the recovery of ChE activity. It should be pointed out that no distinction has been made between "true" and "pseudo" ChE. The highest value for turnover number, approximately 15,000, was obtained for brain ChE. A value of 300,000 has been reported for highly purified bovine red cell ChE.¹ The obvious further experiment, to attempt further purification of the rat-brain ChE, will be carried out when additional DFP³² becomes available. This experiment, however, has shown that we can obtain useful information on the distribution of DFP³², both in regard to fractions and in regard to time. It will be desirable to increase the amount of DFP³² activity used initially. This is feasible, since it had gone through approximately one half life when it became available to us, and we diluted the DFP³² approximately fivefold.

RESPIRATORY METABOLISM OF ACETATE AND GLYCINE AS A FUNCTION OF AGE

Ann M. Hughes and B. M. Tolbert

During the past few years this laboratory has published reports on the respiratory metabolism of organic compounds as a function of a variety of physiologic and pathologic conditions. During this time we have compiled (originally as an incidental observation, but later as an important research in itself) data on the changes that occur in the metabolism of some organic compounds as a function of age. The two compounds that have been studied rather extensively so far are sodium acetate-2-C¹⁴ and glycine-2-C¹⁴.

Long-Evans rats, both male and female, were injected with either acetate-2-C¹⁴ or glycine-2-C¹⁴. The respiratory C¹⁴O₂ was measured in the breath line apparatus developed in this laboratory.

In previous reports we have usually presented the data in two ways, viz., the total respired C¹⁴O₂ for a given length of time and the rate of C¹⁴O₂ respiration (see Chemistry Division Quarterly Reports UCRL-2531, April 1954, et seq.). In an examination of the data for the current report it was obvious that presenting the cumulative and rate curves for every point on the time scale would produce an unwieldy number of graphs. Of the changes occurring in the metabolic pattern with increasing age, one of the most striking is the change in the maximum rate of C¹⁴O₂ excretion. Therefore, although there are many parameters of the curves that must be considered in a complete analysis of the data, we are presenting in this study but one parameter--maximum rate of C¹⁴O₂ excretion--as a criterion of change with age.

¹Cohen, Oosterban, and Warringa, *Biochim. et Biophys. Acta* 18, 228 (1955).

The results are shown in Figs. 14 and 15. All points except the one for 1 day on the acetate-metabolism graph represent the average of at least 12 animals. There is some doubt as to the significance of that one point, since at present we have had time to run only four animals for that age group. Similarly, we have not yet obtained data for the metabolism of glycine by 1-day-old rats.

One of the most interesting observations in the almost complete absence of acetate oxidation in the 2-hour-old rats. The Krebs cycle is such a fundamental reaction in animal biochemistry that heretofore we had found no physiological change that would appreciably vary the respiratory oxidation of acetate. It is evident from our data that the Krebs cycle is not functioning in the newborn rat, but that it starts by the time the newborn is 8 hours old. We hope to devise a procedure for obtaining premature animals to determine whether the Krebs cycle is functioning in the foetus.

Future work will also include the metabolism of glucose as a function of age.

THE INHIBITION OF ASCITES TUMOR GROWTH BY D₂O

Ann M. Hughes

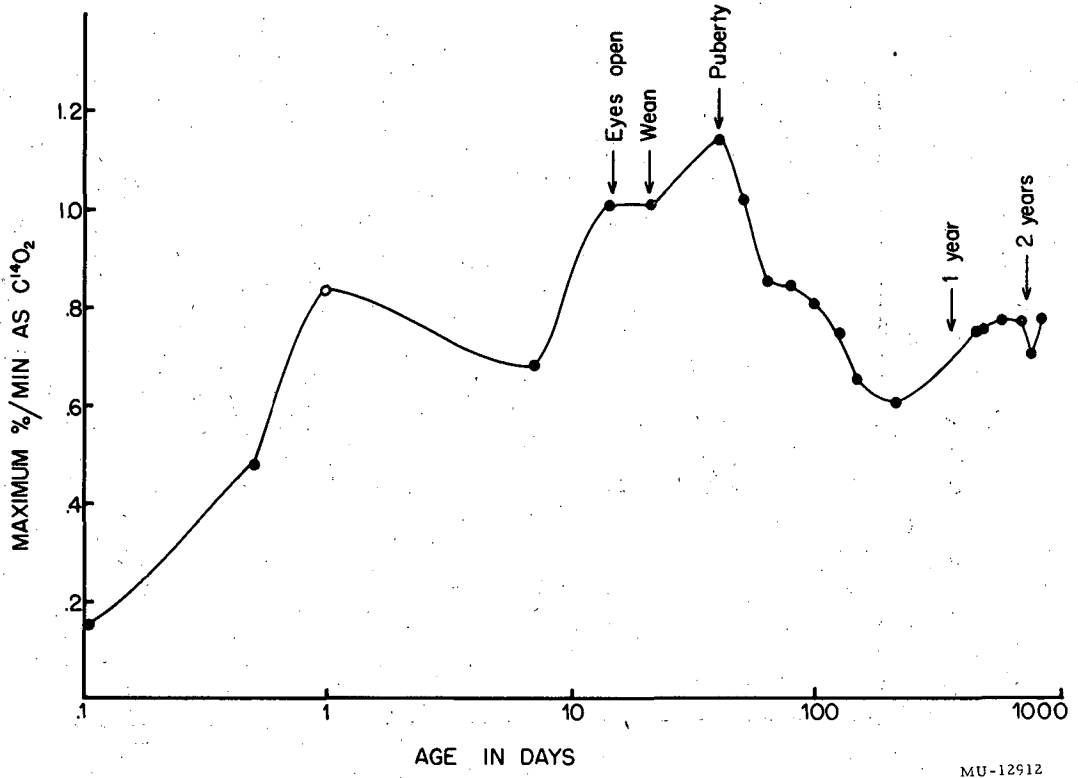
It has been observed in this laboratory that the presence of D₂O in the nutrient media inhibits cell division of growing algae. It is possible that in biological systems involving oxidation-reduction reactions (for example, the formation of nucleic acids) the deuterium might exert a strong isotope effect, thus inhibiting the formation of the nucleic acids. Because of these considerations, it was suggested by Professor M. Calvin that D₂O might selectively retard the multiplication of tumor cells.

Ehrlich's mouse ascites tumor, which has been carried in this laboratory in C₅₇-strain mice for the past three years, was chosen as the first type of tumor for testing the above suggestion. Young adult C₅₇ mice, both male and female, were used.

In order to bring the body concentration of D₂O to a steady state as rapidly as possible before inoculation with ascites tumor, one group of mice was injected intraperitoneally for 2 days with 1.5 ml isotonic D₂O per mouse. On the third day, one half of the group was inoculated with 0.1 ml of a suspension of ascites tumor cells. At the same time an equal number of control mice (not treated with D₂O) was also inoculated with ascites tumor. The first group was continued on D₂O in the drinking water, but without further injections of D₂O. Survival time after tumor inoculation was determined, as a criterion of the ability of D₂O to inhibit tumor growth.

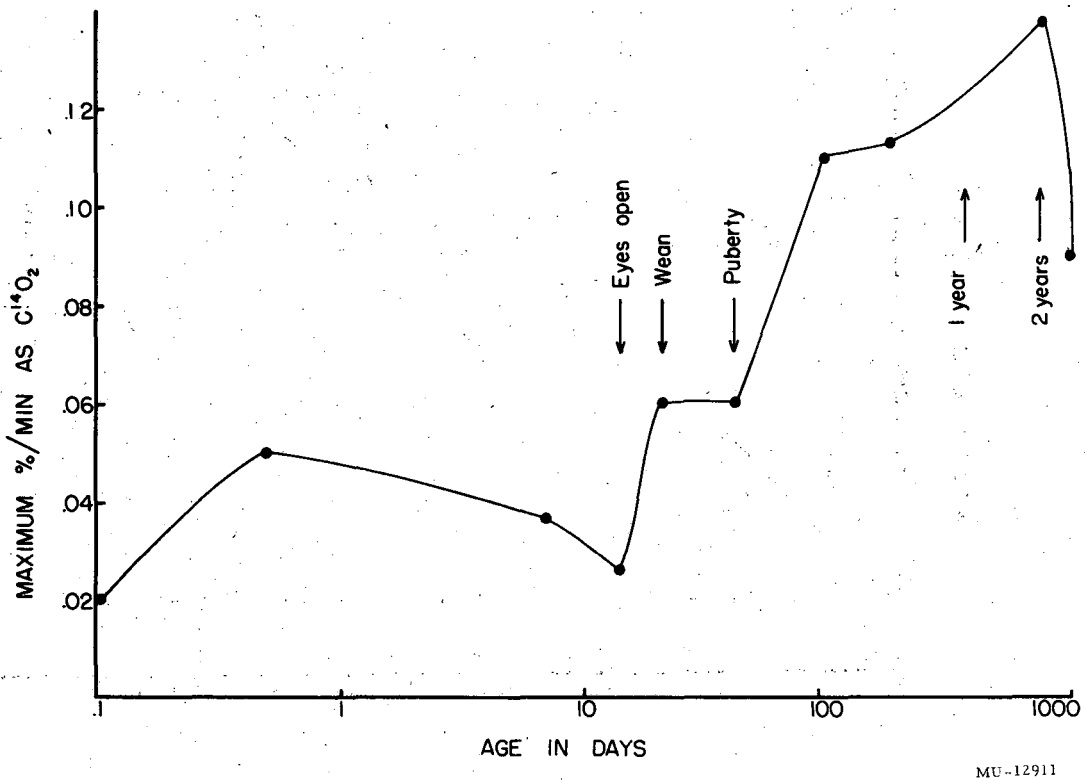
The results for the 30% and 40% D₂O are shown in Figs. 16 and 17. Fifty percent D₂O proved to be too toxic, killing the animals in 2 to 3 days. Thirty percent or 40% D₂O produced no symptoms of toxicity; normal animals

Calvin



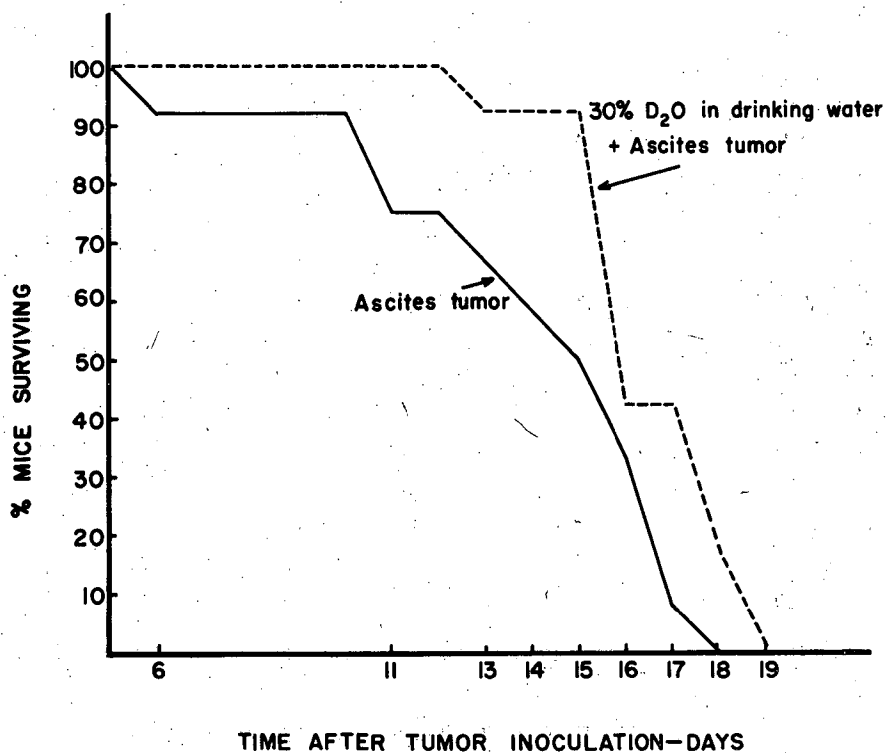
MU-12912

Fig. 14. Acetate metabolism as a function of age.



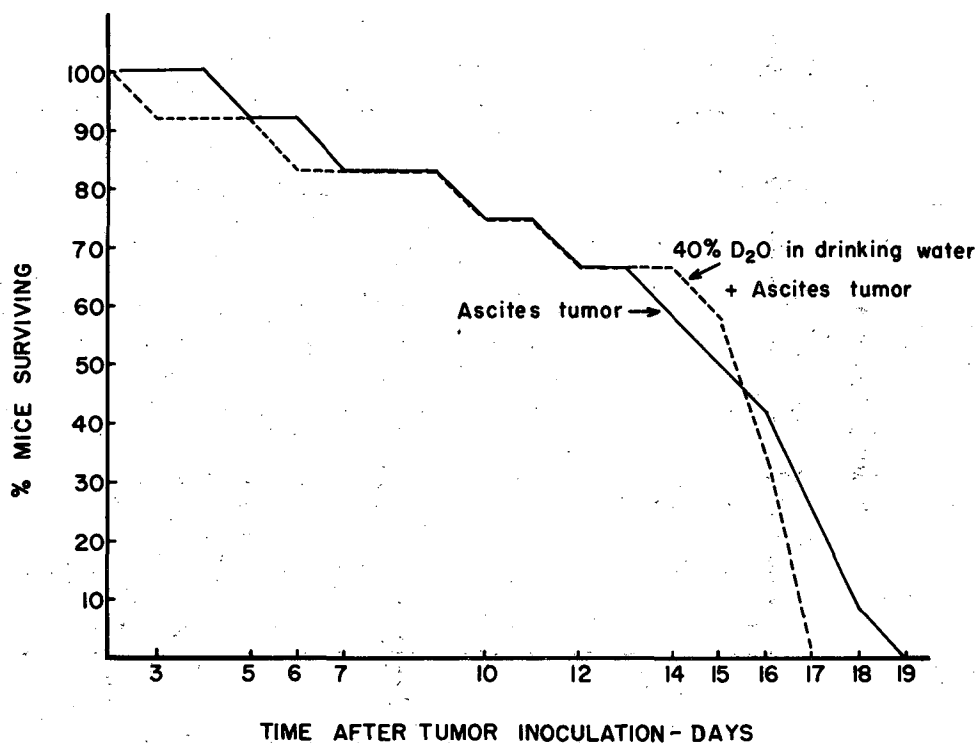
MU-12911

Fig. 15. Glycine utilization (as energy source) as a function of age.



MU-12909

Fig. 16. The effect of 30% D₂O in the drinking water on the survival time of C₅₇ mice inoculated with Ehrlich's mouse ascites tumor cells.



MU-12910

Fig. 17. The effect of 40% D₂O in the drinking water on the survival time of C₅₇ mice inoculated with Ehrlich's mouse ascites tumor cells.

survived indefinitely on such concentrations. There is a definite increase in survival time of tumor-inoculated mice maintained on 30% D₂O, while 40% D₂O affords no protection at all (which suggests that the toxic effect of the D₂O cancels any beneficial effects). Each experiment has been repeated, with comparable results. At the present time the protecting power of 25% D₂O in the drinking water is being tested.

RADIATION EFFECTS ON CHOLINE CHLORIDE

Richard M. Lemmon and Margaret A. Parsons

The abnormal radiation sensitivity of crystalline choline chloride led to a systematic exploration of various choline analogs.¹ No analog was found that exhibited the same high degree of radiation instability. Work aimed at an understanding of the processes taking place in crystalline choline chloride has included determination of (a) the crystal structure by means of X-ray diffraction² and (b) the electron spin resonance spectrum of the irradiated crystals.³ This report describes the rates of decomposition observed when crystalline choline chloride is irradiated (a) at low temperatures, (b) in the presence of added iodide or iodine, and (c) after repeated recrystallization from ethanol-ether or after crystallization from dimethylformamide. The radiation sensitivity of the compound dissolved in different solvents was also investigated.

Low-Temperature Experiments

The target area of the electron linear accelerator, previously described,⁴ was modified to permit the irradiation of samples at liquid nitrogen temperature. A thin-walled well was placed in the vacuum tank in the path of the electron beam. The glass sample holder was then placed inside the well. During an irradiation, nitrogen gas (from boiled liquid nitrogen) was forced through the well at such a rate that the sample was maintained at $-170 \pm 20^\circ$.

Previous work has shown that the chain reaction responsible for choline chloride's radiation decomposition does not proceed at -196° .⁵ It was therefore thought desirable to irradiate samples at liquid nitrogen temperatures and then to determine the extent of decomposition as a function

¹Chemistry Division Quarterly Report, UCRL-3595, Oct. 1956.

²Michael E. Senko, The Crystal Structures of Triazole and Choline Chloride (thesis), UCRL-3521, Sept. 1956.

³Chemistry Division Quarterly Report, UCRL-3629, Jan. 1956

⁴Richard M. Lemmon and Duane F. Mosier, Rad. Res. 4, 373 (1956).

⁵Lemmon, Parsons, and Chin, J. Am. Chem. Soc. 77, 4139 (1955).

of the time of standing at room temperature. For this purpose 18 samples of the crystalline compound were irradiated in the electron beam at $-170 \pm 20^\circ$. The samples all received 5×10^6 rep, an energy dose that would cause approximately 10% decomposition at room temperature. Five of the samples were kept at -196° until they could be analyzed for the amount of undecomposed choline present; the samples were dissolved in water as they were warming up to room temperature and the analyses were performed as previously described.⁵ Two samples each were allowed to stand at room temperature, before analysis, for 2, 4, 7, and 10 hours. Five samples were kept for 15 hours at room temperature before analysis. The amounts of decomposition in these samples are recorded in Table XXIX.

Table XXIX

Radiation decomposition of crystalline choline chloride (5×10^6 rep of 3-Mv electrons). Irradiations at -170° , storage at room temperature.		
No. of Samples	Time of storage (hrs)	Average % decomposition
5	0	0
2	2	1
2	4	5
2	7	7
2	10	7
5	15	9

It is apparent that the free radicals that are responsible for choline chloride's radiation decomposition are quite stable at liquid nitrogen temperature. Furthermore, their half life at room temperature appears to be approximately 4 or 5 hours. The free-radical signal observed in the electron spin resonance apparatus also indicated approximately the same half life.

Addition of Iodide or Iodine

Choline chloride was crystallized from alcohol solutions containing differing concentrations of iodide ion. The amounts of iodide present in the crystals were determined by oxidation with nitrite in acid solution and measuring the iodine by the optical density of the solution at $425 \text{ m}\mu$. The first preparations of the crystalline chloride-iodide contained 4.7 mole % of iodide (i. e., 4.7% of the total anions were iodide). Three samples of these crystals were given a dose of 3×10^6 rep of Co^{60} γ rays. Determinations of amounts of decomposition (% of choline cations decomposed) gave values of 14%, 17%, and 16%. The average G(-M) was 433. The same experiment was also performed on two samples of crystals having 29 mole % of iodide. The energy dose was 5×10^6 rep and the measured amounts of decomposition were 11% and 12%; the average G value was 268. These experiments indicate that the presence of the iodide has led to no decrease in the G value (the difference between the 433 and 268 is probably not significant). The iodide was probably present as separate crystals and thus there was no alteration in the crystal structure of the choline chloride.

Calvin

Two samples of crystalline choline chloride were sealed in evacuated tubes, to each of which a small crystal of iodine had been added. The samples were then given 4×10^6 rep in the Co^{60} source. The measured decompositions in these samples were 18% and 20%, and the average G value was 350. The presence of the iodine, therefore, has no effect on the chain length in the radiation decomposition of choline chloride.

Crystallization Experiments

All previous work has been carried out with choline chloride that was crystallized from alcohol-ether solutions. The salt is obtained as orthorhombic crystals from this solvent. To determine if any possible chain-stopping impurity could be removed by recrystallizations from this solvent mixture, three samples of choline chloride were recrystallized either once, twice, or three times from a mixture of the redistilled solvents. Each sample was subjected to 2.5×10^6 rep from the Co^{60} source. The measured amounts of decomposition were found to be 13%, 13%, and 14%, respectively. It is therefore apparent that repeated recrystallizations from these solvents have no effect on the radiation sensitivity.

A sample of choline chloride, previously crystallized from ethanol-ether, was recrystallized from redistilled dimethylformamide; again, orthorhombic crystals were separately subjected to 2.6×10^6 rep in the Co^{60} source. Reineckate analyses showed decompositions to the extent of 16%, 15%, 13%, and 14%. Therefore, choline chloride crystallized from dimethylformamide has the same radiation sensitivity as it shows after crystallization from alcohol-ether.

Solution Experiments

Fifteen experiments were performed to determine the radiation sensitivity of choline chloride in aqueous solution. These experiments are summarized in Table XXX. These experiments show clearly that choline chloride is normally stable towards radiation decomposition in aqueous solution. Its radiation sensitivity is thus a function only of its crystal structure, and not of any inherent instability in the isolated choline cation. The data of Table XXX also indicate that all of the energy given to the solution is transferred to the choline, and that a given energy dose per gram of solution causes decomposition of the same number of solute molecules, regardless of concentration.

Four experiments were performed to test the radiation sensitivity of choline chloride dissolved in absolute alcohol. These experiments are summarized in Table XXXI.

Table XXX

Radiation sensitivity of choline chloride in aqueous solution (exposed to Co^{60} γ rays)			
Conc. (mg/ml)	Rep x 10^6	Percent Decomp. ^a	G = molecules decomp. 100 ev to soln.
9.4	5.2	15	2.2
33	19	20	2.9
52	19	14	3.2
97	19	3	1.4
97	19	4	1.7
130	22	15	4.4
205	70	19	4.6
205	70	18	4.4
205	70	19	4.6
207	87	8	1.6
207	100	10	1.7
207	100	5	0.9
405	213	16	2.5
405	213	11	1.7
405	200	10	1.5

^aBy reineckate analysis.

Table XXXI

Radiation sensitivity of choline chloride dissolved in absolute alcohol (exposed to Co^{60} γ rays)			
Conc. (mg/ml)	Rep x 10^6	Percent Decomp. ^a	G = molecules decomp. 100 ev to soln.
24	6.9	0	0
24	160	4	2.1
24	140	6	3.5
99	130	3	1.9

^aBy reineckate analysis.

A HIGH-INTENSITY COBALT-60 SOURCE

B. M. Tolbert, Elmer Nielsen, George Edwards, Irville M. Whittemore,
and Nelson B. Garden

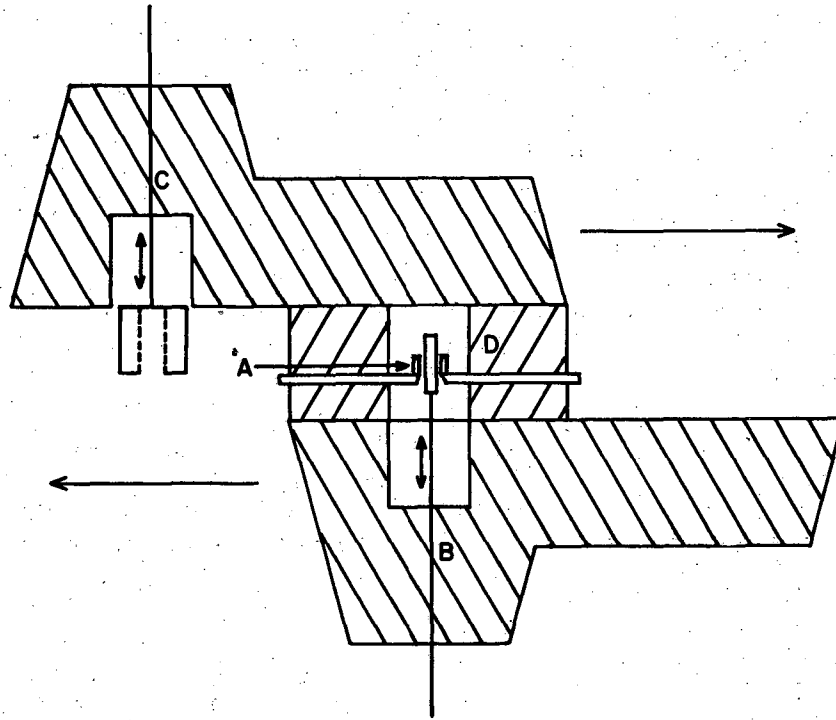
The planning and construction of a high-intensity Co^{60} source for chemical and engineering research has been under way for the past 3-1/2 years. Late in 1953 it was realized that fundamental studies using Co^{60} γ rays in radiation chemistry and in the studies of radiation changes to organic parts of reactors, cyclotrons, and allied equipment would require very high radiation intensities if data were to be obtained in a reasonable length of time. For most organic compounds, 10^7 rep may mean 1% change. Most studies require ~10% change for a reliable chemical measurement. An earlier source, built at the Radiation Laboratory, gave 5×10^5 rep/hr, and 10^8 rep of radiation therefore required 200 hours or 8.3 days--a rather long time between experiments. We had also observed radiation resistance in some compounds, where 10^8 to 10^{10} rep were required for a reasonable percent change. In addition, the original source here at the Laboratory had a very limited usable volume. Therefore, a second Co^{60} source was planned.

In order to produce a source with such high intensities, it is necessary to have Co^{60} of very high specific activity. The cobalt for the new source was therefore to be irradiated at the MTR reactor at Arco, Idaho, in a high-neutron-flux region. The source was, furthermore, to have an optimum space arrangement for the cobalt, in order to be versatile and to have a maximum usable radiation volume.

A sketch of the source holder devised to fill these requirements is shown in Fig. 18. The cobalt is held in a center unit, and moving shields and sample holders are placed above and below it. The lower shield and sample holder introduces a sample within a ring of vertically held Co^{60} -containing tubes. The length of Co^{60} in each tube is 1.5 in. The upper shield-and-sample-holder unit permits the introduction of a sample in the annular space between the outer center shield and the Co^{60} tubes. Since the shields may be moved separately, several samples may be handled at one time.

In addition, the ring of vertically held Co^{60} tubes may be changed in diameter from 1 in. to about 7 in. The area inside the source ring was designed to have a nearly uniform radiation field. At minimal Co^{60} ring diameter, the usable volume should be about 3/4 in. diam by 1 in. long. For a very uniform field, the volume would be about 3/8 in. by 1 in. long.

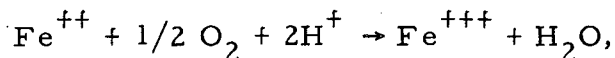
Preliminary measurement of the Co^{60} being placed in the source holders showed a total activity of about 2000 curies. Chemical calibration of the radiation field has now been carried out to determine the radiation field in the unit with Co^{60} source holders at their minimum diameter, i. e., 1 inch. The field has been determined in two ways. The absolute measurements have been made by using the oxidation of Fe^{++} in an oxygen-saturated solution. Relative fields have been determined by glass dosimetry by the darkening of strips of ordinary window glass.



MU-12907

Fig. 18. Diagram of 2000-curie Co^{60} source.
A, Co^{60} source holders, 16 arranged in circle.
B, lower movable shield with sample holder for center volume irradiation facility.
C, upper movable shield with annular basket sample holder lowered.
D, fixed shield for Co^{60} .
Scale: approx. 1 in. = 1 ft.

The first method depends on the reaction



in which the yield of Fe^{+++} is 15.5 $\mu\text{moles Fe}^{+++}$ per liter per 1000 rep. As the optical density of Fe^{+++} at 304 $\text{m}\mu$ in acid solution is 2130 (our determination), very small quantities of Fe^{+++} may be determined by the spectrophotometric method. The above reaction is zero-order, with respect to Fe^{++} and O_2 , as long as the two species are present. Saturating a solution of Fe^{++} with pure oxygen increases the total amount of radiation that may be applied to a given sample fivefold over air-saturated solutions. This was proved important in the work reported here, because of the short exposure times with which it has been necessary to deal.

With the source holders at minimum diameter, the field in the center of the unit, as determined by Fe^{++} dosimetry, averages 10^7 rep/hr in a tube 1 in. long with an i.d. of 10 mm. When two concentric tubes of Fe^{++} solution were irradiated--the outer tube, 10 mm i.d., and the inner tube, 6 mm i.d.--the contents of the outer tube received $\sim 10\%$ larger dose than the solution in the smaller tube.

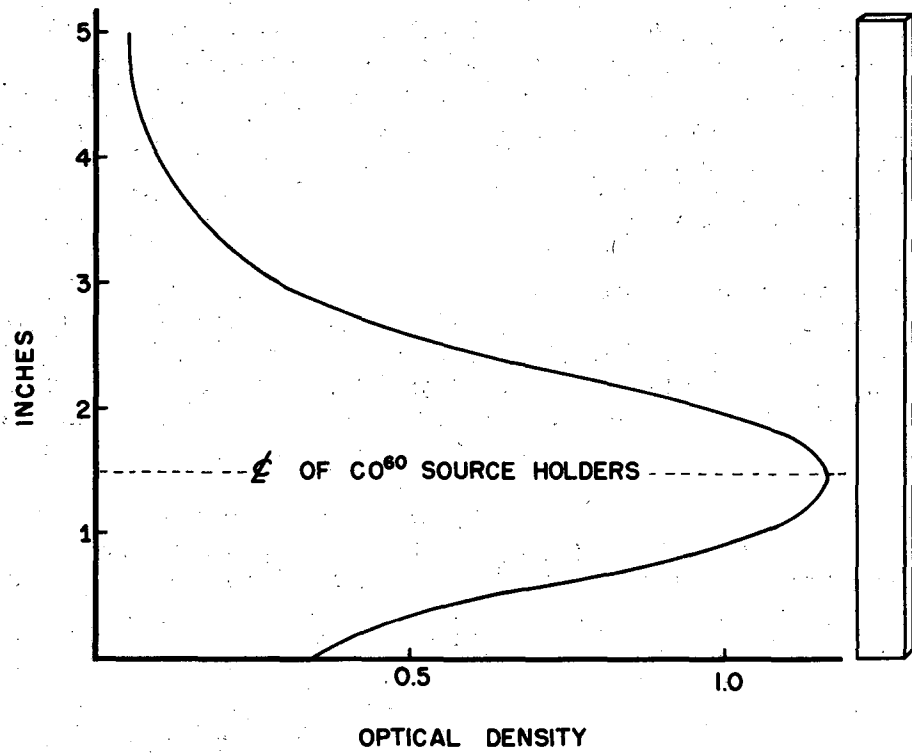
Outside the circle formed by the source holders, six different positions were studied for the irradiation of samples. These positions take the form of six circles concentric with the Co^{60} source holders. When the diameter of the sources is 1 in. then the diameter of the first circle is 2-1/8 in. and the other five are at successive 1-inch-larger diameters. The fields at these positions are as follows:

- No. 1, at 3.4×10^6 rep/hr;
- No. 2, 1.9×10^6 rep/hr;
- No. 3, 1.2×10^6 rep/hr;
- No. 4, 7.2×10^5 rep/hr;
- No. 5, 4.9×10^5 rep/hr; and
- No. 6, 3.7×10^5 rep/hr.

Glass dosimetry has been done in the following manner: A glass bar 3/8 by 1/8 by 5-1/16 in. was placed on the vertical axis of the Co^{60} sources in such a way that the glass extended about 1.5 in. below the centerline of the slugs, and the rest of the length above. After a suitable exposure (about 5 min) the glass was removed from the source and placed in a special slide made to accommodate it and also to fit into the filter-slit slot in a Beckman DU spectrophotometer. The density of the darkening is read at 450 $\text{m}\mu$. As the glass is not uniformly darkened, the gradient is measured by moving different portions of the glass in front of the slit and the optical density is measured. A typical curve obtained is shown in Fig. 19. As may be seen, the field intensity drops to about 5% of center value at 3.5 in. above the centerline of the Co^{60} source.

When this method was applied to obtaining the field at the six positions outside the circle formed by the Co^{60} source holders, estimates were obtained that were in good agreement with those values previously listed, which were obtained by the Fe^{++} dosimetric method.

Calvin



MU-12906

Fig. 19. Variation of field strength along vertical axis as determined by darkening of bar of glass; 5-minute exposure.

SPECTRA OF COPPER AND CHROMIUM COMPLEXES

Robert Feltham

The spectra of copper complexes have been extensively investigated by Belford¹ and Balhausen.² In the visible spectrum of copper bisacetylacetonate there are two absorption bands. In order to interpret the spectra in terms of crystal field theory the two bands were analyzed into three Gaussian components.¹ There is no reason, in view of the observed spectra of other molecules such as benzene, to suppose that the absorptions should be Gaussian. As a matter of fact, one would expect that this would not be the case.

Let us use copper bisacetate monohydrate as a model for the other copper chelates. The crystal structure shows that as a solid this compound is a dimer, with the following structure:³

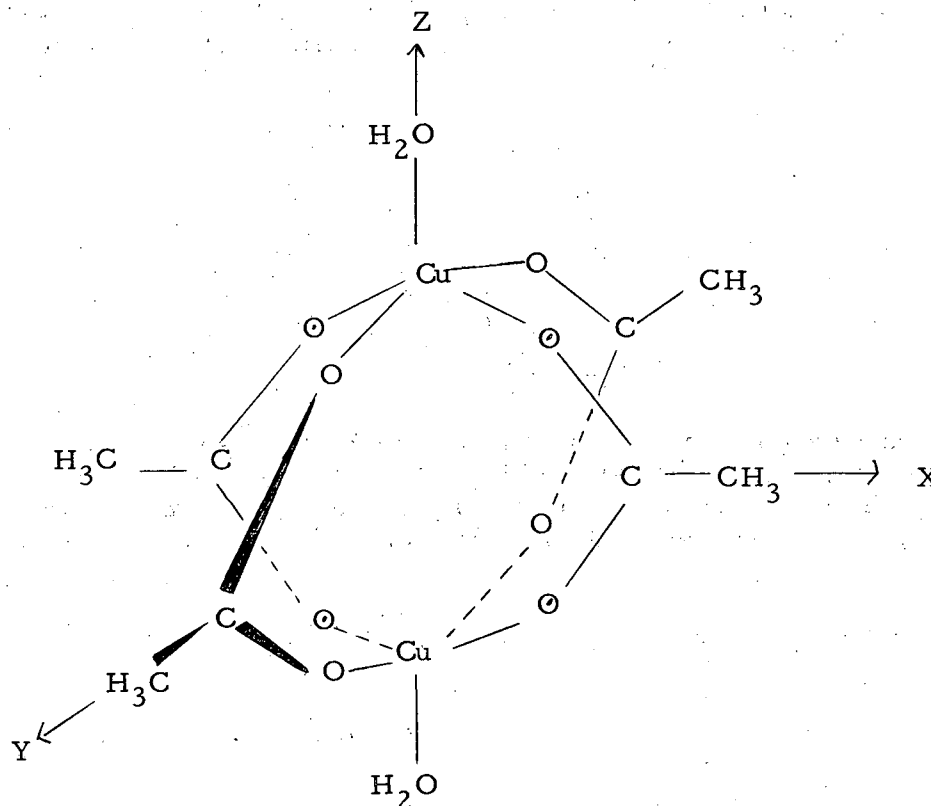


Fig. 20. Crystal structure of copper bisacetate monohydrate.

¹R. Linn Belford, *Bonding and Spectra of Metal Chelates: Ultraviolet, Visible, Infrared, and Electron Resonance Absorption. Near-Infrared Spectra of Alcohols* (thesis), UCRL-3051, June 1955.

²C. J. Balhausen, *Dan. Mat. Fys. Medd.* 29, no. 4 (1954).

³J. N. van Nierkerk and F. R. Schoening, *Acta Cryst.* 6, 227 (1953).

Tsuchida and Yamada have recently reported the polarized spectra for this compound.⁴ They show that the band at 3700 Å is z polarized, while the two bands in the visible are x, y polarized.

Van Vleck first suggested that these were electric dipole transitions and that the absorptions took place by means of vibrational interaction.⁵ The intensity of absorption is proportional to

$$\int \psi_E^{*0} \psi_V^{*0} e \cdot \vec{r} \psi_E^i \psi_V^l d\tau$$

if the transition is allowed by simultaneous electronic and vibrational excitation. ψ_E^{*0} refers to the ground-state electronic wave function, ψ_V^{*0} to the zero or ground-state vibrational mode, ψ_V^l to the first excited vibrational mode, and ψ_E^i to the particular excited electronic state involved in the transition.

If we use crystal field theory to arrange the energy levels in order of increasing energy we find the following scheme for D_{4h} symmetry:⁶

	<u>Class</u>
$d_{xz, xy}$	E_g
d_{xy}	B_{1g}
d_{z^2}	A_{1g}
$d_{x^2-y^2}$	B_{2g}

In order that the integral not vanish the product under the integral must have A_{1g} symmetry.⁷ The only stretching mode that will allow this integral for the highest-energy transition to be nonzero in D_{4h} symmetry is E_u (the Cu-O stretching). The symmetry of the product of wave functions under the integral signs is

$$B_{2g} \times E_g \times E_u = B_{2g} \times (A_{1u} + B_{1u} + A_{2u} + B_{2u}). \quad \text{Now we have}$$

$$B_{2g} \times \begin{cases} x, y \\ \text{or} \\ z \end{cases} = E_u \text{ or } B_{1u}.$$

Therefore, the only component of the electric dipole that makes this integral nonvanishing is z, that is, the absorption is z polarized. This result is in agreement with the experiments by Tsuchida. Using the same approach, we would conclude that the absorption at 6700 Å should be x, y polarized, and this is also the case.

⁴R. Tsuchida and S. Yamada, *Nature* 176, 1171 (1955).

⁵J. H. Van Vleck, *J. Chem. Phys.* 7, 72 (1939).

⁶B. N. Figgis and R. L. Martin, *J. Chem. Soc.* 3837 (1956).

⁷E. B. Wilson, *Molecular Vibrations* (McGraw-Hill New York, 1955)p. 161. Calvin

The assumptions involved in the above analysis are: first, that we are dealing only with electric dipole absorption; second, that the only important vibrational interactions in this transition are the stretching modes; and, third, that the copper-copper interaction is small. The 3700 \AA should be split owing to spin-orbit coupling by $2\lambda' = 1328 \text{ cm}^{-1}$, that is, a second component at 3528 or at 3891 \AA . This band has not been observed.

What does this tell us about the copper bisacetylacetonate? This compound has approximately the same symmetry around the copper as the acetate, and the spectra of the two compounds are almost identical. Apparently the copper-copper interaction is small in comparison with the crystalline electric field, and the similarity of the spectra of the two compounds is not accidental. This would predict the same polarization of the bands in the copper bisacetylacetonate. Investigations are now under way to determine whether or not this is the case. A single crystal of the compound has been prepared and a Dewar has been made in order to take the polarized spectra at liquid nitrogen temperatures.

Investigation of the electron spin resonance of the monodeuterodibenzene chromium, benzene diphenyl chromium, and bisdiphenyl chromium cations is also in progress.

NUCLEAR CHEMISTRY

Glenn T. Seaborg and Isadore Perlman in charge

NEW ISOTOPE: SULFUR-38

David R. Nethaway and Albert A. Caretto, Jr.

It was previously reported in the Quarterly Report (September - November 1956, UCRL-3629) that a new isotope of sulfur, S^{38} , had been identified by the separation of its daughter activity, 37.3-min Cl^{38} , from a previously purified sulfur sample. The half life was estimated to be ~ 5 min by comparison of the amount of S^{38} expected to be produced by the $Cl^{37}(\alpha, 3p)S^{38}$ reaction and the amount of Cl^{38} that was found to be present at a later time. The cross section for the formation of S^{38} by the above reaction was assumed to be approximately the same as that for the $Al^{27}(\alpha, 3p)Mg^{28}$ reaction, which was measured in each experiment. Later experiments have shown that the amount of S^{38} produced was very much lower than expected from the estimated cross section, even when provision was made in the experiment for exchange between the various oxidation states of sulfur and chlorine. Therefore, the previously reported half life for S^{38} is in error.

Bombardments were made by exposing ~ 100 -mg quantities of NaCl powder, covered with aluminum foil, to the 48-Mev alpha-particle beam of the 60-inch cyclotron. The activated NaCl was then placed in a crucible with K_2SO_4 carrier, Na_2CO_3 , K_2CO_3 , aluminum powder, and charcoal. This was heated to $850^\circ C$ for 20 minutes in a muffle furnace. The sulfide produced was then distilled from 6 N HCl into a solution of Pb in 2 N NaOH. The PbS was collected and oxidized with bromine water. The sulfate was precipitated as $BaSO_4$. This was then metathesized with a Na_2CO_3 -NaOH solution and the $BaCO_3$ was removed. The solution was boiled with HCl and HNO_3 , and $BaSO_4$ reprecipitated. The beta and gamma radiations from this sample were then measured.

The beta activity of two separate samples showed a half life of 172 to 176 min with no detectable contamination. The measurements were made through 40 mg/cm^2 of aluminum absorber to remove the beta particles from the 87-day S^{35} present. The beta activity was observed to grow initially, with a 37-min half life, until the Cl^{38} was in equilibrium. Aluminum absorption curves taken repeatedly on one sample indicated the presence of one beta group with an end-point energy of ~ 1.1 Mev.

Gamma-ray measurements have thus far failed to show the presence of any gamma rays of less than 1.6 Mev. The 1.6-Mev gamma ray of Cl^{38} was observed to grow in and decay with ~ 3 hr half life. A photopeak at 510 keV was assumed to be due to the annihilation of positrons produced by pair production from the high-energy gamma rays of the Cl^{38} .

The decay energy of S^{38} was estimated to be ~ 0.8 Mev by use of the Metropolis mass tables. It therefore appears likely that the principal mode of decay of S^{38} is by negatron emission to the Cl^{38} ground state. The calculated log ft value is ~ 5.3 , indicating an allowed transition.

An additional experiment was performed to repeatedly milk out the Cl^{38} daughter at constant time intervals from a sulfur sample. The sulfur was purified of all chlorine activities and then allowed to stand for periods of 90 min, after which the chlorine was separated and its radioactivity measured. Final values of the sulfur chemical yields are not yet available, but a preliminary plot of the Cl^{38} activities found, extrapolated to the time of separation from S^{38} , versus the separation time, gives a value for the S^{38} half life of about 2 hr.

The apparent cross section for the reaction $\text{Cl}^{37}(\alpha, 3p)\text{S}^{38}$ is around 0.3 microbarn. The measured cross section for the reaction $\text{Al}^{27}(\alpha, 3p)\text{Mg}^{28}$ is 500 times as large. Future experiments are being planned to study this anomalous effect more closely and to also provide more accurate values for the beta energy and half life of S^{38} .

PREPARATION OF GADOLINIUM-162 AND TERBIUM-162 BY DOUBLE NEUTRON CAPTURE

Kenneth T. Faler and Jack M. Hollander

A 300- μg sample of $\text{Gd}_2^{160}\text{O}_3$ containing 3% Gd^{158} was irradiated in the Materials Testing Reactor for 1 day. The bulk of the resulting activity was due to Tb^{161} formed by beta decay of 3.7-min Gd^{161} . Chemical separation of the terbium and gadolinium fractions produced a gadolinium fraction containing Gd^{159} and Gd^{162} . The former has an 18-hr half life, and the sample decayed rapidly to an activity of longer half life, which was presumably Gd^{162} .

Half-life determinations currently in progress indicate a figure of about 190 days. The amount of activity indicates a cross section near 10^5 barns for Gd^{161} on the basis of this half life. This seems reasonable compared with those for Gd^{155} and Gd^{157} , which are 7×10^4 and 1.8×10^5 respectively.

The sample of Gd^{162} will also contain the daughter Tb^{162} , which was tentatively reported as having a half life of about 14 min.¹

The gamma spectrum of the two isotopes in equilibrium was determined by means of a 100-channel pulse-height analyzer with a NaI crystal detector. The following photon peaks were observed:

41 keV, 117 keV, 340 keV, 237 keV, 760 keV, 955 keV, 1080 keV, 1250 keV, and 1390 keV.

The 41-keV peak might be expected to be K x-rays from internal conversion processes; however, the energy was quite well determined and is lower than the expected value of at least 43 keV. It is suspected that this peak may be due to a nuclear gamma transition. Its intensity is twice that of the 117-keV peak.

¹F. D. S. Butement, Nature 165, 149 (1950); Proc. Phys. Soc. (London) A64, 395 (1951).

A study is in progress to attempt separation of the daughter and identification of each peak with its nuclide. In addition, an attempt will be made to obtain sufficient activity to make an electron-spectrometer study.

STUDIES OF NEUTRON-DEFICIENT TERBIUM ISOTOPES

Kenneth S. Toth and John O. Rasmussen

A 19-hr terbium alpha emitter was first reported by Rasmussen et al.¹ A tentative mass assignment of the activity as Tb^{151} or possible Tb^{150} was then indicated by Rasmussen and Rollier.² Later, Handley³ reported that no alpha activity was seen in 14.0- and 22.4-Mev proton bombardments on gadolinium enriched in Gd^{152} . The conclusion was then reached that the alpha emitter was Tb^{150} . Consequently, the most recent General Electric Chart of the Isotopes has the activity placed as Tb^{150} .

A 60-inch cyclotron stacked-foil bombardment experiment was carried out to mass-assign the 19-hr terbium. Natural europium (48% Eu^{151} , 52% Eu^{153}) was painted on four aluminum foils. Suitable absorber aluminum foils were placed between the targets to give desired energies. These energies are listed below, together with the reactions most likely to occur:

- (a) 48 Mev, Foil One, $(\alpha, 4n)$, $(\alpha, 3n)$;
- (b) 40.6 Mev, Foil Two, $(\alpha, 3n)$, some $(\alpha, 4n)$;
- (c) 31.2 Mev, Foil Three, $(\alpha, 2n)$, some $(\alpha, 3n)$;
- (d) 20.2 Mev, Foil Four, (α, n) , $(\alpha, 2n)$.

No chemical separations were made, and the four foils were alpha-counted directly. Foil One contained the 19-hr activity in a large amount. The only half life seen on Foil Two was also 19 hr. However, the total activity for the latter foil was diminished by a factor of 20. Foil Three had very few alpha counts.

If the 19-hr activity were Tb^{151} it could have appeared on Foils One and Two by $(\alpha, 4n)$ reactions on Eu^{151} . However, if the activity were Tb^{150} it would have had to be produced by $(\alpha, 5n)$ reactions on Eu^{151} . Such a reaction is improbable at 48 Mev, especially if it has to account for a substantial amount of activity. Furthermore, an $(\alpha, 5n)$ reaction at 40.6 Mev seems to be even more improbable.

¹Rasmussen, Thompson, and Ghiorso, Phys. Rev. 89, 33 (1953).

²M. A. Rollier and J. O. Rasmussen, Studies of Neutron-Deficient Terbium Nuclides, UCRL-2079, Jan. 1953.

³T. H. Handley and W. S. Lyon, Phys. Rev. 99, 1415 (1955).

Samples 1, 3, and 4 have been counted on a 100-channel gamma-pulse analyzer, beginning approximately a month after bombardment so as to allow time for short-lived activities to die out. Sample 2 was lost when chemical separation was attempted. Two prominent peaks appeared in each sample, x-rays and 95-kev gamma rays.

Sample	Peak	Half life and isotope
1	x-ray	~ 150 d (Gd^{151})
	95-kev γ	~ 250 d (Gd^{153})
3 and 4	x-ray	~ 5 d (Tb^{153} and Tb^{156})
	and an	~ 250-d tail (Gd^{153})
	95-kev γ	~ 5 d (Tb^{153})
	and an	~ 250-d tail (Gd^{153})

The results can all be accounted for by using known isotopes Tb^{153} , Tb^{154} , Tb^{156} , Gd^{151} , and Gd^{153} and assuming Tb^{152} and Tb^{155} to be either very long- or short-lived.³ The fact that Gd^{151} appears in Foil One indicates that Tb^{151} was originally made in the bombardment. We feel that our results definitely mass-assign the 19-hr alpha emitter as Tb^{151} .

FURTHER STUDIES IN NEUTRON-DEFICIENT DYSPROSIUM ISOTOPES

Kenneth S. Toth and John O. Rasmussen

In the preceding quarterly report, three new dysprosium isotopes were reported, Dy^{149} , Dy^{153} , and Dy^{155} . Evidence from several experiments has accumulated that indicates the existence of another new activity in this region. It is believed to be Dy^{154} .

A stacked-foil bombardment that mass-assigned Dy^{152} and Dy^{153} was reported in the preceding report. At that time it was indicated that a tail appeared in alpha-counter decay curves that had a half life of approximately 15 hr.

It is considered that this tail represented a new alpha emitter, Dy^{154} . Gadolinium enriched in Gd^{154} was bombarded with full-energy alpha particles on the 60-inch cyclotron. A chemical separation was carried out and the dysprosium fraction followed on an alpha-pulse analyzer.

Alpha activity was low. At the bombarding energy the two principal reactions are $(\alpha, 4n)$ and $(\alpha, 3n)$. In spite of the fact that Gd^{154} represented 33% of the material bombarded and Gd^{152} only 0.3%, three peaks appeared with almost the same total activity. The one with the highest energy decayed with a 2.5-hr half life (Dy^{152}). The second peak, with the next-to-highest energy, had a 4.5-hr half life (Dy^{153}). The lowest-energy peak decayed

with an 11-hr half life. The sample was followed on an alpha counter approximately 48 hr after bombardment time, for a period of 12 hr. The activity decayed with a 13- to 15-hr half life.

Recently this experiment was repeated. The chemically separated sample was again followed on the 48-channel pulse analyzer, 20 hr after bombardment time. Two peaks appeared. The lower-energy peak dominated the spectrum. Its half life was 13 hr, and that of the higher-energy one was 5 hr. With the 5-hr peak as one standard (3.48 Mev) and Gd^{148} as the other (3.16 Mev), the 13-hr peak was calibrated. The average value obtained was 3.37 Mev.

It must be added that a bombardment was made wherein the same material was bombarded with 27-Mev alphas. No alpha activity could be detected. Since this energy is below the $(\alpha, 3n)$ threshold, Dy^{152} and Dy^{153} could not have been produced. Dy^{154} could have been made only by $(\alpha, 2n)$ on Gd^{152} (0.3% of bombarded material). This produces, evidently, an insufficient amount of alpha activity to be detected.

An experiment is planned for the near future in which the material will be irradiated at an energy just below the $(\alpha, 4n)$ threshold. Dy^{152} and Dy^{154} should not appear, but a 5-hr peak, representing Dy^{153} , should be in evidence. The mass assignment of Dy^{154} would then be completed.

The gamma spectra of two dysprosium isotopes, Dy^{155} and Dy^{157} , have been studied. Both isotopes decay by electron capture, and their gamma spectra were obtained by following samples on a 100-channel gamma-pulse analyzer.

Dysprosium-155 is produced in large amounts in irradiations by full-energy alphas on the 60-inch cyclotron of gadolinium enriched in Gd^{154} . The separated dysprosium fraction was studied on the gamma analyzer approximately 9 days after bombardment time. The only activity seen at this point in the decay curve is the 5-day Dy^{155} . A number of peaks were seen and assigned to Dy^{155} by virtue of their half life. They were:

- (a) 10-kev L x-rays;
- (b) 40-kev K x-rays;
- (c) Gammas with energies of 88 kev, 106 kev, 160 kev, 256 kev, 350 kev and 535 kev.

Dysprosium-157 was first reported by Handley¹ as an 8.2-hr EC isotope. The photons given at that time were K x-rays and a 375-kev gamma. Natural gadolinium bombarded with alphas at an energy below the $(\alpha, 3n)$ threshold produces essentially two dysprosium activities, Dy^{157} and Dy^{159} . The latter isotope has a half life of 134 days. If the sample is studied soon after the chemical separation is performed, the spectrum obtained is that of Dy^{157} .

¹Thomas H. Handley and Elmer L. Olson, Phys. Rev. 90, 500 (1953).

The spectrum appeared as follows:

- (a) L and K x-rays;
- (b) A 75-kev peak, which probably is the result of a pile-up of the K x-rays;
- (c) A 325-kev gamma;
- (d) A peak at 160 kev, which is probably the scatter peak of the 325-kev gamma;
- (e) A 660-kev gamma.

THE DETERMINATION OF NUCLEON-NUCLEON CROSS SECTIONS IN NUCLEAR MATTER

Lester Winsberg and Tom Clements

At sufficiently high energies, the interaction of a proton or neutron impinging on a nucleus can be described in terms of direct interactions with individual nucleons inside the nucleus. It is usual to consider that these direct interactions are the same as if the collisions were occurring between free nucleons. Since a large amount of experimental data has been accumulated on proton-proton and neutron-proton interactions, it is now possible to make calculations on the basis of this model. In order to do this, it is necessary to take into account the motion of the struck nucleon and the exclusion of reactions that leave nucleons in states that are already occupied.

For the initial stage in a general program of these calculations, we are now preparing to determine nucleon-nucleon cross sections in nuclear matter from the lowest energies up to 6 Bev as a function of the neutron and proton Fermi energies. A nucleon-nucleon collision can be described by four parameters: the momentum of the struck nucleon, the collision angle, the scattering angle in the center of mass of the two nucleons, and the angle of direction of the outgoing nucleons about the direction of the two nucleons before the collision in the center of mass. The first two parameters determine the total energy in the center of mass, and therefore establish the collision cross-section σ_i had the reaction been allowed. The allowedness of the reaction is determined by all four parameters, which are expressed in terms of four random numbers. In order to get a statistically reliable answer it is necessary to make many such collision calculations for a given bombarding energy and Fermi energy. The nucleon-nucleon cross section in nuclear matter is then given by

$$\sigma_{NM}(E, E_{FN}, E_{FP}) = \frac{\sum_i \sigma_i (d\sigma/d\Omega)_i \begin{pmatrix} 1 \\ 0 \end{pmatrix}_i}{\sum_i (d\sigma/d\Omega)_i}$$

where

E = bombarding energy,

E_{FN} = neutron Fermi energy,

E_{FP} = proton Fermi energy,

$d\sigma/d\Omega$ = differential cross section at the scattering angle chosen;

$\begin{pmatrix} 1 \\ 0 \end{pmatrix}_i = 1$ if allowed, 0 if not allowed.

This problem is now being programmed for the University of California IBM-701 computer. The differential cross-section data for elastic collisions have been expressed in analytical form as a function of E/mc^2 by the least-squares treatment. The inelastic cross sections for single, double, and triple meson production were similarly expressed in analytical form. Since the information on the momenta and scattering angles of the outgoing particles in meson production is incomplete, the calculation of these cross sections in nuclear matter will be repeated for various assumptions concerning the distribution of momenta and scattering angles.

TRITON PRODUCTION IN CYCLOTRON BOMBARDMENTS

William H. Wade and Jose Gonzalez-Vidal

It has previously been reported by us that significant amounts of H^3 are produced in the heavy-element region during proton, deuteron, and helium-ion bombardments with initial energies of 32, 24, and 48 Mev respectively. The same type of investigation has been performed in Mg, Al, Ti, Fe, Cu, Ni, Cd, In, and Ag targets. The evidence shows that, at least for helium-ion bombardments, there is a dual mechanism for tritium production: a non-compound-nucleus process producing H^3 with energies comparable to those of the bombarding He^4 (these integrated cross sections remain roughly constant through the periodic table), and a compound-nucleus process producing H^3 with relatively low energies and whose integrated cross sections seem to decrease exponentially with increasing Z of the target material. Odd-even Z effects have also been noted.

HALF-THICKNESS VALUES FOR GAMMA RAYS IN LEAD

Stanley D. Farrow and John O. Rasmussen

Discrepancies were found between the values of half thicknesses for electromagnetic radiation in lead compiled by Allen¹ and those more recently calculated by Davisson and Evans.² To see which data were more reliable, the half thickness in lead was measured for three gamma-ray energies. The half thicknesses for higher gamma-ray energies were found to agree with the recent data rather than with Allen's values. The results are shown in the table.

γ energy (kv)	Pb half thickness (g/cm ²)		
	Allen	Davisson and Evans	This experiment
662	4.9	6.6	6.9
279	0.95	1.36	1.55
60	0.15	--	0.13

FLUORESCENCE OF U⁺³

John G. Conway, Ralph D. McLaughlin, and George V. Shalimoff

Fluorescence has been observed in crystals of LaCl₃ containing UCl₃. The color of the fluorescence is a deep red. Four crystals prepared from different lots of LaCl₃ and varying concentrations of UCl₃ have been made to date. Additional crystals of UCl₃ in NaCl, MgCl₂, and SrCl₂ were prepared. These did not fluoresce. The color of the UCl₃ in SrCl₂ was very different from the others; it was burgundy where the others were a green-yellow. These crystals will be grown so as to produce single crystals, and their spectra will be taken.

¹S. J. M. Allen, in A. H. Compton and S. K. Allison, X-Rays in Theory and Experiment (Van Nostrand New York, 1935), Table 1, p. 801.

²C. M. Davisson and R. D. Evans, Revs. Modern Phys. 24, 79 (1952).

DEUTERON-INDUCED REACTIONS OF
URANIUM-234, URANIUM-235, AND URANIUM-238

Richard M. Lessler

Uranium-234, U^{235} , and U^{238} have been bombarded on the 60-inch cyclotron. The following cross sections have been determined.

Uranium-234

Energy (Mev)	Cross section (mb)		
	(d, n) Np^{235}	(d, 2n) Np^{234}	(d, 3n) Np^{233}
8.4	---	1.41	---
11.8	---	3.26	---
14.8	11.2	16.6	2.33
16.0	---	(32.0)	(5.64)
16.4	---	29.2	8.33
17.1	---	---	12.9
17.5	---	29.9	19.1
18.9	---	(22.5)	(19.2)
20.0	---	(20.1)	(17.6)
20.6	11.9	18.9	14.9
23.4	12.3	12.3	7.44

Uranium-235

Energy (Mev)	Cross section (mb)			
	(d, n) Np^{236}	(d, 2n) Np^{235}	(d, 3n) Np^{234}	(d, 4n) Np^{233}
9.3	1.41	7.80	---	---
10.7	3.65	33.5	0.754	---
14.7	4.41	---	8.40	---
14.7	4.48	22.1	8.60	---
17.2	4.77	18.0	14.8	---
18.2-19.2 (foil)	(5.00)	(15.5)	(24.7)	---
20.6	5.38	---	25.0	0.315
23.4	6.30	---	10.4	---
23.4	6.10	---	11.4	---
23.4	6.29	---	12.5	4.15

Cross sections given in parentheses are relative cross sections. That is, in U^{234} the d, 2n is relative to the d, 3n and in U^{235} the d, 2n and the d, 3n are relative to the d, n when parentheses are used.

Cross sections for Np^{235} are obtained by assuming that the residual activity remaining in the sample after the decay of shorter-lived neptunium isotopes is due to Np^{235} . Activity due to long-lived alpha emitters is, of course, subtracted out.

The cross section for Np^{236} includes only the 22-hr isomer.

The Nucleometer (windowless proportional counter) was used to count the samples. The following counting efficiencies were used to calculate the cross section:

Np^{236} : 0.95

Np^{235} : 0.40

Np^{234} : 0.65

Np^{233} : 0.60

Uranium-238

Energy Range in foil (Mev)	Cross section (mb)			
	(d, γ)61-min Np^{240}	(d, γ)7-min Np^{240}	Total(d, γ)	(d, 2n) Np^{238}
1.8-6.3	1.57×10^{-3}	$< 4.14 \times 10^{-3}$	5.71×10^{-3}	-----
6.1-9.3	21.0×10^{-3}	$< 35.1 \times 10^{-3}$	56.1×10^{-3}	2.93
9.7-13.0	44.0×10^{-3}	$< 49.0 \times 10^{-3}$	93.0×10^{-3}	48.3
14.5-16.8	44.8×10^{-3}	$< 118.0 \times 10^{-3}$	163.0×10^{-3}	39.7
21.4-23.4	11.5×10^{-3}	$< 63.6 \times 10^{-3}$	75.1×10^{-3}	32.7

These cross sections are tentative.

The cross section for the 7-min Np^{240} is an upper limit. Therefore, the cross section for the 61-min Np^{240} is a lower limit for the true (d, γ) reaction while the total (d, γ) cross section given is an upper limit.

ELECTROSTATIC CALCULATION OF STRUCTURE
FOR YTTRIUM OXYFLUORIDE

David H. Templeton

A paper of this title is to be presented at the Fourth International Congress of Crystallography, Montreal, July 10-19, 1957. The abstract is as follows:

The substance YOF exists in two crystal structures, each of which is an ordered superlattice based on the CaF_2 -type structure. The atomic coordinates were determined by Zachariasen,¹ but the diffraction data did not distinguish O and F. The nearest-neighbor distances are 2.28 and 2.44 Å in the rhombohedral form and 2.30 and 2.47 Å in the tetragonal form. A calculation of the crystal energy, based on a simple model, shows decisively that the shorter distance corresponds to the oxygen neighbor in each structure.

In this treatment the crystal energy is assumed to be given by the expression

$$U = \sum q_i q_j / r_{ij} + \sum B_{ij} / r_{ij}^n$$

The first sum takes account of the Coulomb monopole interactions of all pairs of atoms, and is computed by Bertaut's method² with careful attention to convergence.³ The second sum is computed only for nearest neighbors. The constant B for Y-O (or Y-F) pairs is chosen so that U, calculated in the same way, is a minimum for Y_2O_3 (or YF_3) at the interatomic distances observed experimentally. Various values of the exponent n have been used, but one value is used consistently throughout a single calculation.

For rhombohedral structure is described as follows:¹

space group $R\bar{3}m$ (No. 166)

$a = 6.697 \text{ \AA}$, $\alpha = 33.20^\circ$

2 Y at $\pm (uuu)$, $u = 0.242$ or 0.258

2 F at $\pm (vvv)$, $v = 0.122$ or 0.130

2 O at $\pm (www)$, $w = 0.370$ or 0.378

The structures described by the two sets of parameters differ only in the interchange of O and F atoms. The crystal energy calculated for $u = 0.242$ exceeds that for $u = 0.258$ by about 100 kcal/mole. The minimum in U was sought as a function of a and u, with α held constant. The parameter

¹W. H. Zachariasen, Acta Cryst. 4, 231 (1951).

²F. Bertaut, J. phys. radium 13, 499 (1952).

³R. E. Jones and D. H. Templeton, J. Chem. Phys. 25, 1062 (1956)

v (or w) was determined so as always to equalize the two independent Y-F (or Y-O) nearest-neighbor distances. The value of u giving the minimum energy is 0.259 for either $n = 8$ or $n = 9$. The value of a giving the minimum energy agrees with the experimental value within 0.6% for $n = 8$, and 0.4% for $n = 9$.

Less complete calculations for the tetragonal structure indicate very similar results. It is hoped to extend the calculations to include anion-anion repulsion effects, but these effects are not expected to change the qualitative conclusions. All statements made concerning the structures of YOF are assumed to apply also to the compound LaOF, which is isostructural with both forms of YOF.¹

It is noteworthy that the Y-O distance is about what one estimates for coordination 5 or 6, which is intermediate between the number of oxygen neighbors and the number of anion neighbors. The Y-F distance, on the other hand, corresponds to hardly any repulsive potential and is considerably longer than the sum of ionic radii. A similar effect may be observed in other oxyhalides, for example the rare earth oxychlorides.⁴

⁴D. H. Templeton and C. H. Dauben, J. Am. Chem. Soc. 75, 6069 (1953).

CHEMICAL ENGINEERING (PROCESS CHEMISTRY)

NOTES ON WORK IN PROGRESS

Correlation of Limiting Current Density at Horizontal Electrodes
under Free-Convection Conditions

Eugene J. Fenech and Charles W. Tobias

Complete revamping of all circuits is in process in order to achieve greater control and more precise measurements.

A new cell is being designed to make possible undistorted visual observation of the processes taking place in the cell and to allow the use of sectioned electrodes.

Stability of Perforated-Plate Trays

Robert S. Brown, Donald N. Hanson, and C. R. Wilke

It has been found that momentum of the liquid across the perforations has a significant effect on the dumping rate. Placing an inlet weir on the plate increases the dumping rate by a factor of approximately five. At the same time, the liquid flow required to maintain the desired clear liquid height is decreased by a factor of 1.4.

Multicomponent Distillation Studies
with an IBM 701-2 Frame Digital Computer

J. H. Duffin, Donald N. Hanson, and C. R. Wilke

By the use of the above computer, problems involving distillation of multicomponent mixtures have been and are being solved. This work continues that previously mentioned.

The steam-stripped fractionator continues to give trouble, and work on the solution of this problem is currently being carried on.

Electrochemical Studies in Nonaqueous Solvents

W. S. Harris and Charles W. Tobias

Quantitative solubilities have been determined for a number of salts in propylene carbonate at 25°C. The electrical conductivity of their saturated solutions has also been determined at 25°C.

Equipment has been set up to make the corresponding measurements with ethylene carbonate, whose melting point is 36°C.

Liquid-Liquid Extraction and Agitation Coalescence Rates

in Two-Phase Agitated Systems

J. H. Vanderveen and T. Vermeulen

The determination of coalescence data has been continued, and further empirical analysis of the factors in droplet breakup and droplet coalescence has been made. The rate of breakup increases with decreasing interfacial tension (σ); the limiting (minimum) particle size decreases with decreasing σ , as already known; and the rate of coalescence is then found to increase with σ^n where n (less than one) varies with other physical factors. It appears that the size of dispersed gas bubbles is determined mainly by coalescence effects. Correlation of these results is continuing.

Performance of Sphere-Packed Extraction Columns

G. Jacques and T. Vermeulen

Rate of longitudinal dispersion and of radial dispersion have been measured for three ordered arrangements of 3/4-inch spheres, and for random arrangements of 3/4-inch and 1/4-inch spheres. For longitudinal dispersion, a fairly sharp transition in Peclet number has been observed with varying Reynolds number, which suggests a sharper transition from laminar to turbulent flow than has been apparent from widely available pressure-drop data. The study of two-phase systems will be begun shortly.

Extraction Rates into Single Drops

T. Miyauchi and T. Vermeulen

Nitric acid extraction from single penta-ether droplets into pure water has been measured as a function of droplet size and concentration level. No conclusions have yet been reached regarding the mechanism; experimental measurements are continuing.

Gas-Liquid Partition Chromatography (GLPC)

Robert H. Houston and C. R. Wilke

Work on this problem has been completed and is the subject of a forthcoming report.

GENERAL CHEMISTRY

Leo Brewer, Robert E. Connick, and Kenneth S. Pitzer in charge

METALS AND HIGH-TEMPERATURE THERMODYNAMICS

Absolute-Lifetime Apparatus

Elizabeth Brackett, Leo Brewer, Richard Brewer, John Engelke,
Fred Stafford, and Earl Worden

An electronic bombardment furnace for molecular-beam sources has been built. Intensity measurements of a CN arc-light source are in progress. The modulating and detection systems are virtually complete and ready to be installed in the laboratory for testing.

Ground State of C₂

William T. Hicks

The heats of sublimation of the triplet and singlet states of C₂ have been measured and the work has been written up as a UCRL report (UCRL-3696).

Stability of SiO and GeO Solids

Frank T. Greene and Leo Brewer

Papers describing this work have been written up and submitted for journal publication. The revision of the thermodynamic table in the National Nuclear Energy Series is in progress.

BASIC CHEMISTRY

Ruthenium Chemistry

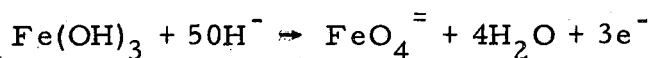
Howard Cady

This work has been completed and a report is being written.

The Heat of Formation of the Ferrate Ion

Robert Wood

The potential of the half reaction



of -0.91 volt given in the preceding quarterly report should be corrected to $-0.71 \pm .02$ volt. An attempt has been made to measure this half reaction directly, using a gold electrode and solutions of K_2FeO_4 in 5 M and 10 M NaOH. A hydrogen electrode was used as the other half cell. Although the E^0 values are independent of the concentration of $\text{FeO}_4^{=}$, they are not independent of the concentration of NaOH. For this reason the data are considered unreliable. The calculated values of E^0 were -0.807 volt in 10.89 M NaOH and -0.768 volt in 5.31 M NaOH.

The Second Ionization Constant of H_2Se

Robert Wood

The solubility of K_2Se as a function of the concentration of NaOH is being measured so that a value of the second ionization constant of H_2Se can be calculated.

Kinetics of Rapid Reactions

Claude Coppel

At the completion of the experiments on the ferric thiocyanate complexing reaction, some experimental difficulties were noted and checked before final calculations were made.

The first problem was due to an overshoot and decay of the oscilloscope. When a constant dc voltage was applied across the scope an initial displacement was observed, then a gradual decay to some equilibrium displacement. This decay was measured as a function of time and as a function of equilibrium displacement. It was found to be both complicated and somewhat irreproducible. Experimental runs of rate data were corrected for a maximum decay effect, and these corrections turned out to be negligible. This indicates that the data obtained previously are acceptable. A new oscilloscope was obtained that does not have this decay property.

The second problem was to check on the sampling method used to obtain final concentrations of solutions in the mixer. This was done by removing small samples continuously from a filled mixer and measuring the ferric thiocyanate concentration. The results indicated that the sampling procedure used may lead to errors of $\pm 4\%$ in the final concentrations. This is within the $\pm 5\%$ used in estimating probable errors.

Since our earlier work on the K and ΔH of the ferric thiocyanate reaction, two publications have been found on measurements of these values. The agreement in all cases is within experimental error.

Following this work a study of the ferric chloride complexing reaction was started. At this time no rates have been observed on this reaction. It appears to be faster than the mixing time of the apparatus, although it may be possible that optimum conditions have not yet been obtained.

Determination of the Molecular Structure of Aluminum Hydride

Robert F. Nickerson

Ether-free aluminum hydride was prepared by a variation of the method described by Rice and Chizinsky in an ONR Technical Report. Upon analysis, the sample proved to be largely lithium chloride with as little as 10% aluminum hydride present. The variation of the reported procedure is probably the reason for the presence of LiCl. However, some preliminary proton-spin resonance spectrograms were made with the sample.

Attempts are now being made to prepare perfluoroethers to be used as solvents in the preparation of aluminum hydride to further the studies on this compound.

Heat Capacities of Metals between 0.1° and 4.2° K

Norman E. Phillips

The apparatus has been completed and some measurements on Cu and Al have been made. The temperature of the metal specimen is measured by a carbon resistance thermometer. Above 1°K the resistance thermometer is calibrated directly against the vapor pressure of liquid He; thermal contact to a vapor-pressure bulb is made by a mechanical heat switch. Use of the mechanical switch instead of the usual He gas improves the thermal insulation obtained during heat-capacity measurements and makes possible an accuracy of better than 1% even near 1°K.

For the measurements below 1°K the metal is connected to a paramagnetic salt pill through a superconducting thermal switch, and the mechanical switch is used to make thermal contact between the salt and He bath. The resistance thermometer is calibrated against the susceptibility of the salt, which is in turn calibrated against the vapor pressure of liquid He. Susceptibility measurements are made with a low-frequency mutual-inductance bridge. Under the most favorable conditions the heat leak to the salt is about 10 ergs/min.

Hydrogen Bonding in Formic Acid Systems

Jefferson C. Davis, Jr.

Studies of hydrogen bonding in formic acid and formic acid solutions are now in progress utilizing nuclear magnetic resonance techniques. It is well known that in systems where there is rapid exchange of protons between two species a single resonance is observed, its position depending upon the relative amounts of the two species present. It is thus possible to determine the degree of hydrogen bonding by observing the shifts of the -COOH proton resonance with temperature and at various degrees of dilution with inert solvents. Formic acid and a solution of approximately 0.1 mole % formic acid in carbon tetrachloride have been studied between 0° and 140°C, and the expected shifts have been observed. The investigation is continuing with more accurate methods over a greater temperature range.